ZEBRAFISH AS A MODEL TO STUDY BETA-CELL DEVELOPMENT AND REGENERATION

by

Maria Chiara Toselli

B.HSc., The University of Calgary, 2013

A THESIS SUBMITTED IN PARTIAL FULFILLMENT OF

THE REQUIREMENTS FOR THE DEGREE OF

DOCTOR OF PHILOSOPHY

in

THE FACULTY OF GRADUATE AND POSTDOCTORAL STUDIES

(Cell and Developmental Biology)

THE UNIVERSITY OF BRITISH COLUMBIA

(Vancouver)

March 2020

The following individuals certify that they have read, and recommend to the Faculty of Graduate and Postdoctoral Studies for acceptance, the dissertation entitled:

Zebrafish as a Model to Study Beta-Cell Development and Regeneration

submitted by Maria Chiara Toselli in partial fulfillment of the requirements for

the degree of Doctor of Philosophy

in Cell and Developmental Biology

Examining Committee:

Dr. Timothy Kieffer, Professor, Cellular and Physiological Sciences
Supervisor

Dr. Cheryl Gregory-Evans, Professor, Ophthalmology and Visual Sciences
Supervisory Committee Member

Dr. James Johnson, Professor, Cellular and Physiological Sciences
Supervisory Committee Member

Dr. Bradford Hoffman, Associate Professor, Surgery
University Examiner

Dr. Alice Mui, Associate Professor, Biochemistry and Molecular Biology
University Examiner

Additional Supervisory Committee Members:

Dr. Francis Lynn, Associate Professor, Surgery
Supervisory Committee Member

Abstract

Diabetes is characterized by insufficient amounts of insulin, a hormone produced by the beta-cells in the pancreatic islets. While current treatment options such as insulin injections provide a way to manage blood glucose levels, these methods provide suboptimal glucose control. Islet transplantation shows significant therapeutic promise, but the lack of available islets is an obstacle for this therapy. Restoration of beta-cell mass through cell therapy or stimulation of endogenous regeneration to replace beta-cell loss and dysfunction could potentially cure diabetes. Hence, investigating beta-cell development and regeneration is extremely valuable. Because zebrafish and mammalian pancreas development are highly conserved, we utilized zebrafish as a model to study beta-cell development and regeneration in the work described in this thesis. We developed and characterized a lineage tracing model that allowed us to differentiate beta-cells arising from the dorsal and ventral pancreatic buds. We lineage traced the dorsal bud derived beta-cells during development until the adult stage. While we observed that dorsal bud derived beta-cells constitute a small percentage of the total beta-cells in the adult pancreas, we did not identify transcriptional differences between beta-cells that arise from dorsal and ventral pancreatic buds, suggesting that developmental origin does not dictate transcriptional profile. Second, we characterized the role of islet vessels during beta-cell formation. We found that islet vessels are dispensable for alpha-cell and beta-cell development. Finally, we determined the cell sources important in beta-cell maintenance and regeneration. We observed that beta-cell proliferation is the main mechanism of beta-cell maintenance in the adult zebrafish, but that a non-beta-cell source may contribute to beta-cell regeneration. By providing a better understanding of zebrafish beta-cell development and regeneration, the findings in this thesis may help guide cell therapies and regenerative strategies for diabetes.

Lay Summary

Diabetes affects 425 million people worldwide. Diabetes is characterized by insufficient amounts of insulin, a hormone produced by the beta-cells in the pancreas. Finding ways to increase or replace insulin-producing beta-cells is a major priority in diabetes research. This thesis uses the zebrafish as model to investigate beta-cell development and beta-cell replacement strategies. Zebrafish develop beta-cells within the first 14 hours of life, and upon beta-cell destruction, zebrafish are able to regenerate their beta-cells within 3 weeks. Zebrafish pancreas development is similar to mammalian pancreas development, and hence zebrafish are a valuable model to study how beta-cells develop and regenerate. This work provides a better understanding of beta-cell biology and regeneration, and hopefully provides insights into the development of potential therapies for diabetes.

Preface

The studies presented in this dissertation were conceived, designed, and performed Chiara Toselli, with assistance as described below.

Studies in Chapter 2 were performed by Chiara Toselli. FACS was performed by Justin Wong and Andy Johnson at the UBC Flow Cytometry & Cell Sorting Facility. RNA sequencing and alignments were performed by Ryan Vander Werff and Yiwei Zhao at the UBC Biomedical Research Center. Cara Ellis performed RNA sequencing analysis and generated Figures 2-10A-H.

Studies in Chapter 3 are published in the following article Toselli CM, Wilkinson BM, Paterson J, and Kieffer TJ. (2019) Vegfa/vegfr2 signalling is necessary for zebrafish islet vessel development but is dispensable for beta-cell and alpha-cell formation. *Scientific Reports.* Studies were performed by Chiara Toselli. Brayden Wilkinson performed experiments in Figures 3-9A-C and Joshua Paterson assisted with the experiments performed in Figures 3-10A-J. This publication was written by Chiara Toselli with editing by Timothy J. Kieffer.

Studies in Chapter 4 were performed by Chiara Toselli. Double blind experiments in Figure 4-4 and 4-6 were performed by Stephanie Tarazi. Stephanie Tarazi helped perform experiments in Figure 4-4G-H.

Animal studies described in this dissertation were approved by the University of British Columbia Animal Care Facility (Certificates: #A18-0051, #A18-0052).

Table of Contents

List of Tables

List of Figures

List of Abbreviations

4-OHT	4-Hydroxytamoxifen
Actb2	Actin beta 2
Anova	Analysis of variance
Arx	Aristaless-related homeobox protein
Ascl1b	Achaete-scute family bHLH transcription factor 1b
BMP	Bone Morphogenetic Protein
BrDU	5-Bromo-2′-Deoxyuridine
CAC	Centroacinar cells
CAII	Carbonic anhydrase II
Cas9	CRISPR associated protein 9
Cdkn	Cyclin-dependent kinase Inhibitor
cDNA	Complementary deoxyribonucleic acid
CFP	Cyan fluorescent protein
Cre	Cre recombinase
CreERT2	Cre recombinase - estrogen receptor T2
CRISPR	Clustered regularly interspaced short palindromic repeats
Cryaa	Crystallin, alpha A
DAPI	4’,6-diamidino-2-phenylindole
DAPT	N-[N-(3,5-Difluorophenacetyl-L-alanyl)]-S-phenylglycine t-Butyl Ester
DMSO	Dimethyl sulfoxide
DNA	Deoxyribonucleic acid
DOX	Doxycycline hyclate
dpa	Days post ablation
dpf	Days post fertilization
DsRed	Discosoma red fluorescent protein
DTA	Diphtheria toxin A
DYRK1A	Dual-specificity tyrosine-regulated kinase 1A
E3 media	Embryo media
EBFP	Enhanced blue fluorescent protein

EdU	5-ethynyl-2’-deoxyuridine
Ef1α	Eukaryotic translation elongation factor 1 alpha 1
EGFP	Enhanced green fluorescent protein
FACS	Fluorescence-activated cell sorting
FGF	Fibroblast growth factor
Fli1	Fli-1 proto-oncogene
FLP	Flippase
FRT	Flippase recognition target
GCG	Glucagon
Gcgb	Glucagonb
GCK	Glucokinase
GECI	Genetically encoded calcium indicator
GFP	Green fluorescent protein
GLP-1	Glucagon-like peptide-1
Glut2	Glucose transporter 2
Grn2	Granulin 2
GSIS	Glucose-stimulated insulin secretion
H2B	Histone 2B
HBSS	Hanks' balanced salt solution
Hes1	Hairy and enhancer of split 1
hpf	Hours post fertilization
hPSCs	human pluripotent stem cells
Hsp70l	heat shock cognate 70-kd protein, like
htBID	Human truncated BH3 interacting-domain death agonist
Ins	Insulin
IPD	Intrapancreatic duct
IRES	Internal ribosome entry site
Isl1	ISL LIM homeobox 1
kb	Kilobase
kdr	Kinase insert domain receptor

kdrl	Kinase insert domain receptor like
Krt18a.1	Keratin 18a, tandem duplicate 1
LoxP	Locus of X-over P1
Mafaa	Musculoaponeurotic fibrosarcoma oncogene homolog Aa
MO	Morpholino
mRNA	Messenger ribonucleic acid
MS-222	Tricaine methanesulfonate
MTZ	Metronidazole
Muc1	Mucin 1
Myl7	myosin, light chain 7, regulatory
Neurod1	Neurogenic differentiation 1
NfsB	Oxygen-insensitive NAD(P)H nitroreductase
Neurog3	Neurogenin 3
Nkx2-2	Homeobox Protein Nkx-2.2
Nkx6-1	Homeobox Protein Nkx-6.1
NOD	Non-obese diabetic
NTR	Nitroreductase
pA	Polyadenylation
Pax4	Paired box 4
PBS	Phosphate buffered saline
PCNA	Proliferating cell nuclear antigen
PDL	Pancreatic duct ligation
Pdx1	Pancreatic and duodenal homeobox 1
PP	Pancreatic polypeptide
Ptf1a	Pancreas Associated Transcription Factor 1a
PTU	1-phenyl-2-thiourea
RA	Retinoic Acid
RNA	Ribonucleic acid
RT-PCR	Reverse transcription polymerase chain reaction
RT-qPCR	Reverse transcription quantitative polymerase chain reaction

SCID	Severe combined immunodeficiency
SHH	Sonic Hedgehog
SIV	Sub-intestinal vein
Sox9	Sex determining region Y box-9
SST	Somatostatin
Sst1.1	Somatostatin1.1
Sst2	Somatostatin2
STZ	Streptozotocin
SU5416	Z-3-{(2,4-dimethylpyrrol-5-yl) methylidenyl}-2-indolinone
T2A	2A peptide from thosea asigna virus 2A from
TagRFP	Tagged red fluorescent protein
TCF7L2	Transcription factor 7-like 2
TBF	Tebufenozide
Ubb	ubiquitin B
UMAP	Uniform Manifold Approximation and Projection
UTR	Untranslated region
Vegf	Vascular endothelial growth factor
Vegfr	Vascular endothelial growth factor receptor
Wnt	Wingless-Type MMTV Integration Site Family
WT	Wild-type
YFP	Yellow fluorescent protein

Acknowledgements

I first want to thank my PhD supervisor, Dr. Timothy Kieffer. I am grateful for his patience, guidance, encouragement, and advice he has provided throughout my PhD. I would also like to thank my supervisory committee including Dr. Francis Lynn, Dr. James Johnson, and Dr. Cheryl Gregory-Evans for all of your guidance. I am grateful for the sources of graduate school salary funding including the Natural Sciences and Engineering Research Council and the University of British Columbia.

I would also like to thank past and present graduate students, technicians, and postdoctoral research associates in the lab for their constant source of support. In particular, I would like to thank Dr. Cara Ellis for her mentorship and who contributed to the data in this thesis. I thank Josh Paterson, Stephanie Tarazi, and Brayden Wilkinson, all of whom I had the pleasure of supervising as they helped contribute to the data in this thesis. Special thanks to all the volunteer undergraduate students who helped with the maintenance of the zebrafish animal facility throughout the last 6 years.

Finally, I thank my family and friends for their abundant and continuous support throughout my thesis. To my partner Jarred, I really cannot express my appreciation for your unconditional love and support during my PhD. Thank you for being the person I can always count on.

Chapter 1: Introduction

1.1 Diabetes

Diabetes mellitus is a metabolic disorder that is largely characterized by elevated levels of blood glucose due to insufficient amounts of the blood lowering hormone insulin. In 2017, diabetes was estimated to affect over 425 million people worldwide including more than 2.6 million Canadians and over 30 million Americans (1,2). The number of cases worldwide is expected to increase to 629 million people by 2045 (1). The associated costs of diabetes to the health care systems is astonishing. Annually, approximately $17 billion in Canada and $350 billion in the United States is spent on healthcare costs related to diabetes (1). These medical costs are mostly attributed to type 2 diabetes which makes up approximately 90% of the cases, while type 1 diabetes makes up for most of the remaining 10% of diabetes cases.

Type 2 diabetes is characterized by insufficient insulin levels to meet the body's demands. The high demands of insulin produced by the beta-cell results in beta-cell exhaustion and leads to the eventual loss of functional endocrine cells. Genetics and major environmental risk factors such as physical inactivity and obesity contribute to the development of type 2 diabetes. Genetic variants such as single nucleotide polymorphisms in genes like Gli-similar 3 (*GLIS3*) and transcription factor 7-like 2 (*TCF7L2*) are associated with type 2 diabetes (3,4). Type 1 diabetes is characterized by uncontrollable hyperglycemia due to insufficient insulin production from pancreatic beta-cells. The immune system plays a dominant role in the pathogenesis of type 1 diabetes as CD8+ cytotoxic cells and macrophages can be found around islets in many patients with type 1 diabetes (5), and the presence of autoantibodies against known beta-cell autoantigens are found in more than 90%

of individuals with newly diagnosed type 1 diabetes (6). Type 1 diabetes is a polygenic disease (7) with unknown environmental triggers.

Insulin or insulin analogue treatments are the main approach for treating type 1 diabetes and some cases of type 2 diabetes. While exogenous insulin can be a life-saving cure for people, insulin injections do not mimic the fine control of physiological blood glucose levels mediated by intact islets. As a result, complications such as cardiovascular disease, kidney disease, and nerve damage can occur (1). Furthermore, potential fatal hypoglycemic episodes can happen when the action of insulin cannot be decreased once blood glucose levels are lowered. Insulin pumps and continuous glucose monitoring have been developed in order to improve glycemic control; however, fluctuations in blood glucose beyond the physiological range are still common (reviewed in (8) and (9)). This has led researchers to focus on treatment options that would mimic the pattern of physiological insulin secretion which would allow for optimal glycemic control.

Islet transplantation

The pancreas is divided into two components: the exocrine component containing acinar and ductal tissue and the endocrine component which is made up of Islets of Langerhans. The pancreatic islet consists of the hormone-producing alpha-, beta-, delta-, epsilon-, and PP-cells which secrete glucagon, insulin, somatostatin, ghrelin, and pancreatic polypeptide, respectively, into the surrounding vasculature system. In 2000, a breakthrough development with an improved islet transplantation protocol successfully induced insulin independence in patients with long standing type 1 diabetes (10). Patients with implanted cadaveric islets displayed near-optimal glycemic control and were protected against severe hypoglycemic events (10). The latest trials report that ~50% of adult patients remained independent of exogenous insulin 5 years after islet

transplantation (11). Ongoing research focusing on new methods including the use of biomaterials, encapsulation techniques, and improving vascularization are being conducted to improve islet transplantation (reviewed in (12–14)). However, the limited supply of cadaveric islets creates a major limitation for this method of cell therapy. This has fueled efforts into finding a readily available supply of beta-cells.

Pluripotent stem cell therapy

Derivation of beta-like cells from human pluripotent stem cells (whether embryonic stem cells (ESCs) or induced pluripotent stem cells (iPSCs)) are a promising source for cellular replacement therapy. Human pluripotent stem cells (hPSCs) have the capacity to differentiate into cells of all somatic lineages. The last few decades of islet biology and pancreatic development research have allowed an understanding of the factors that are important for the efficient and rapid differentiation of hPSCs into pancreatic insulin-producing cells (15–20). However, the function of these hPSC-derived beta-like cells differ significantly from that of primary beta-cells as they exhibit higher basal insulin secretion and poor glucose-stimulated insulin secretion (GSIS) *in vitro* (15–20). Interestingly, hPSC-derived hormone-producing cells become glucose-responsive after implantation in rodents, suggesting the need for additional factors to drive the maturation of these cells *in vitro* (17,19,20). A detailed analysis of cellular and molecular signalling events at each step of pancreatic endocrine differentiation and maturation could improve differentiation protocols. *In vivo* systems are therefore ideal for identifying the relevant differentiation mechanisms.

Endogenous beta-cell regeneration in humans

While restoration of beta-cell mass can be achieved through exogenous cell sources such as differentiation of hPSCs into beta-cells, stimulation of endogenous repair mechanisms offers an alternative strategy to replace lost beta-cell mass. There is some evidence to suggest that there is regeneration of the endocrine pancreas in humans. For example, while the majority of beta-cells are destroyed during type 1 diabetes, studies have shown that patients with long term type 1 diabetes have detectable C-peptide levels and endogenous insulin secretion (21–24). The secretion of C-peptide increases after a meal, indicating the presence of functional beta-cells in these individuals (21). Moreover, insulin-immunoreactive cells have been found in patients with type 1 diabetes in spite of on-going apoptosis (24,25), and increases in beta-cell proliferation in patients with newly onset type 1 diabetes compared to age matched controls suggest the occurrence of endogenous beta-cell regeneration (26). Patients with type 2 diabetes have a modest reduction in beta-cell mass (0-65%) at the time of onset (27,28) and there is good evidence to suggest that there is an eventual loss of beta-cells in patients with type 2 diabetes (27,29). Scattered endocrine cells appear throughout the exocrine pancreas in patients with type 2 diabetes, suggesting possible beta-cell regeneration in these individuals (30). Hence, finding mechanisms to stimulate or augment endogenous beta-cell regeneration may provide promising future directions in type 1 and type 2 diabetes treatments.

1.2 Pancreas development

1.2.1 Morphogenesis and patterning of the pancreatic endoderm

Decades of research using rodent, zebrafish, frog, and chicken embryos have helped uncover critical molecular and morphological events that regulate pancreatic development. Pancreatic development begins with the specification of definitive endoderm. Molecular signals,

in particular the TGF-beta family member Nodal, induces the formation of Sox17, FoxA2 co-expressing endodermal tissue (31–34). The resulting endodermal tissue can be patterned into oesophagus, lungs, thyroid, thymus, stomach, pancreas, liver, and intestine (35). The endodermal regions destined to become the dorsal and ventral pancreas are specified through various secreted molecules. Retinoic acid (RA), Sonic Hedgehog (SHH), and fibroblast growth factor (FGF) signalling from the paraxial mesoderm and notochord allow for patterning of the dorsal pancreatic endoderm, while FGF and bone morphogenetic protein (BMP) signalling from the cardiac mesoderm and mesenchyme affect the patterning of ventral pancreatic endoderm (36–43). These factors induce the expression of *Pdx1*, a transcription factor that is required for the production of pancreatic tissue in rodents and humans (44–48). Despite the difference in signals that initiate dorsal and ventral pancreatic bud development, both buds give rise to exocrine and endocrine cells (49). In successive developmental stages, growth and rotation of the gut causes the fusion of the dorsal and ventral pancreas at embryonic day 12.5 (E12.5) in mice (50) (Figure 1-1).

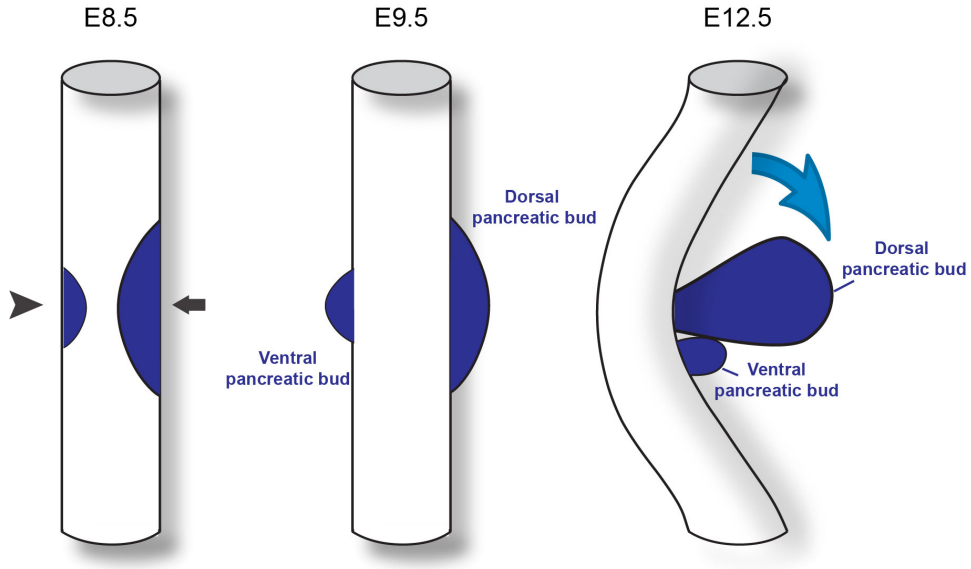

Figure 1-1 Development and rotation of the pancreatic buds

At E8.5, signals from the notochord and dorsal aorta are important for the induction of Pdx1 (blue) in the region that will give rise to the dorsal pancreatic bud (arrow), while signals from the vitelline vein and inhibition of BMP signalling is important to specify the ventral bud (arrowhead). At E9.5, the dorsal and ventral pancreas buds begin to form. At E12.5, gut rotation causes the ventral and dorsal pancreatic buds to fuse.

During the early development of the pancreatic epithelium, endocrine cells emerge in two waves of differentiation, both initiated by *Neurog3* (*Ngn3)* expression which is necessary for commitment to the endocrine fate in rodents and humans (51–53). In mice, the first endocrine cells appear during early branching morphogenesis (called the 'primary transition') at E9.5. Most of these primary endocrine cells are glucagon-expressing cells. Insulin-expressing cells appear at E10.5-11.5 and often co-express glucagon (54–57). This primary wave of alpha-cells and beta-cells are not robustly proliferative and hence are thought to not significantly contribute to mature islet cell mass (55,57). At E12.5, the epithelium undergoes a massive wave of expansion and differentiation termed the 'secondary transition' (49,58). This extensive growth allows for the formation of a complex tubular epithelial system which regionalizes into multipotent 'tip' and bipotent 'trunk' domains (59). The PTF1a+ multipotent 'tip' progenitor cells fuel branching until their fate becomes restricted to acinar cell differentiation around E14.5 (60). The SOX9+/HNF1B+/NKX6-1+ bipotent 'trunk' cells are destined to differentiate into ductal or endocrine fates. NGN3+ cells located in the 'trunk' region delaminate and differentiate into endocrine cells (51). Endocrine differentiation during the secondary transition is thought to make the majority of endocrine cell mass. While mice have two waves of endocrine differentiation, in humans, there is no evidence for two waves of endocrine cell development (61,62). Insulin-expressing cells are the earliest observed endocrine cell type in humans, suggesting some species differences in pancreatic endocrine development (63).

After *Ngn3* expression, pro-endocrine cells delaminate from the trunk into the mesenchyme and trigger downstream endocrine genes such as *Pdx1, Nkx6-1, Sox9, Nkx2-2, NeuroD1, Pax4, Arx,* and *Pax6* which orchestrate the formation of the five individual endocrine cell types (alpha-, beta-, delta-, epsilon- and PP-cells) present in adult islets (49). Significant increases in beta-cell mass and formation of large islet aggregates occurs during the postnatal stages (64). The expansion in beta-cell mass during the postnatal stages is mostly attributed to beta-cell proliferation (65–68).

1.2.2 Vasculature instruction during pancreas development

While the primary function of the circulatory system in the adult pancreas is the exchange of nutrients, gases, and wastes, endothelial cells also play a critical role in pancreas development. From E8.75-E9.5 in mouse, the fusing aorta is adjacent to the dorsal pancreatic bud. Early studies using recombination assays with isolated E8.25 embryonic tissues revealed that the induction of *Pdx1* expression was dependent on signals from endothelial cells (69). Later studies revealed that endothelial cells are necessary to maintain the FGF10-producing mesenchyme which is required for proliferation of the *Pdx1*-expressing progenitor cells, the induction of PTF1a, and dorsal pancreas budding (70–73).

Not only are signals from the endothelial cells important in initiating early pancreas development, but the blood it carries also may constitute sources of signals (74,75). For example, oxygen has been proposed to be an important factor in endocrine differentiation. There is a correlation between the appearance of blood perfused vessels and endocrine cell differentiation during the secondary transition (74). Moreover, embryos from pregnant rats exposed to a hypoxic environment (8% O_2) from E13.5-E14.5 exhibited significantly reduced *Ngn3* expression in

comparison to embryos from the control pregnant rats exposed to a normoxic environment (21% O_2) (75), suggesting the importance of oxygen in endocrine cell differentiation.

In addition to pancreas specification, developmental crosstalk between vessels and pancreatic epithelium is important at later development stages to control pancreas outgrowth and islet innervation. Overexpression of vascular endothelial growth factor A (*VegfA*) in the developing mouse pancreas resulted in pancreas hypervascularization, reduced pancreas branching and growth, deficient formation of exocrine and endocrine cells, and increased islet innervation (76–78). Conversely, hypovascularization using pancreas specific knockdown of *VegfA* or Vegf-blocking drug SU5416 resulted in increased pancreas branching and growth, excessive differentiation of endocrine and exocrine fates, and decreased islet innervation (76–78). Crosstalk between blood vessels and islet cells is also important in the adult rodent pancreas. Rodent pancreatic islets have a dense capillary network which allow for efficient sensing of blood glucose and proper secretion of hormones. Reductions of islet vasculature by a pancreas specific knockout of *VegfA* leads to defects in blood glucose homeostasis in adult mice (79,80). In addition, endothelial cells supply beta-cells with a vascular basement membrane which produce factors such as laminin and vascular collagen IV which are necessary for proper insulin expression and secretion, as well as beta-cell proliferation and survival (69,79–81). Altogether, it is evident that the vasculature is an important signalling center during murine pancreas organogenesis and tissue homeostasis.

While research of human pancreas development has been limited to developmental 'snapshots', studies have shown that endothelial cells begin to associate with small endocrine cell clusters at gestation week 10 (G10w) (82), and developing vessels penetrate the fetal islets by G14w (82,83), suggesting a possible interaction between these cell types during prenatal pancreas

development. Adult human islets have fewer blood vessels than mouse islets (84). The physiological implications of the differences between mouse and human islet vessel architecture are not known.

Despite the differences in islet vessel architecture, understanding the interplay between endothelial cells and islet cells will likely have implications in replacement strategies for diabetes. For example, co-culturing either isolated adult mouse or human islet tissues with vascular endothelial cells or human mesenchymal stem cells generated pancreatic islet-organoids which when transplanted into diabetic mice, significantly improved the survival compared to conventional islet transplantation (85). hESC-derived pancreatic progenitor cells transplanted into a pre-vascularized subcutaneous site in diabetic animals reached euglycemia within 100 days, while the majority of diabetic mice with transplanted hESC-derived pancreatic progenitor cells in a non-pre-vascularized subcutaneous site remained hyperglycemic post-transplant (86), suggesting the importance of vascularization in cell therapy.

Blood vessels may also play an important role in beta-cell regeneration and diabetes pathogenesis. In adult mice, short term overexpression of *VegfA* in beta-cells resulted in islet hypervascularization, increased beta-cell proliferation, and protection from alloxan mediated beta-cell death (87). In addition, there is evidence to support that islet endothelial cells may also develop a dysfunctional phenotype that can contribute to age related beta-cell dysfunction (88,89) as well as beta-cell loss in diabetes (90). In patients with type 2 diabetes, capillary thickening, capillary fragmentation, and increased vessel density in islets have been observed (84). These intra islet vessel changes were associated with amyloid deposition (84), which can subsequently exacerbate beta-cell loss and dysfunction. Dissecting the signals and dynamics of endothelial cells and islet

cells may have profound implications in the development of effective cell and regenerative therapies for diabetes.

1.2.3 Beta-cell heterogeneity

Molecular and functional heterogeneity

Recent studies have revealed molecular heterogeneity between insulin-expressing cells, including variations in gene expression in mice and humans (91–100). Functional variability among dispersed primary beta-cells has been identified by measurements of glucose-induced redox state (101), calcium signalling (102), biosynthetic activity (103), and insulin secretion (104). These beta-cell subpopulations could reflect a temporal cross-section through a cell population that are at different stages in their life cycle. Indeed, single cell RNA sequencing of rodent neonatal and juvenile beta-cells revealed that heterogeneity reflects distinct cell-cycling phases and maturation states (105). Molecular and functional heterogeneity may also be a result of aging (106–110) or may reflect natural fluctuations in gene expression which can occur throughout the lifetime of adult beta-cells (94,111,112). For example, fluctuations in GFP fluorescence in *Ins2*$^{GFP/+}$ isolated beta-cells have been observed, indicating the dynamic transcriptional activity at the *Ins2* promoter (112).

Exposure to endogenous and exogenous cues can further lead to changes in molecular signature. Beta-cells in patients with type 2 diabetes have increased ER stress markers (113). A model of chronic hyperglycemia in mice caused beta-cell dedifferentiation, observed by the expression of immature endocrine markers in a subset of beta-cells (114). Beta-cell dedifferentiation has also been suggested in humans with type 2 diabetes as an increase in beta-cell transcription factors in glucagon-expressing cells and somatostatin-expressing cells have been

observed (115,116). These results suggest that the beta-cell transcriptome can change under pathophysiological conditions.

An alternative hypothesis is that distinct molecular signatures represent beta-cell subpopulations with specialized phenotypes. Recent identification of pancreatic hub leader cells provides support of this latter hypothesis (117). Pancreatic hub cells express higher levels of GCK and GLUT2 than the more populous follower beta-cells allowing them to sense glucose faster and coordinate Ca^{2+} synchronization for insulin secretion. Silencing hub cells via the light-gated Cl^{-} pump, halorhodopsin, abolished Ca^{2+} synchronization and reduced insulin granule exocytosis from isolated islets, suggesting that hub beta-cells represent a functionally distinct population of beta-cells (117). Another report has found a subpopulation of beta-cells that are multipotent. This subpopulation of beta-cells express insulin and low levels of GLUT2 and can form islet and neural cells in culture (97). The concept of specialized beta-cell populations has considerable implications on the understanding of beta-cell differentiation. Understanding how subpopulations arise and if they are functionally differently may offer valuable knowledge for the ongoing research of hPSC-derived beta-cells.

Beta-cell heterogeneity during development

Regional differences exist at the earliest stage of fetal development. The pancreas is formed from the dorsal and ventral pancreatic buds. Because of their anatomical position during development, different signals induce the dorsal and ventral pancreatic buds (36–40). For example, signals such as RA from the lateral plate mesoderm and FGF2 and activin secreted by the notochord are necessary for dorsal pancreatic bud induction (38,41,42). FGF signalling from the cardiac mesoderm inhibits the formation of ventral pancreatic bud (43). Signals from the aortic

endothelium induce formation of the *Pdx1* and *Ptf1a*-expressing dorsal pancreatic bud, whereas development of the ventral pancreas is not dependent on cues from the endothelium (69,71).

Differences in islet cell composition are found between dorsally and ventrally derived islets. Islets derived from the ventral pancreatic bud (which gives rise to the inferior part of the head and the uncinate process of the pancreas) have more pancreatic polypeptide cells but fewer alpha- and delta-cells than the dorsal bud (which gives rise to the superior part of the head, the body, and the tail of the pancreas) in both rodents (118–120) and humans (121,122). Differential beta-cell responses to the disruption of *Isl1,* in which *Isl1* mutant mice display dorsal pancreatic bud agenesis and loss of the first wave of endocrine cells while the ventral pancreatic bud is still able to form, provide additional evidence for beta-cell heterogeneity during development (123).

There are also variations in islet blood supply and innervation dependent on ontogeny. Blood supply for the dorsal bud is supplied by the coeliac artery and innervated by the coeliac ganglion, while the ventral bud receives blood via the mesenteric artery and receives innervation from the superior mesenteric ganglion (124). These variations in innervation and blood supply as well as developmental ontogeny may promote functional differences between beta-cells. For example, rat islets in the pancreatic tail are found to have higher rates of stimulated insulin biosynthesis and secretion than islets located in the head of the pancreas (119,125). Higher rates of beta-cell proliferation are observed in the splenic region compared to the duodenal and gastric regions of the pancreas (120). More recently, a higher percentage of mature beta-cells was observed in the tail of the pancreas in comparison to the head (93). Interestingly, the loss of beta-cells was more prominent in the head region than the tail region of the pancreas among patients with type 2 diabetes (126).

At the islet level, location of the beta-cells could also lead to functional heterogeneity. For example, homologous contacts between beta-cells potentiates insulin secretion when compared to single beta-cells in both rodents and humans (127–129). Increased insulin secretion is observed between alpha- and beta-cell contacts (128,129), but not delta- and beta-cell contacts (129,130). In addition, not all beta-cells receive axon terminals (131) and differences in the proximity to capillaries, which carry nutrients and oxygen, may be additional causes of molecular and functional variances.

Collectively, beta-cell heterogeneity exists with differences extending from the islet level to regional differences at the organ level. Identifying and characterizing the subpopulations, such as populations that are more susceptible to metabolic stress or have an increased replicative and/or functional capacity, can have a profound impact on beta-cell replacement and regenerative therapies.

1.3 Beta-cell regeneration

1.3.1 Models of pancreas regeneration

While cell therapies offer a viable path for a cure to diabetes, research has also focused on expanding the existing beta-cell population in patients with lost beta-cell mass. Much of the regeneration studies have utilized rodent injury models, including surgical injury models, chemically induced beta-cell injury models, or genetic models to ablate the beta-cells.

Surgical injury models

In pancreatectomy, an ablation method that involves surgical removal of up to 90% of the pancreas, mice and rats show tissue growth and sprouting at the cut site (132–134). Significant

increases in beta-cell proliferation and beta-cell mass have been documented in both 90% pancreatectomy and less extensive pancreas resections (40-60%) (133–139). Other studies have also reported beta-cell neogenesis in pancreatectomized rodents (134,139–141). Similarly in humans, rare pancreatectomy cases in children have suggested tissue growth at the cut site (142). However, this regenerative capacity declines sharply in older pancreatectomized animals (143–145) and is absent in adult humans (146).

Pancreatic duct ligation (PDL) is another surgical injury model used to study pancreas regeneration. PDL mimics obstructive pancreatitis by stimulating massive acinar destruction. While beta-cell neogenesis after PDL has been proposed (147), more recent studies have shown that non-beta-cell progenitors do not contribute to the beta-cell lineage, nor is there a significant increase in beta-cell mass or proliferation after PDL (65,148,149). Despite minimal beta-cell regeneration, *Ngn3*, a critical transcription factor during pancreatic mammalian development and a hallmark for fetal pancreatic endocrine progenitors, is significantly upregulated in the pancreas after PDL (147–149), possibly suggesting the activation of developmental pathways.

Chemically induced beta-cell injury models

In another injury rodent model, beta-cell destruction is achieved through the administration of chemical toxins such as alloxan or streptozotocin (STZ). These compounds structurally mimic glucose and are imported into the beta-cells. High dose of STZ or alloxan results in beta-cell destruction and renders the animals diabetic (150,151). Increases in proliferating insulin-expressing cells and non-beta-islet cells shortly after high dose STZ administration have been reported (152–156). Interestingly, more robust levels of regeneration have been shown in STZ-treated neonatal rats which reach normoglycemia within 6 weeks (152). In addition, autoimmune

diabetic NOD mice have significantly increased levels of beta-cell proliferation after STZ treatment compared to non-diabetic NOD mice after STZ (157,158). These results suggest that beta-cell regeneration may be dependent on multiple factors such as age and genetic background.

Genetic ablation of beta-cells mediated by diphtheria toxin has also been used to study beta-cell regeneration. In this method, the beta-cell specific expression of the diphtheria toxin receptor results in beta-cell destruction upon addition of the diphtheria toxin (159,160). This method kills >95% of beta-cells and under this extreme regenerative loss, transdifferentiation of alpha- and delta-cells have been observed (159,160). Interestingly, the delta-to-beta-cell transdifferentiation was only observed in neonatal mice, while alpha-to-beta-cell transdifferentiation is observed in adult mice, suggesting that age may be an important factor in determining cell plasticity and the mechanism of beta-cell regeneration (159,160).

1.3.2 Regeneration of beta-cells by induced proliferation

While the proliferative capacity of adult beta-cells is low and declines rapidly with age (107,108,161–164), under certain physiological stresses such as pregnancy, obesity, or insulin resistance, beta-cell proliferation is significantly increased (120,165–169). During pregnancy, rodent beta-cell mass significantly increases, stimulated largely by the pregnancy hormones placental lactogen and prolactin (170,171). Under high fat diet induced obesity or under experimental models of induced insulin resistance such as the insulin receptor liver-specific knockout mice, significant increases in beta-cell proliferation and mass have been found (120,166–168). Proliferation can also be stimulated in various regenerative rodent models such as the STZ-induced diabetes model (152,156). Interestingly, beta-cells of old mice readily proliferate when

exposed to a young environment (89), suggesting that extrinsic factors can stimulate beta-cell proliferation.

In humans, very few replicating adult beta-cells can be found under physiological and pathophysiological conditions (164,172,173); however, some beta-cell proliferation can be stimulated. Human transplanted beta-cell grafts exhibit significant increases in proliferation in *ob/ob* and high fat diet fed obese mice compared to lean mice, suggesting that human beta-cells can respond to overnutrition *in vivo* (144,174). Indeed, hyperglycemia stimulates beta-cell proliferation *in vivo* in a variety of model systems including human transplanted beta-cell grafts in mice (167,175–177). Various growth factors that simulate Nodal or Wnt signalling pathways can promote human beta-cell proliferation *in vitro* (178,179). The inhibition of DYRK1A has also been shown to stimulate human beta-cell proliferation (180). Moreover, this increase in beta-cell proliferation by DYRK1A inhibitors was potentiated with GLP-1 agonists (181). These results highlight the proliferative potential of human beta-cells. Identifying factors that augment or stimulate proliferation may help replace lost beta-cell mass in patients with diabetes.

1.3.3 Reprogramming of pancreatic endocrine cells into beta-cells

Transdifferentiation, the conversion of a differentiated cell type into another cell type, is rare if at all absent under normal physiological conditions. However, lineage tracing studies have shown that under certain stressors such as models of extreme beta-cell loss in rodents, alpha-cells and delta-cells can convert into insulin-expressing cells (159,160), In humans, an increase in the frequency of polyhormonal cells have been found in patients with type 2 diabetes (115) and nondiabetic insulin resistant subjects (182), possibly suggesting cell transdifferentiation. Alternatively, these polyhormonal cells could also represent dedifferentiated beta-cells (114,183).

Genetic manipulation of non-beta-cells can result in their conversion into insulin-expressing cells. For example, *in vivo* ectopic expression of *Pax4* in alpha-cells or delta-cells resulted in their conversion to glucose responsive beta-cells (184,185). Inhibition of *Arx* expression or inhibition of *Arx* in combination with DNA methyl transferase 1 (*Dnmt1*) in alpha-cells can reprogram alpha-cells into glucose responsive beta-cells (186,187). In humans, overexpression of *PDX1* and *MAFA* can convert human alpha-cells and PP-cells into insulin-producing cells (188). Moreover, the reprogrammed human alpha-to-beta-cells were able to restore normoglycemia in mice with STZ-induced diabetes, providing evidence for human islet cell plasticity (188). Although more research is needed to understand the precise control of cell transdifferentiation, islet cells represent endogenous cell sources that may be reprogrammed into functional beta-cells.

1.3.4 Reprogramming exocrine tissue into beta-cells

The acinar cells provide an attractive cell source given that it makes up >90% of the pancreas. Transdifferentiation of acinar cells to beta-cells is rare under physiological conditions; however, under regenerative pressures, the conversion of acinar cells into insulin-expressing cells was observed in PDL-induced mice (189). Acinar-to-beta-cell transdifferentiation was also observed in alloxan induced diabetic mice and this conversion was enhanced by administration of epidermal growth factor and ciliary neurotrophic factor (190). In addition, adenoviral mediated overexpression of *Ngn3, MafA*, and *Pdx1* in rodent exocrine cells leads to the downregulation of exocrine specific genes and the expression of insulin *in vitro* and *in vivo* (191–193). Moreover, these converted beta-like cells were able to reverse diabetes in STZ-treated NOD-SCID (non-obese diabetic severe combined immunodeficiency) mice (191) and STZ-treated immunodeficient *Rag*

knockout mice (193). The mechanism of acinar-to-beta-cell conversion is uncertain, although some work suggest that acinar-to-beta-cell reprogramming is dependent on euglycemia (194), while another report suggests a role of inflammation and macrophages (195). Isolated human exocrine tissue can also be reprogrammed to islet-like cells by adenoviral overexpression of *PDX1, NGN3, MAFA* and *PAX4* in combination with growth factors (196). Collectively, these studies suggest acinar cell plasticity in mice and humans.

Pancreatic ductal cells are also a potential source of beta-cells. Given the developmental model of islet genesis, ductal cells are a logical cell source to convert into beta-cells. Under physiological conditions, lineage tracing experiments reveal that there is limited conversion of pancreatic ducts to beta-cells in the adult pancreas (65–68). However, under certain regenerative conditions, some studies have proposed the formation of new beta-cells from ductal cells (66,147,197–199). For example, an increased frequency of *Ngn3*-expressing cells and *Pdx1*-expressing cells along pancreatic ducts have been reported in PDL and pancreatectomy respectively (147,197), suggesting the activation of endocrine transcriptional pathways in ductal cells. Another report observed rare insulin-expressing cells located on the pancreatic ducts during pancreatectomy in rats (140). Moderate hyperglycemia with low dose growth factors or inflammatory cytokines have also been shown to promote the formation of endocrine cells from ducts (198,199). However, lineage tracing studies of ductal cells using *Sox9* (65), *Hes1* (68), *CAII* (66), *Hnf1b* (67), or *Muc1* (200) promoters in the adult pancreas or during adult beta-cell regeneration have demonstrated limited evidence for ductal cell contribution to endocrine cell mass. It is worth noting that some of the ductal cell lineage tracing models had low recombination efficiencies (20-40%) which could make it difficult to detect small amounts of duct-to-beta-cell conversion.

In humans, insulin-positive cells expressing ductal markers such as *CK19* were found in graphs of purified duct cells (201), and increases in CK19, insulin co-positive cells have been observed in insulin resistant subjects (182,202). Moreover, *in vitro* expansion of human ductal tissue have been observed to form islet structures (203,204). Another study found the induction of *NKX6-1* (an endocrine cell specific transcription factor in adult beta-cells) on ductal cells in human islet grafts implanted underneath the kidney capsule in mice (174). In addition, adenoviral overexpression of transcription factors *NGN3, PAX6, MAFA,* and *PDX1* in both human and rodent ductal cells induced formation of islet-like clusters (205,206). These results suggest that the exocrine tissue in rodents and humans may serve as possible beta-cell sources, although more research is needed to understand and control the mechanism of transdifferentiation in order to develop effective and replicable clinical approaches.

1.3.5 Reprogramming endoderm-derived tissues into beta-cells

Genetic manipulation of endodermal tissue into beta-cells also demonstrates their cellular plasticity (207). For example, *FoxO1* ablation in *Ngn3*-expressing enteroendocrine cells in mice converted gut cells into glucose responsive insulin-expressing cells (208). Overexpression of *Ngn3, MafA*, and *Pdx1* in rodent liver cells *in vivo* resulted in the expression of pancreatic endocrine markers (209). Reports have also found that the overexpression of *Ngn3, MafA*, and *Pdx1 in vivo* caused ‘neo-islets’ to form in intestinal crypts (210) and the antral stomach (211). These studies highlight the use of several different cell sources that may be reprogrammed into beta-cells; however, a better understanding of cellular plasticity and the delicate regulation of cell differentiation in adult tissues is needed before possible clinical translatability.

1.3.6 Adult pancreatic stem cells

It is been hypothesized that pancreatic progenitor cells exist in the adult animal and human pancreas. Although some progenitor cell markers can be histochemically defined in the adult pancreas particularly after injury (147,197), it is unclear if these progenitor cells originate from a pancreatic stem cell population or are the result of general cell plasticity. The lack of clear pancreatic progenitor marker(s) and the uncertain location of these pancreatic stem cells make the search for pancreatic stem cells difficult.

The pancreatic duct has been proposed as a potential niche for pancreatic progenitor cells. This hypothesis is based on histological observations of single islet cells and small islets clusters embedded or in close proximity to adult pancreatic ducts, which is suggestive of the emergence of new islets cells from ducts (140,147,197). However, the majority of lineage tracing of exocrine tissue reveals limited contribution of the exocrine pancreas to endocrine cells during normal physiological conditions and under various pancreatic injury models (65–68,147,200).

Other work has suggested a progenitor population within the islet (97,212–214). Islet cells that were positive for Nestin and PDX1 but negative for endocrine hormones were able to differentiate into hormone-expressing endocrine cells *in vitro* (212). However, lineage tracing of Nestin+ cells *in vivo* and in *ex vivo* explants did not reveal contribution of Nestin+ cells to endocrine cells (215). A progenitor population of insulin-expressing cells that express low levels of *Glut2* have also been described (97,213,214). Furthermore, these rare insulin-expressing, low *Glut2*-expressing cells could form islet and neural cells in culture, suggesting the multipotent nature of this cell type (97). More recently, immature beta-cells located on the islet periphery were identified to have a similar transcriptome to endocrine progenitors and are capable of differentiating into mature beta-cells or alpha-cells (216). Future directions understanding cell fate

decisions and cell plasticity at the single cell level can provide important insights that can be harnessed to regenerate or replace beta-cell loss in diabetes.

1.4 Zebrafish as a model for beta-cell development and regeneration

1.4.1 Zebrafish as a model organism

Zebrafish has emerged as a powerful vertebrate model organism for studies relating to development and physiology. Of the protein coding genes, 71.4% of human genes have at least one zebrafish orthologue (217). Organ development is similar between zebrafish and mammals suggesting that studies in this system can have broadly applicable insights. High fecundity, rapid development, and genetic tractability in zebrafish are a few advantages of this model system. Zebrafish embryos develop *ex-utero* and are also transparent during the first week of life. Hence, they are amendable for *in vivo* imaging of developmental processes (Figure 1-2A). Zebrafish also have a remarkable ability to regenerate their organs, including the endocrine pancreas. For example, upon chemical or physical ablation of the pancreatic beta-cells in the adult animal, zebrafish are able to normalize blood glucose levels and regenerate their beta-cells in less than 3 weeks without the need for insulin therapy (218,219). The robust regenerative response of zebrafish is a distinct advantage to study beta-cell renewal in this model.

1.4.2 Zebrafish pancreas morphology

The zebrafish pancreas consists of islets scattered throughout the exocrine tissue. The exocrine tissue runs along the intestinal tube. The exocrine structure is similar to that of mammals: acinar tissue secrete digestive enzymes into the pancreatic ducts which form a complex branched network that is connected to the intestine and the hepatic ducts through the hepatopancreatic ductal

system (220). The adult zebrafish pancreas consists of one principal islet with smaller secondary islets (ranging from several endocrine cells to hundreds of endocrine cells) in addition to single endocrine cells scattered throughout the body of the pancreas (Figure 1-2B). The zebrafish pancreas contains all 5 hormone secreting cells-types. A dense vasculature and innervation network are present in the adult islets (221–224), similar to rodent islets.

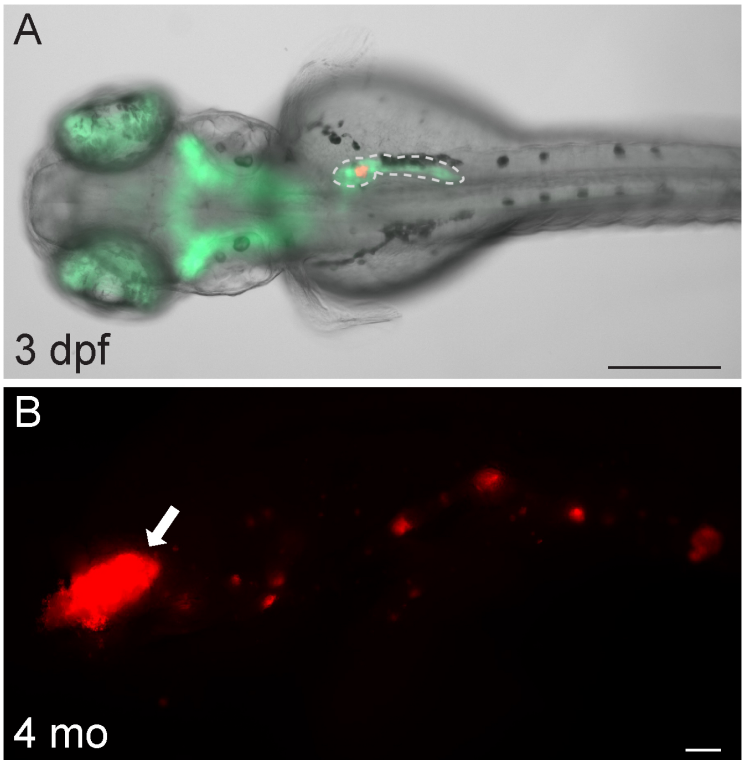

Figure 1-2 Zebrafish pancreas morphology
A) A *Tg(ptf1a:GFP ; ins:TagRFP)* zebrafish larvae at 3 days post fertilization (dpf) shows pancreatic beta-cells (red) and *ptf1a*+ tissue (green). Exocrine pancreas is outlined in white dotted lines. Scale bar = 200 µm. **B)** An adult zebrafish with a principal islet (arrow) and secondary islets in a 4 month old *Tg(ins:TagRFP)* fish. Scale bar = 200 µm.

1.4.3 Zebrafish pancreas development

Similar to the mammalian system, the zebrafish pancreas forms from two pancreatic buds which develop from the *pdx1*-expressing posterior foregut endoderm (225). The first endocrine

cells to appear are insulin-expressing cells at 14 hours post fertilization (hpf), followed by somatostatin-expressing cells at 17 hpf, and glucagon-expressing cells at 21 hpf (221,225,226) These cells form the dorsal pancreatic bud which is clearly discernable at 24 hpf, when the endocrine cells have coalesced into the principal islet (221,225). The *ptf1a*+ ventral pancreatic bud begins to emerges at 32 hpf (225). Around 52 hpf, the gut rotates and the principal islet becomes engulfed by the ventral pancreatic bud (225). The use of *heart and soul* mutant zebrafish embryos, in which the pancreatic buds do not fuse, have shown that the dorsal pancreatic bud gives rise to exclusively endocrine cells, while the ventral pancreatic bud generates ductal, acinar, and endocrine tissue (225). Beta-cells from the dorsal pancreatic buds are largely non-proliferative during early embryonic development (226), and hence, it is thought that the beta-cells originating from the ventral pancreatic bud give rise to the majority of adult beta-cells in the adult zebrafish (226). The principal islet contains endocrine cells originating from the dorsal and ventral pancreatic buds, while the secondary islets which begin to emerge at 120 hpf along the length of intrapancreatic duct (IPD) originate from the ventral pancreatic bud (Figure 1-3). The secondary islets arise from a population of pancreatic progenitors, the Notch-responsive cells, within the IPD (227). These Notch-responsive cells also persist in the adult zebrafish pancreas as centroacinar cells which are located in a terminal duct position within the lumen of the acinus (227,228).

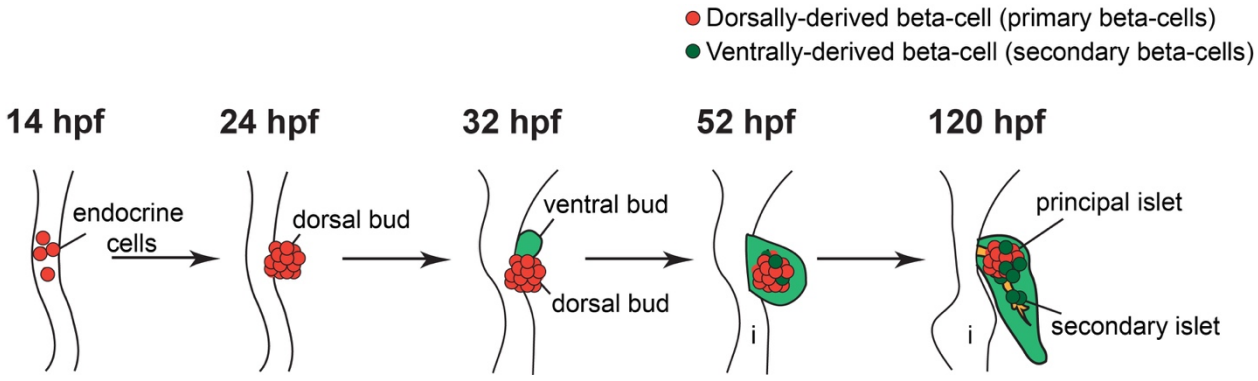

Figure 1-3 Endocrine pancreas development in zebrafish
The first endocrine cells begin to form at 14 hours post fertilization (hpf) (red). By 24 hpf, the endocrine cells are clustered into a principal islet and solely make up the dorsal pancreatic bud. The ventral pancreatic bud emerges at 32 hpf. The dorsal and ventral pancreatic buds fuse by 52 hpf and early ventrally-derived endocrine cells (dark green) begin to appear. Secondary islets, derived from the ventral pancreatic bud, begin to appear after 120 hpf along the intrapancreatic duct (yellow). i = intestine

Molecular signals and transcription factors involved in zebrafish pancreas development

Many of the molecular signals that are important in specifying mammalian pancreatic tissue are necessary in zebrafish pancreas development as well. TGF-beta/Nodal signalling induces the Sox17, FoxA2 co-expressing endodermal tissue (229,230). RA, SHH, BMP, FGF signalling are important in specifying pancreatic fate (231–234). For example, zebrafish embryos deficient in RA synthesis or signalling have severely disrupted pancreas development (36), a similar phenotype to RA knockout mice which have complete dorsal pancreatic bud agenesis (41). Knockdown of *fgf10* in zebrafish severely blunts the formation of the exocrine pancreas (231), similar to the pancreatic growth defect observed in *Fgf10*-deficient mouse embryos (235). Inhibition of Bmp signalling is also needed to specify the pancreatic fate in zebrafish (233,234). Many transcription factors necessary in directing endocrine formation are shared between mouse and zebrafish (236–239) (Figure 1-4). For example, zebrafish and mouse embryos with severe or complete loss of HNF1B exhibit defects in foregut regionalization which subsequently results in dorsal and ventral pancreatic bud agenesis (240–243). Knockdown of *pdx1* in zebrafish severely impairs endocrine and exocrine pancreas formation (244,245), similar to the phenotype of *Pdx1*-knockout mice (46,47). Knockdown of *ptf1a* in zebrafish impairs endocrine and exocrine formation, although it does not affect dorsal pancreatic bud formation which is solely comprised of endocrine cells (246,247). Similarly in mice, a subset of endocrine cells appear in *Ptf1a* knockout animals; however, endocrine and exocrine development are severely compromised

(72,73), suggesting that *Ptf1a* has similar roles in mouse and zebrafish. *Sox9b* is expressed in the early zebrafish hepatopancreatic endoderm, in the anterior *pdx1*-expressing domain, which marks both the dorsal pancreas and the prospective ventral pancreas (248). *Sox9* expression in the early pancreatic rudiment is also found in the mammalian pancreas (249). Similar to *Sox9* ablation in the mouse pancreas, *sox9b* homozygous mutant zebrafish show a reduction in pancreatic ductal cells and endocrine cells (248,249). However, the formation of acinar cells in the *sox9b* mutant zebrafish are unaffected, while *Sox9* ablation in the mouse pancreas leads to a severe reduction in acinar tissue (248,249), suggesting species differences in acinar cell formation.

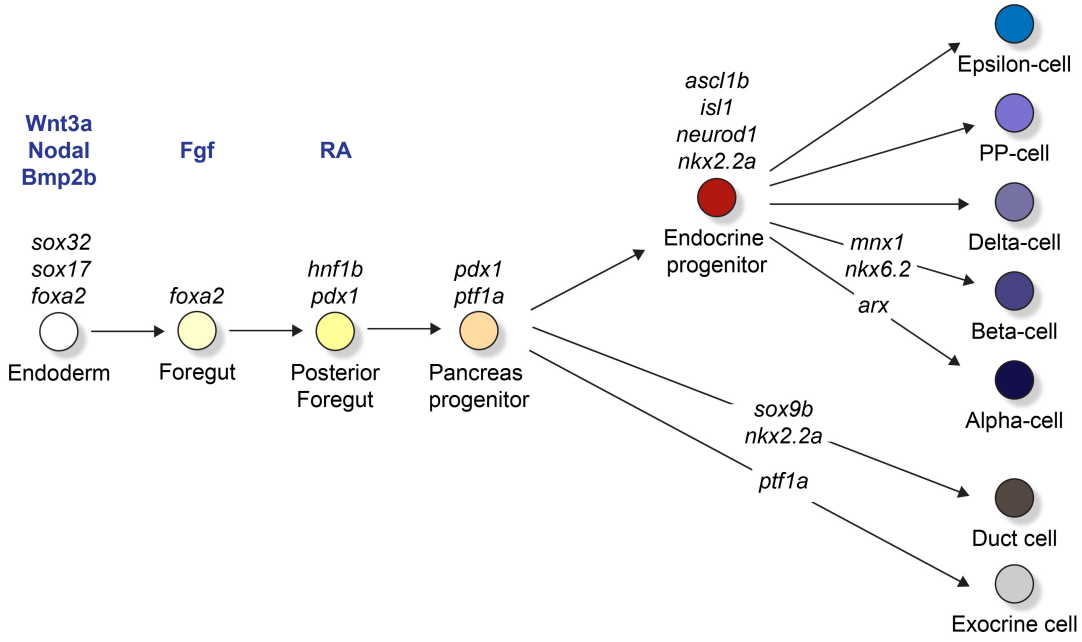

Figure 1-4 Zebrafish pancreatic cell lineages
Diagram of key secreted molecules (blue) and transcription factors (black) in regulating zebrafish pancreas development. Modified from (239).

One surprising difference in the developmental islet transcriptional cascade is *ngn3*, which while essential for endocrine cell development in mammals, is dispensable in zebrafish pancreas endocrine formation. *Ngn3* is not expressed in the developing zebrafish pancreas, and *ngn3* null mutants do not display any defects in zebrafish endocrine development (250,251). Instead, another bHLH transcription factor, *ascl1b,* works with *neurod1* to regulate endocrine formation (250). Indeed, morpholino knockdown of *ascl1b* and *neurod1* completely impairs endocrine formation - a more severe phenotype than single knockdown of *ascl1b* or *neurod1* in which some endocrine cells still form (250,252). Beyond endocrine specification, the beta-cell transcriptional factor program appears to be conserved between mammals and zebrafish. For example, *mnx1* knockdown in zebrafish display a significant reduction in the number of beta-cells (253,254), a phenotype similar to *Mnx1* mutant mice which exhibit a significant decrease in beta-cell numbers (255,256). Zebrafish knockdown studies of *nkx2.2a* (257) or *nkx6.2* (258), a homolog and functional equivalent to mouse *Nkx6-1*, show impairments in the formation of dorsally and ventrally-derived beta-cells, phenotypes similar to mouse gene knockout studies (259–261). *Pax6b* knockdown in zebrafish leads to a significant reduction in beta-cells and alpha-cells, while significant increase in the number of ghrelin-producing cells are observed (262), a similar phenotype to *Pax6* mutant mice (263).

The antagonist action of *Arx* and *Pax4* that control the ratio of alpha-cells and beta/delta-cell in mouse (264) are also important in zebrafish, albeit solely in alpha-cell formation (265). Knockdown of *arx* in zebrafish embryos leads to a significant decrease in alpha-cell number and a significant increase in *pax4* expression, similar to what is observed in *Arx* mutant mice (264). Knockdown of *pax4* causes an increase in alpha-cell number and an increase in *arx* expression; however, there is no significant alterations in beta-cell or delta-cell numbers (265), a contrast to

mouse *Pax4* mutant mice which show significant decreases in both of these endocrine cell populations (264,266).

Knockdown of *isl* genes in zebrafish results in a significant reduction in dorsal bud derived endocrine cell numbers, although ventral bud derived endocrine cells can still form (267). Similarly, gut explants of *Isl1* mutant mice display dorsal pancreatic bud agenesis and loss of the first wave of endocrine cells, although the ventral pancreatic bud is still able to form (123). Altogether, the conservation of pancreas transcriptional pathways has defined zebrafish as a unique and powerful model to investigate molecular mechanisms important in pancreatic endocrine development.

1.4.4 Beta-cell heterogeneity in zebrafish

Beta-cells arise from the dorsal and ventral pancreatic buds. The dorsal and the ventral pancreatic progenitors are specified at different developmental time points. The dorsal pancreatic bud is specified early during somitogenesis, with the first insulin-expressing cells appearing at around 14 hpf (herein termed primary beta-cells) (221,268). Progenitors destined to constitute the ventral pancreatic bud are specified after mid-somitogenesis, between 21-28 hpf (241). The ventral bud derived beta-cells (herein termed secondary beta-cells) appear later on during development around 48 hpf. Cell tracking studies have revealed that only medial cells positioned adjacent to the notochord give rise to the dorsal pancreatic bud, while cells positioned more laterally give rise to the ventral pancreatic bud, intestine, and liver (234,268), indicating that endocrine cells in the dorsal and ventral buds come from different precursor populations.

Other work additionally supports this notion that different precursor populations give rise to primary and secondary endocrine cells. A difference in proliferative activity between the two

precursor populations was demonstrated when an injection of a H2B-RFP tag at the one cell stage was able to transiently label the dorsal derived primary beta-cells but not the ventral derived secondary beta-cells (226,267). Primary beta-cells were able to retain the label for the first 12 days, suggesting limited proliferative capacity during early development. Interestingly, purification sorting of the primary beta-cells at 12 dpf led the authors to discover that primary beta-cells express increased levels of cell cycle inhibitors and decreased levels of insulin and mature beta-cell markers in comparison to secondary beta-cells at 12 dpf (226). Whether primary beta-cells represent a subpopulation of beta-cells with a distinct molecular signature in the adult pancreas is unknown. A more recent study found that both primary and secondary beta-cells were glucose responsive during early development and during the juvenile stages (269), suggesting that despite potential transcriptional heterogeneity, both populations respond to glucose. Given the difference in time of formation, the zebrafish provides a unique advantage to differentially label the dorsal bud derived primary beta-cells and the ventral bud derived secondary beta-cells.

1.4.5 Functional and molecular markers of beta-cell heterogeneity

Molecular and functional beta-cell heterogeneity has recently been described in zebrafish. One study reported a subpopulation of beta-cells expressing *anxa4* (270), while another report identified beta-cells with high NF-kB signalling activity (271). Age leads to an increase in the number of beta-cells with high NF-kB signalling activity (271), suggesting that beta-cell heterogeneity can be influenced with age. More recently, a subpopulation of leader beta-cells have been identified (272). These leader cells possess a unique transcriptional profile compared to the more populous follower beta-cells (272). Like in mice, leader beta-cells are first to exhibit a Ca^{2+} increase in response to glucose, and they coordinate the Ca^{2+} responses from follower beta-cells

(117,272). Photoablation of these leader beta-cells, but not follower cells, leads to an abolished Ca^{2+} response to glucose (272), suggesting that the leader beta-cells are a functionally distinct beta-cell population. Investigating the origin and development of these leader cells will be of great interest in furthering our understanding of beta-cell development and biology.

1.4.6 Modeling diabetes in zebrafish

Type 1 diabetes is characterized by a significant loss in beta-cell mass. Surgical, chemical, and genetic methods have been utilized in the zebrafish system to model beta-cell destruction. Using transgenic fluorescent reporter fish to mark the islets, pancreatectomy has been utilized by several groups to cause significant beta-cell loss in adult zebrafish (218,219). However, due to the technical difficulty, this method is not commonly used. Chemical ablation via STZ or alloxan are alternative ways to destroy beta-cells. Alloxan administration in zebrafish larvae has shown the selective ablation of beta-cells (273,274). Intraperitoneal injections of STZ causes significant beta-cell destruction, observed by increases in fasting blood glucose and reduced insulin levels (219,275,276). Multiple STZ injections over 4 weeks to achieve hyperglycemia leads to diabetes complications including retinopathy and impaired fin regeneration (275–277). However, the toxicity of these compounds can be a concern (278,279). Genetic models for beta-cell destruction are most commonly used in zebrafish to model beta-cell loss observed in type 1 diabetes. Several beta-cell ablation models have been created including beta-cell specific inducible expression of a truncated Bid protein, tBid (280), and the beta-cell specific expression of DTA (281). However, the most common beta-cell ablation system is the nitroreductase/metronidazole system. In this system, beta-cell specific expression of the bacterial gene *nfsB,* which encodes for the enzyme nitroreductase (NTR), converts the prodrug metronidazole (MTZ) into a cytotoxic compound

resulting in rapid beta-cell death (218,282–284). Remarkably, adult zebrafish are able to normalize blood glucose levels and regenerate their beta-cells within 3 weeks of beta-cell ablation (218,219). This rapid tissue regeneration make zebrafish an attractive model to investigate the cellular and molecular pathways involved during beta-cell renewal.

Models of type 2 diabetes in zebrafish have also been created through nutritional and genetic methods. Diet induced obesity caused by high fat diet or overfeeding leads to significant increases in body weight, adipose tissue, insulin resistance, elevated fasting blood glucose, and impaired glucose tolerance (285–288). Immersion of adult zebrafish in 2% glucose solutions leads to elevated blood glucose levels, impaired response to exogenous insulin, and diabetic complications such as retinopathy and impaired wound healing (289–291). Genetic models of insulin resistance, a major driver in type 2 diabetes, have also been created. For example, liver specific CRISPR/Cas9 knockdown of the insulin receptors (*IRa* and *IRb*) resulted in postprandial hyperglycemia (292). The transgenic expression of dominant negative *Igf1* receptor in skeletal muscle of zebrafish results in impaired glucose uptake and blunted Akt phosphorylation, indicative of impaired insulin signalling in the skeletal muscle (293). Given that insulin resistance is believed to be a major driver for type 2 diabetes, these skeletal and liver insulin resistance zebrafish models may be helpful in dissecting the progression of type 2 diabetes. Overall zebrafish is a powerful model to gain an understanding of normal physiology as well as insight into beta-cell regeneration and the pathophysiology of diabetes.

1.4.7 Zebrafish beta-cell regeneration

Relative to mammals, zebrafish have a high capacity for beta-cell pancreatic regeneration. Regardless of the ablation method used (surgical, chemical, or genetic), upon extreme beta-cell

destruction in adult zebrafish animals (>90%), blood glucose levels are restored to control levels within a week, and beta-cell mass is comparable to controls within three weeks after ablation (218,219). The mechanism of beta-cell regeneration is still unclear. Increased proliferation at the islet periphery is observed in STZ-treated adult zebrafish at 3 days post ablation (dpa) (219). In the *nfsB*/MTZ system, lineage tracing of alpha-cells in larval fish have shown alpha-to-beta-cell transdifferentiation in response to beta-cell ablation (283). This alpha-to-beta-cell conversion was further enhanced with transgenic overexpression of *igfbp1a* (294). *Sox9b* mutants, which display a significant reduction in the formation of ductal cells, exhibit blunted beta-cell regeneration in larval fish compared to controls (248), suggesting the contribution of ductal cells to beta-cell renewal in the larval model. Possible duct-to beta-cell transdifferentiation has also been suggested in adult zebrafish as there is a significant increase in the number of insulin, *nkx6.1* (ductal marker in the adult) co-expressing cells during beta-cell regeneration in the adult pancreas (295). Increases in ductal cell proliferation have also been observed during adult beta-cell regeneration (295). More recently, lineage tracing of centroacinar cells (CACs), a specialized type of ductal cells, revealed that 43% of new beta-cells arise from CACs after *nfsB*/MTZ mediated beta-cell ablation (218).

The role of proliferation during beta-cell regeneration is not clear. Similar to rodents, zebrafish beta-cell proliferation in adult animals is low (~1%) (271). BrdU or EdU labelling during regeneration shows increases in beta-cell proliferation in regenerating islets (218,282). However, it is unclear if these proliferating beta-cells come from pre-existing beta-cells or their precursors. Staining for proliferative markers during STZ-induced adult beta-cell ablation revealed *pdx1*+ cell proliferation, but not insulin+ cell proliferation (219). Lineage tracing of pre-existing beta-cells during beta-cell regeneration would help define the contribution of beta-cell proliferation during beta-cell renewal. It is possible that the type of regenerative method (proliferation,

transdifferentiation, or neogenesis) may be dependent on a number of factors including ablation method, extent of ablation, and age (larvae versus adult). In addition, a combination of regenerative methods may be important in restoring beta-cell mass. Understanding the cell sources that are responsible for zebrafish beta-cell development will allow for a better understanding of the regenerative mechanism(s) used by this model and possibly lead to insights into activating and/or stimulating these cell sources in mammalian beta-cell renewal.

1.5 Thesis investigation

Zebrafish have emerged as a powerful model to study beta-cell development and regeneration, and the similarity in pancreas development programs between zebrafish and mammals suggests that studies in this model system can have broadly applicable insights. This thesis will provide insight into zebrafish beta-cell development and regeneration in three main data chapters – characterizing primary and secondary beta-cells arising from the dorsal and ventral pancreatic bud (Chapter 2), determining the role of endothelial cells in early beta-cell development (Chapter 3), and investigating the new sources of beta-cells during physiological and regenerative conditions (Chapter 4).

Our first aim was to determine the contribution of beta-cells arising from the dorsal and ventral pancreatic bud to adult beta-cell mass and investigate if transcriptome differences exist between these two populations of pancreatic beta-cells, which has not been previously addressed in the adult zebrafish. The zebrafish is a good model to study beta-cells arising from different pancreatic buds as dorsally-derived and ventrally-derived beta-cells arise at different timepoints during development. We created a Cre/LoxP lineage tracing model to label primary and secondary beta-cells into adulthood, and we subsequently investigated the transcriptomes of the two

populations of beta-cells using single cell RNA sequencing in the adult animal. Second, we aimed to investigate the angiogenic factors necessary for islet vascularization which has not been previously identified in zebrafish. We used genetic and pharmacological means to inhibit Vegf signalling and consequently endothelial cell formation during early endocrine development. We characterized early alpha-cell and beta-cell formation in vessel deficient animals. Finally, we sought to determine the new sources of beta-cells during physiological and regenerative conditions. While previous research has utilized lineage tracing models for non-beta-cells, we utilized our Cre/LoxP lineage tracing model to lineage trace pre-existing beta-cells to assess their contribution to beta-cell mass during normal physiology and beta-cell regeneration. Collectively, the studies in this thesis allowed for the development of a useful genetic tool to lineage trace beta-cells, provide insight into beta-cells arising from the dorsal and ventral pancreatic bud, elucidate the angiogenic factors necessary for islet vascularization and the role of endothelial cells in early beta-cell development, and clarify the new sources of beta-cells during aging and regeneration. These findings highlight the zebrafish as a model to study beta-cell development and regeneration.

Chapter 2: Primary and secondary beta-cells contribute to principal islet mass and they share similar transcriptional profiles

2.1 Background

The pancreas develops from dorsal and ventral buds that eventually fuse during embryonic development to form one organ. In mammals, both the dorsal and ventral pancreatic bud give rise to exocrine and endocrine tissues. Because of the surrounding tissues, different signals induce the dorsal and ventral pancreatic buds (36–40). For example, signals from the aortic endothelium induce the formation of the *Pdx1* and *Ptf1a*-expressing dorsal pancreatic bud, whereas development of the ventral pancreas is not dependent on cues from the endothelium (69,71). The dorsal pancreatic bud eventually generates the superior part of the head, the body, and the tail of the pancreas, whereas the ventral pancreatic bud give rise to the inferior part of the head and the uncinate process of the pancreas (118–120). Endocrine composition, vascularization, and innervation differ between islets in the head and tail of the pancreas (124,296), and functional differences between regions of the pancreas have been described (119,125). Interestingly, patients with type 2 diabetes exhibit preferential loss of beta-cells in the head region compared to the tail region of the pancreas (126). Understanding if developmental differences lead to beta-cell subpopulations with distinct molecular signatures and/or functions might unravel important insights into beta-cell biology and dysfunction.

Like mammals, endocrine cells arise from dorsal and ventral pancreatic buds in the zebrafish. Zebrafish represents a unique model whose rapid, *ex-utero* development, high fecundity, ease of genetic manipulation, and transparency during development provide it with distinctive

advantages over that of other model organisms. Zebrafish beta-cell development is also similar to mammalian beta-cell development suggesting studies in this system can have broadly applicable insights. In zebrafish, medial cells directly adjacent to the notochord give rise to the dorsal pancreatic bud, while the ventral pancreatic bud arises from the more lateral cells (268,297). Dorsal derived beta-cells (herein termed primary beta-cells) first begin to express insulin at 14 hpf. The next wave of beta-cells (herein termed secondary beta-cells) appear after 48 hpf and originate solely from the ventral pancreatic bud. It is thought that the beta-cells that appear after 48 hpf give rise to the majority of adult beta-cells. It is not known the contribution of the primary beta-cells to adult beta-cell mass. Transcriptional differences between dorsally-derived primary and ventrally-derived secondary beta-cells have been described at 12 dpf in which primary beta-cells express significantly less insulin and beta-cell maturation markers in comparison to secondary beta-cells (226). However, whether primary and secondary beta-cells have distinct molecular signatures in the adult pancreas is not known. Understanding if ontogeny and time of formation leads to a distinct molecular signature in beta-cells may give us insight into the development of beta-cell heterogeneity.

In this Chapter, we took advantage of the difference in time of formation between the early appearing dorsal pancreatic bud and later appearing ventral pancreatic bud in order to differentiate between primary and secondary beta-cells. We developed a novel Cre/LoxP genetic lineage tracing model to track primary beta-cells during larval and adult stages and we performed single cell RNA sequencing to determine if transcriptional differences exist between primary and secondary beta-cells in the adult pancreas.

2.2 Methods

Zebrafish lines

Adult zebrafish were housed in a ZEBTEC zebrafish housing system (Tecniplast, Buguggiate, Varese, Italy) at 28 °C in a 14 hr light/10 hr dark cycle. Larvae and juvenile zebrafish (up until 1-month post fertilization) were fed with Gemma micro-150 (Skretting, Westbrook, ME, USA) once daily and artemia twice daily (Aquatic Eco-Systems, Apopka, FL, USA). Adults were fed Gemma micro-300 (Skretting) once daily and artemia (Aquatic Eco-Systems) twice daily. Fertilized eggs were collected from adult zebrafish and placed in E3 media (5 mM NaCl, 0.17 mM KCl, 0.33 mM $CaCl_2$•$2H_2O$, 0.33 mM $MgSO_4$) at 28°C in an incubator with a 14 hr light /10 hr dark cycle. The following zebrafish lines were used in experiments: *Tg(actb2:LOXP-STOP-LOXP-DsRedEx)*^{sd5} (298)*, Tg(hsp70l:mCherry-T2A-CreER*^{T2}*)*^{tud104} (299), *Tg(-1.5hsp70l:Cre)*^{vu297} (300), *Tg(-3.5ubb:CreER*^{T2}*, myl7:EGFP)*^{cz1702} (301), and *Tg(ins:nfsB-Flag, cryaa:mCherry)*^{s950} (abbreviated *Tg(ins:nfsB)*). The *Tg(ins:nfsB)* line was a kind gift from Christian Helker. We genotyped the *Tg(actb2:LOXP-STOP-LOXP-DsRedEx)* line by performing RT-PCR on DsRed (forward primer: 5'- GTAATGCAGAAGAAGACTATGGGCTGGGAG-3'; reverse primer: 5'-ATGTCCAGCTTGGAGTCCACGTAGTAGTAG-3').

Generating the *Tg(ins:FRT:EGFP:LOXP:IRES:FLP:LOXP:FRT:RFP), Tg(ins:FRT:EGFP:LOXP:IRES:FLP:LOXP:FRT:nfsB-T2A-RFP),* and *Tg(ins:FRT:nfsB-T2A-EGFP:LOXP:IRES:FLP:LOXP:FRT:RFP)* lines

To create our novel transgenic lines, we utilized Golden Gate cloning (302). Due to the complexity of the transgenes, we divided the transgenes into 3 modules whereby these modules would be eventually ligated together to produce the final DNA constructs (Figure 2-1A,B). All

cloning pieces were amplified using Phusion High-Fidelity DNA Polymerase (Life Technologies, Carlsbad, CA, F530S) with specific primers listed in Table 2.1. Primers contained *BsmB1, Bsa1,* or *Bbs1* cut sites on the 5' ends (underlined). The IRES sequence was amplified from the p3E-IRES-EGFP from the Tol2Kit (303,304) and FLP sequence was amplified from pCAG-Flpe. pCAG-Flpe was a gift from Connie Cepko (Addgene plasmid #13787; http://n2t.net/addgene:14797; RRID:Addgene 13787). The pieces were ligated into modified pBluescript vectors, transformed into NEB® 5-alpha Competent *E. coli* following the manufacturer's instructions (New England BioLabs, C2987H, Ipswich, MA). Vectors were isolated and subsequently cut with either *BsmB1, Bsa1,* or *Bbs1* to generate complimentary sticky ends. Cloning pieces were ligated into the appropriate cloning module. Modules were transformed in NEB® 5-alpha Competent *E. coli* (New England BioLabs, C2987H), isolated, and cut with the *BsmB1* to generate complementary sticky ends and ligated to a modified Tol2 vector backbone. Transposase mRNA was generated via the mMESSAGE mMACHINE T7 Transcription Kit as per the manufacturer's instructions (Life Technologies, AM1344). Co-injection of 30 pg Tol2 vector and 30 pg transposase mRNA was performed at the one cell stage in wild-type AB embryos as previously described (303). Microinjection was performed using a MM-33 micromanipulator (Sutter Instrument, Novato, CA, USA) and a PicoSpritzer III pressure injector (Parker Hannifin Corp, Pine Brook, NJ, USA). Founder fish were screened for EGFP or RFP expression at 3 dpf, raised, and outbred to wild-type AB fish to determine germline transmission.

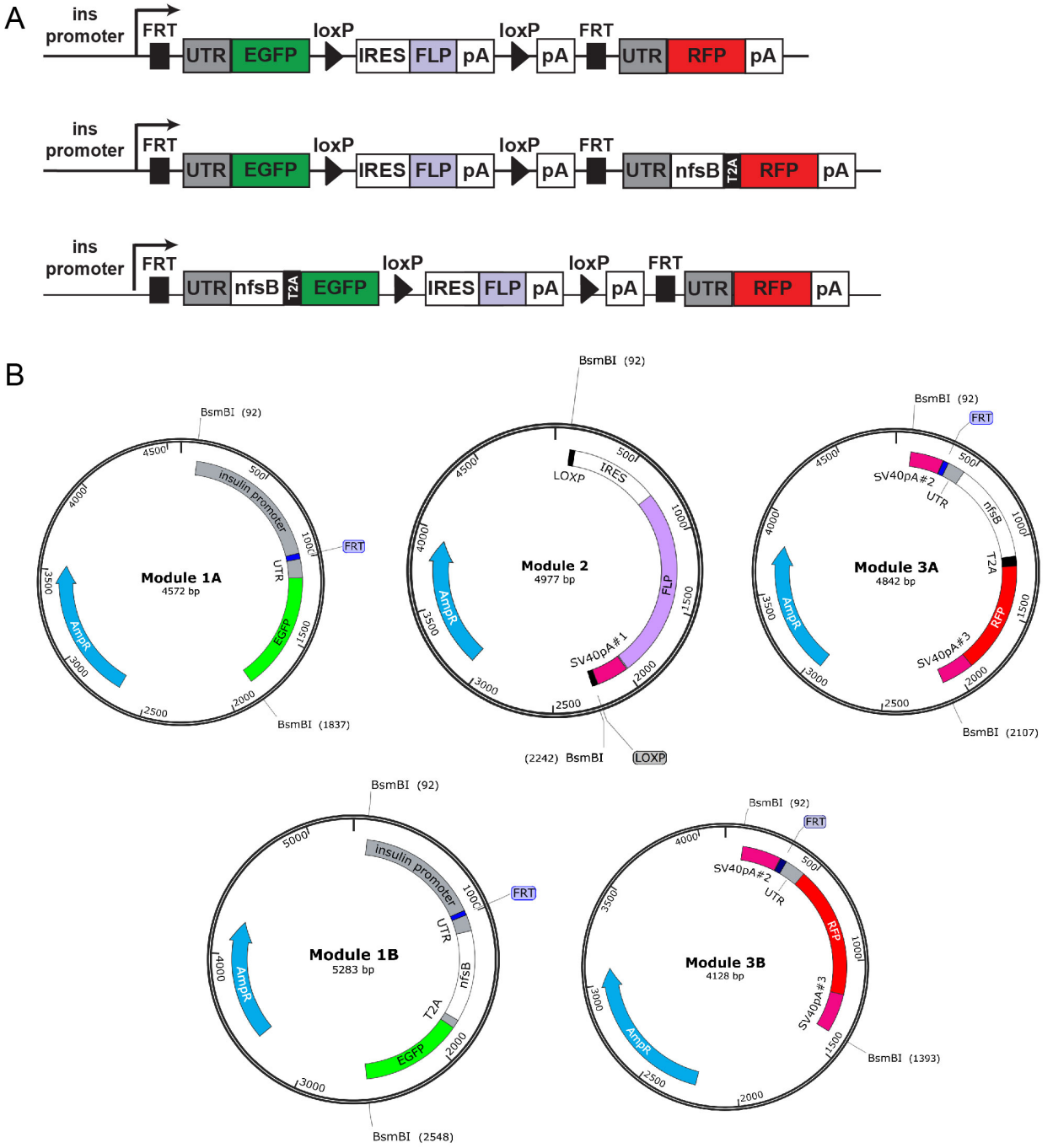

Figure 2-1 Cloning strategy to generate novel transgenic lines.
A) Schematic of the *Tg(ins:FRT:EGFP:LOXP:IRES:FLP:LOXP:FRT:RFP), Tg(ins:FRT:EGFP:LOXP:IRES:FLP:LOXP:FRT:nfsB-T2A-RFP),* and *Tg(ins:FRT:nfsB-T2A-EGFP:LOXP:IRES:FLP:LOXP:FRT:RFP*) transgenes. The FRT was placed within the 5' UTR, 114 bp upstream of the *ins* ATG start codon. The UTR refers to the endogenous sequence that is 114 bp upstream of the *ins* ATG start codon. The UTR was added upstream of EGFP; as such, any sequences that may be involved with 5' capping of the RNA or with ribosome recognition of the

start codon would be present. **B)** Maps of plasmid modules flanked by *BsmB1* cut sites that were used to generate the final transgenes observed in **A)**.

Table 2-1 *Tg(ins:FRT:EGFP:LOXP:IRES:FLP:LOXP:FRT:pA:nfsB-T2A-RFP)* transgene primer sequences

Target	Forward Primer	Reverse Primer
1.0 kb *ins* promoter	CACACAGGTCTCAGCCAATTTAACTTCAGCCCACAGTC	CACACAGGTCTCACAGAGGCGAGGAATGGTG
FRT oligo	TCTGGAAGTTCCTATACTTTCTAGAGAATAGGAA	GAAGTTCCTATTCTCTAGAAAGTATAGGAACTTC
ins 5' UTR	CACACAGGTCTCACTTCGAGAACAGGTGAGTGTC	CACACAGGTCTCAGGTCACACTGACACAAACACA
EGFP for Mod 1A	CACACAGGTCTCAGACCATGGTGAGCAAGGGCG	CACACACGTCTCATGATCTTGTACAGCTC
EGFP for Mod 1B	CACACAGGTCTCACCCTATGGTGAGCAAGGGCG	CACACACGTCTCATGATCTTGTACAGCTC
5' loxP oligo	ATCAATAACTTCGTATAGCATACATTATACGAAGTTATGCCCCT	GGAGAGGGGCATAACTTCGTATAATGTATGCTATACGAAGTTAT
IRES	CACACAGGTCTCACTCCCTCCCCCCCCCCTAACGTTA	CACACAGGTCTCATGTGGCCATATTATCATCGTGTTTTTC
FLP	CACACAGGTCTCACACAATGCCACAATTT	CACACAGGTCTCATCAGCTAAATGCGTCT
SV40pA #1	CACACAGGTCTCACTGAGATCATAATCAGCCATACCACA	CACACAGGTCTCATGCTAGTTTGGACAAACCACAACTAGAATG
3' loxP oligo	AGCAATAACTTCGTATAGCATACATTATACGAAGTTAT	GCATATAACTTCGTATAATGTATGCTATACGAAGTTAT
SV40pA #2	CACACAGGTCTCAATGCGATCATAATCAGCCATACCACA	CACACAGGTCTCACAGAAGTTTGGACAAACCACAACTAGAATG
nfsB	CACACAGGTCTCAGACCATGGATATCATTTCTGTCGCCTTAAAG	CACACAGGTCTCATGCCCACTTCGGTTAAGGTGATGTTTTGCG

T2A oligo	GGCAGCGGAGAGGGCAGAGGAA GTCTTCTAACATGCGGTGACGTG GAGGAGAATCCCGG	AGGGCCGGGATTCTCCTCCACGT CACCGCATGTTAGAAGACTTCCT CTGCCCTCTCCGC
RFP for Mod 3A	CACACACGTCTCACCCTATGGTG TCTAAG	CACACACGTCTCAGTTGAGTCCG GAATT
RFP for Mod 3B	CACACACGTCTCAGACCATGGTG TCTAAG	CACACACGTCTCAGTTGAGTCCG GAATT
SV40pA #3	CACACAGGTCTCACAACGATCAT AATCAGCCATACCACA	CACACAGGTCTCAAGTTTGGACA AACCACAACTAGAATG

Generating the *Tg(ins:EGFP-T2A-CreER^{T2})* line

Primers were designed to amplify 1.0 kb of the zebrafish insulin promoter, EGFP, and CreER^{T2} with a SV40 poly adenylation site. Pieces were amplified with Phusion High-Fidelity DNA Polymerase (Life Technologies, F530S). Primers included *BsaI* or *BbsI* cut sites on the 5' ends (underlined) (Table 2-2). pCAG-CreER^{T2} was a gift from Connie Cepko (Addgene plasmid # 14797; http://n2t.net/addgene:14797; RRID:Addgene 14797) (305). The amplified products were cut with *BsaI* or *BbsI* to generate complimentary sticky ends, purified, and ligated to a modified Tol2 backbone (304) (Figure 2-2A,B). Transposase mRNA was generated via the mMESSAGE mMACHINE T7 Transcription Kit as per the manufacturer instructions (Life Technologies, AM1344). Co-injection of 30 pg Tol2 vectors and 30 pg transposase mRNA was performed at the one cell stage in wild-type AB embryos as previously described (303). Founder fish were screened for EGFP expression at 3 dpf, raised, and bred to determine germline transmission. *Tg(ins:EGFP-T2A-CreER^{T2})* F1 lines were raised and backcrossed to wild-type AB strain 3 times before crossing to the *Tg(actb2:LOXP-STOP-LOXP-DsRedEx)* line (298).

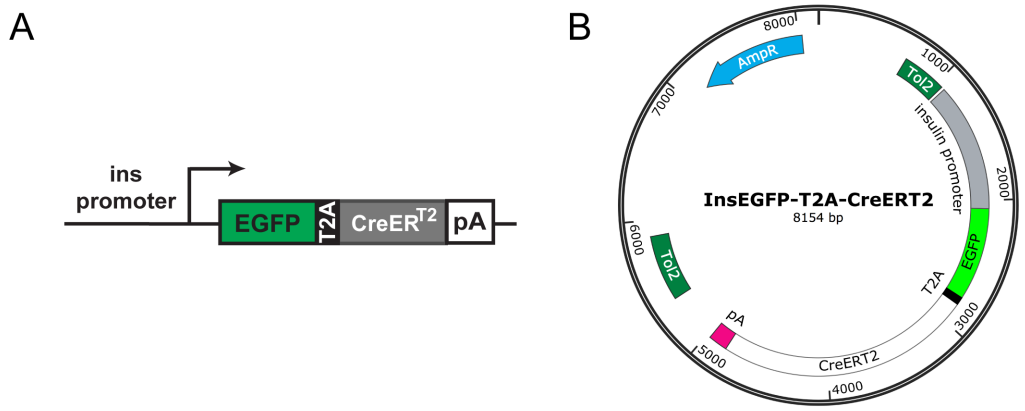

Figure 2-2 *Tg(ins:EGFP-T2A-CreER^{T2})* transgene and plasmid map
A) Schematic of the *Tg(ins:EGFP-T2A-CreER^{T2})* transgene. **B)** Map of the Tol2 plasmid with the *ins:EGFP-T2A-CreER^{T2}* insert which is flanked by transposon terminal sequences (Tol2).

Table 2-2 *Tg(ins:EGFP-T2A-CreER^{T2})* transgene primer sequences

Target	Forward Primer	Reverse Primer
1.0 kb *ins* promoter	CACACAGGTCTCAGCCAATTTAA CTTCAGCCCACAGTC	CACACAGGTCTCAGGTCACACTG ACACAAACACA
EGFP	CACACAGGTCTCAGACCATGGTG AGCAAGGGCG	CACACAGGTCTCAAGGGCCGGGA TTCTCCTCCACGTCACCGCATGTT AGAAGACTTCCTCTGCCCTCTCC GCTCTTGTACAGCTCGTCCATGC (primer contains the viral T2A)
CreER^{T2}	CACACAGAAGACAACCCTATGT CCAATTTACTGACCGTACACC	CACACAGAAGACAAGTTGACAA ACCACAACTAGAATGCAGTG

Chemical treatments and heat shock

(Z)-4-Hydroxytamoxifen (4-OHT) (Sigma-Aldrich, Oakville, ON, Canada H7904) was dissolved in DMSO to 10 mM and stored at -20°C. Embryos were treated with 10 µM 4-OHT or 0.1% DMSO in E3 media from 12-42 hpf or 2-8 hpf. The embryos were kept at 28°C in the dark

during 4-OHT administration. For 4-OHT removal, we placed embryos in fresh E3 media for 5 minutes and repeated this step with fresh E3 media at least 5 times. For beta-cell ablation studies, 10 mM MTZ or 0.1% DMSO in E3 media was administered from 12-30 hpf and embryos were kept from light. Embryos were washed with fresh E3 media 5 times to remove MTZ. For mannitol and glucose administration, 6 dpf larvae were placed in E3 media containing 0.5% or 2% w/v glucose or 2% w/v mannitol. Glucose or mannitol was removed after 8 hrs or after 2 days and fish were sacrificed at 6.5 dpf or 8 dpf. Animals that were treated from 6-8 dpf with glucose, mannitol or control (E3 solution) were fed once at 6.5 dpf, and solutions were refreshed at 7 dpf. For heat shock treatments, embryos were placed in 50 mL conical tube in 38ºC pre-heated E3 media. They were placed in a 38ºC water bath for one hour before being placed in fresh E3 media or 10 μM 4-OHT.

Cell dissociation and FACS

For isolating adult primary and secondary beta-cells, the principal islet was dissected from 2.5-3 month old adult *Tg(ins:EGFP-T2A-CreER^{T2}; actb2:LOXP-STOP-LOXP-DsRedEx)* fish and digested as previously described (306). Briefly, adult pancreata were digested in 1.4 mg/ml collagenase-P at 37°C for 20 min, pelleted, and resuspended in 0.05% trypsin/HBSS at 37°C for 15 min. To stop digestion, 5% fetal bovine serum was added. Dispersed cells were filtered through a 40 μm filter and subsequently sorted based on EGFP expression using BD Influx Cell Sorter (BD Biosciences, Mississauga, ON, Canada).

Single-cell RNA sequencing library generation

The principal islet was isolated from 40 *Tg(ins:EGFP-T2A-CreER^{T2} ; actb2:LOXP-STOP-LOXP-DsRedEx)* 2.5 month old adult zebrafish. Single-cell RNA sequencing was done using the Chromium Single-Cell 3′ Reagent version 2 kit and Chromium Single-Cell Controller (10x Genomics, CA). In short, 10,000 cells were loaded onto a 10x Genomics Single Cell 3′ Chip, and cDNA synthesis and library construction were performed as per the manufacturer's protocol for the Chromium Single Cell 3′ v2 protocol (10x Genomics). Libraries are loaded into the NextSeq 500 System for a 75-cycle sequencing run.

Single cell data analysis

Following sequencing, cellranger mkfastq (10X Genomics) was used to generate FASTQ files from the raw sequencing data. Cell ranger count aligned to reference zebrafish genome (GRCz11) generated single-cell counts. Zebrafish reference genome was annotated to include *DsRed* and *GFP* sequence. Scater was used to filter out low quality cells (307). Cells with greater than 5% of mitochondrial DNA and less than 200 expressed features were discarded. Seurat R package (308,309) was used to identify differentially expressed genes in each cluster, generate violin plots, and the heat matrix. For our experiment, we selected that for a gene to be differentially expressed in a cluster, the gene must be expressed in 25% of the cells, have a log fold change of greater than 0.25, and reach statistical significance of an adjusted $p<0.05$ as determined by the Wilcox rank sum test.

Quantitative PCR

For qPCR on adult beta-cells, RNA was isolated from primary DsRed+/EGFP+ beta-cells or secondary EGFP+ cells using TRIzol (Invitrogen, Carlsbad, CA, USA). For qPCR on zebrafish

embryos, RNA was isolated from 20 whole body zebrafish using TRIzol (Invitrogen, Carlsbad, CA, USA). cDNA was prepared using the iScript cDNA synthesis kit (Invitrogen) and amplified with SsoFast EvaGreen Supermix (BioRad, Richmond, CA, USA) on a CFX96 Touch™ Real–Time PCR Detection System (BioRad). The relative expression of each sample was determined after normalization to *elongation factor 1α* (*ef1α*). Non-template control reactions and reactions with genomic DNA, but not cDNA (to determine cDNA primer specificity), were conducted for each primer set. Primers used are listed in Table 2-3. PCR cycling conditions were as follows: 3-min denaturation step at 95 °C, followed by 40 cycles of denaturation at 95 °C for 15 s, annealing at 55 °C for 15 s, and extension at 72 °C for 25 s.

Table 2-3 RT-qPCR primer sequences

Gene	Forward Primer	Reverse Primer	Accession
ef1α	TCAAGGACATCCGTCGTGGTA	ACAGCAAAGCGACCAAGAGG	NM_131263
insulin	TCTGCTTCGAGAACAGTGTG	GGAGAGCATTAAGGCCTGTG	NM_131056
pdx1	GGGCGCGAGATGTATTTGTTGA	CAAATCTCACACGCACGCATG	NM_131443
neurod1	TCATGCTTTCCTCGCTGTATGACT	CCACGAAGGGCATGAAACTATCA	NM_130978
gck	ATCCTCATGGTGGACCAA	ATCACCAACCTCGGAGC	NM_001045385
grn2	TGGCAAATGGACATGTTGTCC	GCCGGGCAGTAGAAATTTCC	NM_212756
krt18a.1	TCATGCTTTCCTCGCTGTATGACT	CCACGAAGGGCATGAAACTATCA	NM_178437
DsRed	CCCCGTAATGCAGAAGAAGACT	GGCTACTACTACGTGGACTCCAA	NA
GFP	AAGTTCATCTGCACCACCG	TCCTTGAAGAAGATGGTGCG	NA
sst2	TGAACTCTGCACTACAGGCGTC	GATCCGAGTTACTGAGCAGCC	NM_131727

gcga	AAGGCGACAGCACAAGCACA	GCCCTCTGCATGACGTTTGACA	NM_001271770

Immunofluorescence

For whole mount larval zebrafish, immunofluorescence was performed as previously described (310). Briefly, zebrafish embryos were anaesthetized with ethyl 3-aminobenzoate methanesulfonate (MS222, 0.01% w/v) and then fixed with 4% paraformaldehyde overnight at 4°C. Embryos were washed three times with 0.3% Triton X-100 in PBS. The embryos were blocked for 1 hr in PBS with 5% donkey serum (Jackson Immunoresearch Laboratories, West Grove, PA, USA) and 0.3% Triton X-100. Both primary and secondary antibodies were incubated overnight at 4°C. Washes were done with 0.1% Tween/PBS for 30 min three times. Antibodies used were rabbit anti-DsRed (1:200, Clontech, 632496) and goat anti-rabbit Alexa Fluor 594 antibody (1:1000, Life Technologies, A11037). Cell nuclei were visualized with 4′,6-diamidino-2-phenylindole (DAPI) DNA stain (1:1000, Thermo Fisher Scientific D1306). Samples were mounted in 75% glycerol on concave glass slides (EISCO). All fluorescent images were obtained with a LSM800 Zeiss upright confocal and imaged with a 40X objective. Whole mount tissues were scanned by confocal microscopy. Cell numbers were counted manually. The Shapiro–Wilk normality test was used to assess normality of data distribution and when all groups passed the test for normality, a Student's t-test or one-way ANOVA and Tukey post-hoc test were used for statistical analysis for cell counts.

For paraffin embedded sections, the pancreata were dissected out of fish using fine tip needles and fixed in 4% paraformaldehyde overnight at 4°C. Tissues were transferred to 70% ethanol for long-term storage before paraffin embedding and sectioning (5 μm thickness; Wax-It Histology Services, Vancouver, Canada). Briefly, sections were deparaffinized in xylene (15

minutes) and rehydrated in graded ethanol washes (100% 2x5 mins, 95% 5 mins, 70% 5 mins, and PBS 10 mins). Rehydrated sections underwent heat induced epitope retrieval in an EZ Retriever microwave oven (BioGenes, Fremont, CA) for 10 minutes at 95°C in 10mM citrate buffer (0.5% Tween 20, pH 6.0; ThermoFisher Scientific, Waltham, MA). Samples were blocked in DAKO Protein Block, Serum Free (Dako, Burlington, Canada) for 15 minutes at room temperature and subsequently incubated with primary antibodies diluted in Dako Antibody Diluent (Dako, Burlington, Canada) overnight at 4°C. The following primary antibodies were used: mouse anti-EGFP (1:100, Millipore Sigma, MAB3580) and rabbit anti-DsRed (1:200, Clontech, 632496). The following day, slides were washed and incubated in secondary antibodies: goat anti-rabbit Alexa Fluor 594 antibody (1:1000, Life Technologies, A11037) and goat anti-mouse Alexa Fluor 488 antibody (1:1000, Life Technologies, A11029) for 1 hr at room temperature before mounting with VECTASHIELD Hard Set Mounting Medium with DAPI (Vector Laboratories, Burlingame, CA, H-1500). All fluorescent images were obtained with a LSM800 Zeiss upright confocal and imaged with a 40X objective. Pancreatic sections were cut 20 to 50 μm apart and at least 5 sections per animal were used in quantification. Cell numbers were counted manually.

2.3 Results

Creation of novel transgenics to differentially label and ablate primary and secondary beta-cells

To differentially label primary and secondary beta-cells, we generated the *Tg(ins:FRT:EGFP:LOXP:IRES:FLP:LOXP:FRT:RFP), Tg(ins:FRT:EGFP:LOXP:IRES:FLP:LOXP:FRT:nfsB-T2A-RFP),* and *Tg(ins:FRT:nfsB-T2A-EGFP:LOXP:IRES:FLP:LOXP:FRT:RFP*) lines. The lines were to be crossed to a ubiquitous Cre driver line. The resulting double

transgenic would differentially label primary beta-cells (red) and secondary beta-cells (green) after Cre recombinase activation before 48 hpf (Figure 2-3A). In addition, our transgenics would also allow for the specific ablation of either the primary or secondary beta-cells (dependent on the location of the inducible *nfsB* suicide gene) (Figure 2-1A). The success of this labelling strategy relies on the efficiency of the FLP and Cre recombinases (Figure 2-3A). The *Tg(ins:FRT:EGFP:LOXP:IRES:FLP:LOXP:FRT:RFP), Tg(ins:FRT:EGFP:LOXP:IRES:FLP:LOXP:FRT:nfsB-T2A-RFP),* and *Tg(ins:FRT:nfsB-T2A-EGFP:LOXP:IRES:FLP:LOXP:FRT:RFP*) exhibit FLP recombination, as we observed RFP expression at 32 hpf (Figure 2-3B). At 120 hpf, most of the beta-cells expressed RFP, suggesting successful FLP recombination (Figure 2-3B).

We next tested out three different ubiquitous Cre models: *Tg(hsp70l:Cre), Tg(hsp70l:mCherry-T2A-CreER^{T2}),* and *Tg(-3.5ubb:CreER^{T2}, myl7:EGFP).* We crossed our *Tg(ins:FRT:EGFP:LOXP:IRES:FLP:LOXP:FRT:RFP)* to either the *Tg(hsp70l:Cre), Tg(hsp70l:mCherry-T2A-CreER^{T2}),* or the *Tg(-3.5ubb:CreER^{T2}, myl7:EGFP)* and administered either heat shock at 30 hpf at 38°C for 1 hr, and/or administered 4-OHT from 31 hpf until 42 hpf, depending on the Cre line (Figure 2-3C). It has been previously established that around 20 primary beta-cells and 15 secondary beta-cells are present at 5 dpf (226). Hence, in our initial screening for successful FLP and Cre recombination, we expected to see similar RFP+ and EGFP+ cell proportions at 7 dpf. However, our double transgenic lines did not match our predictions. In both the *Tg(ins:FRT:EGFP:LOXP:IRES:FLP:LOXP:FRT:RFP ; hsp70l:mCherry-T2A-CreER^{T2})* and the *Tg(ins:FRT:EGFP:LOXP:IRES:FLP:LOXP:FRT:RFP ; -3.5ubb:CreER^{T2}, myl7:EGFP)* lines, we observed that the majority of beta-cells are RFP+, suggesting unsuccessful Cre recombination (Figure 2-3D,F). In the *Tg(ins:FRT:EGFP:LOXP:IRES:FLP:LOXP:FRT:RFP ;*

hsp70l:Cre) line, we observed mostly EGFP+ cells, indicating leaky Cre expression from the *hsp* promoter during early development (Figure 2-3E).

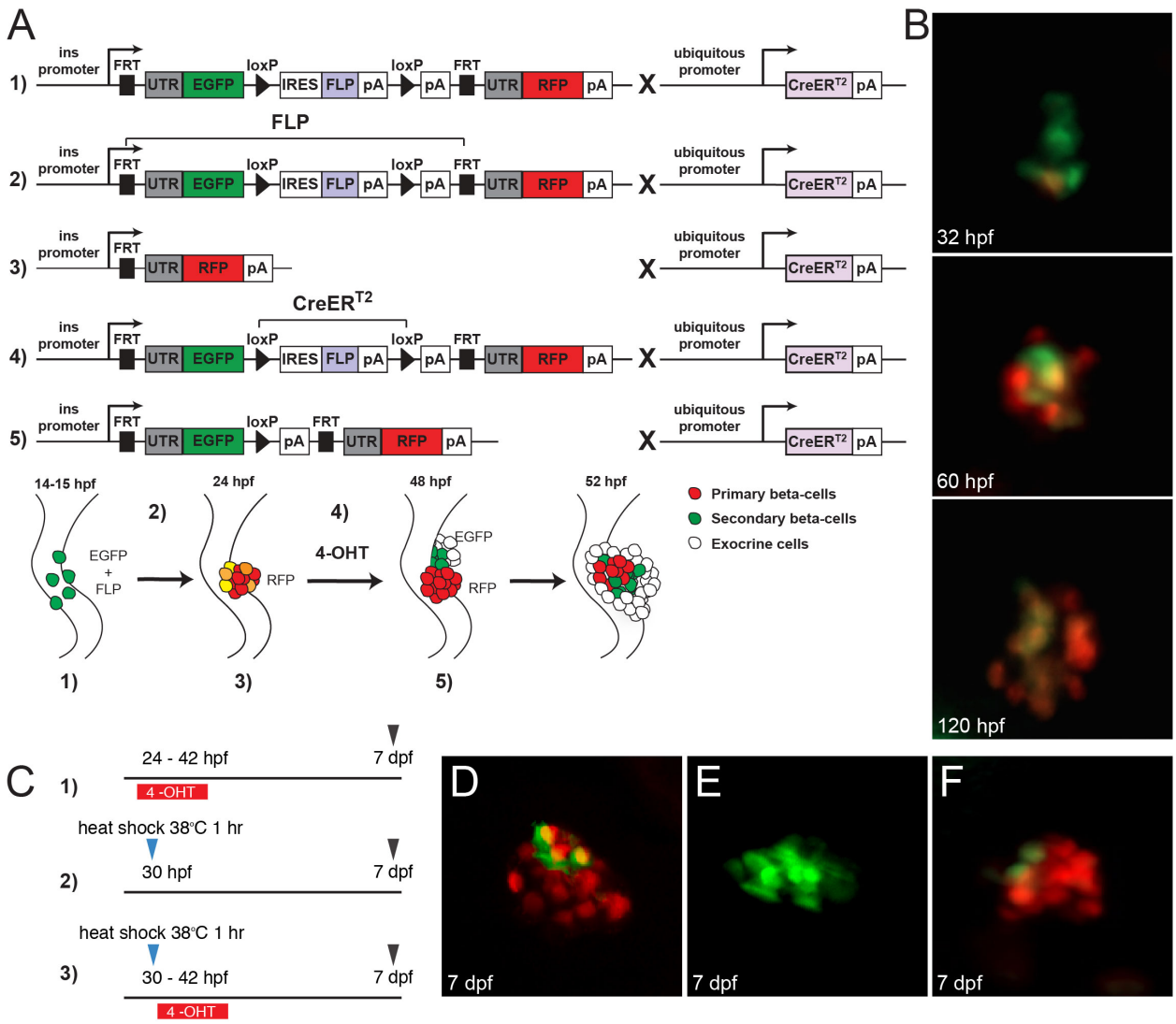

Figure 2-3 Transgenic model for labelling primary and secondary beta-cells during zebrafish pancreas development

A) Schematic of the *Tg(ins:FRT:EGFP:LOXP:IRES:FLP:LOXP:FRT:RFP)* line crossed to a ubiquitous Cre driver: 1) insulin promoter drives expression of EGFP and labels primary beta-cells in green around 14 hours post fertilization (hpf). 2) FLP recombinase removes the expression cassette containing EGFP and the transcription termination signal. 3) Starting from 24 hpf, the insulin promoter drives expression of RFP in primary beta-cells with different shades of red, orange, and yellow depending on the residual amount of cytosolic EGFP. 4) 4-OHT administration

induces nuclear translocation of CreER^{T2}, leading to subsequent excision of the cassette expressing FLP, leaving a transcription termination signal in frame after EGFP. 5) Starting from 48 hpf, new emerging beta-cells (secondary beta-cells) will be labelled in green whereas primary beta-cells maintain red labelling. **B)** FLP recombination activity in *Tg(ins:FRT:EGFP:LOXP:IRES:FLP:LOXP:FRT:RFP)* line at 32 hpf, 60 hpf, and 120 hpf. The fish were not treated with 4-OHT; hence, the majority of the beta-cells are expected to have FLP recombination, resulting in RFP expression. **C)** Experimental timeline for testing out 1) *Tg(ins:FRT:nfsB-T2A-EGFP:LOXP:IRES:FLP:LOXP:FRT:RFP;-3.5ubb:CreER^{T2},myl7:EGFP)*, 2) *Tg(ins:FRT:nfsB-T2A-EGFP:LOXP:IRES:FLP:LOXP:FRT:RFP ; hsp70l:Cre),* and 3) *Tg(ins:FRT:nfsB-T2A- EGFP:LOXP:IRES: FLP:LOXP:FRT:RFP; hsp70l:mCherry-T2A-CreER^{T2}).* **D-F)** Representative images of an islet at 7 dpf from *Tg(ins:FRT:nfsB-T2A-EGFP:LOXP:IRES: FLP:LOXP:FRT:RFP)* crossed to the **D)** *Tg(-3.5ubb:CreER^{T2}, myl7:EGFP),* **E)** *Tg(hsp70l:Cre),* and **F)** *Tg(hsp70l:mCherry-T2A-CreER^{T2}).* For **E)** and **F)** embryos were heat shocked at 38°C for 1 hr starting at 30 hpf. 10 μM 4-OHT was administered to embryos from **D)** 24-42 hpf or **F)** 31-42 hpf. Images were taken with Zeiss Axio Zoom.V16 stereo microscope. n = 10.

To better characterize the Cre lines, we crossed the *Tg(hsp70l:Cre), Tg(hsp70l:mCherry-T2A-CreER^{T2}),* or the *Tg(-3.5ubb:CreER^{T2}, myl7:EGFP)* to the existing *Tg(act2b:LOXP:STOP:LOXP:DsRedEx).* In the *Tg(hsp70l:Cre ; act2b:LOXP:STOP:LOXP:DsRedEx)*, we expected DsRed expression only upon heat shock. However, we found that at 28.5°C and 24°C, DsRed expression was evident in a subset of 24 hpf embryos, suggesting leaky activation of the *hsp70l* promoter. Leaky activation of the *hsp70l* promoter has been previously described in other transgenic lines (299) (Figure 2-4A,B). In the *Tg(hsp70l:mCherry-T2A-CreER^{T2} ; act2b:LOXP:STOP:LOXP:DsRedEx)* double transgenic line, heat shock at 38°C for 1 hr induced mCherry expression, suggesting activation of the heat shock promoter (Figure 2-4C-E). We found that mCherry expression was variable between individuals (Figure 2-4D,E). When we stained for DsRed and insulin at 6 dpf, we are unable to detect DsRed expression in the insulin-producing cells, suggesting that the *hsp70l* promoter was not induced in the beta-cells (Figure 2-4F). In the *Tg(-3.5ubb:CreER^{T2}, myl7:EGFP ;*

act2b:LOXP:STOP:LOXP:DsRedEx), we administered 4-OHT from 24 until 42 hpf. We observed stochastic expression of DsRed at 5 dpf (Figure 2-4G); however, DsRed expression was not found in the insulin-expressing cells (Figure 2-4H). Overall, these results suggested that *Tg(-3.5ubb:CreER^{T2}, myl7:EGFP), Tg(hsp70l:Cre),* and *Tg(hsp70l:mCherry-T2A-CreER^{T2}*) were not appropriate Cre lines to use with our *Tg(ins:FRT:EGFP:LOXP:IRES:FLP:LOXP:FRT:RFP), Tg(ins:FRT:EGFP:LOXP:IRES:FLP:LOXP:FRT:nfsB-T2A-RFP),* and *Tg(ins:FRT:nfsB-T2A-EGFP:LOXP:IRES: FLP:LOXP:FRT:RFP*) transgenic lines.

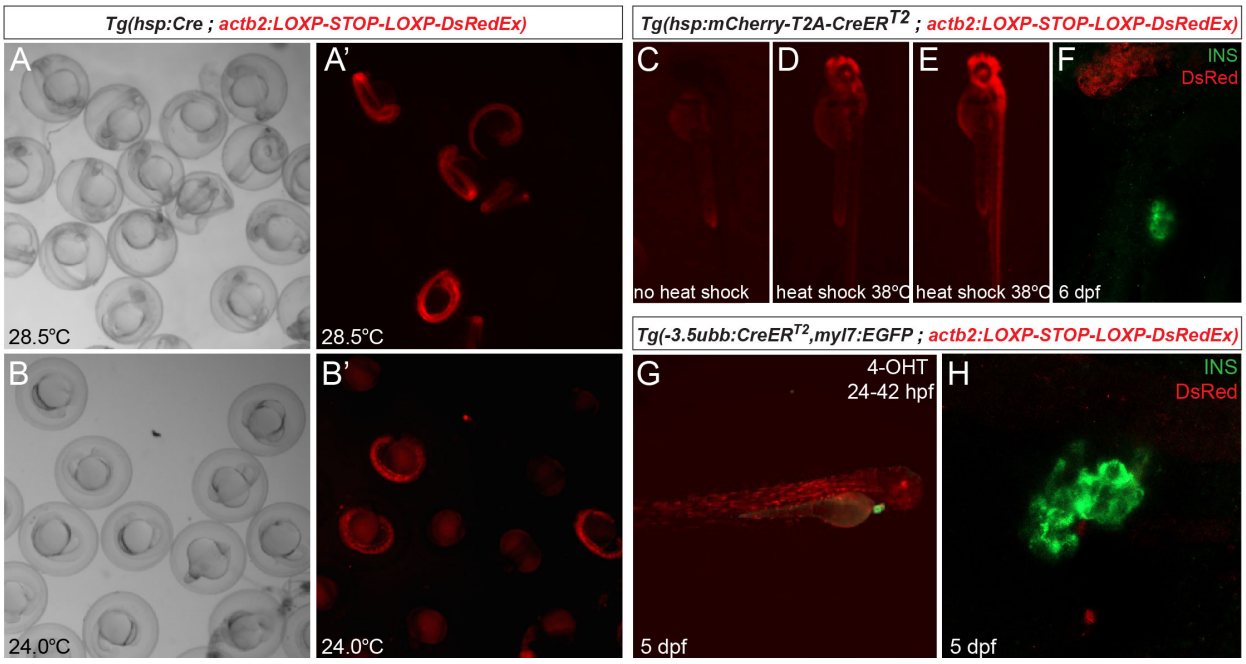

Figure 2-4 The efficiency of Cre recombination in 3 separate Cre transgenic lines
A-B) *Tg(hsp70l:Cre ; act2b:LOXP:STOP:LOXP:DsRedEx)* 24 hpf embryos at 28.5°C and 24°C. No heat shock was applied. **C-E)** *Tg(hsp70l:mCherry-T2A-CreER^{T2} ; act2b:LOXP:STOP:LOXP:DsRedEx)* 48 hpf embryos that received **C)** no heat shock or **D-E)** heat shock at 38.0°C for 1 hr at 30 hpf. **F)** *Tg(hsp70l:mCherry-T2A-CreER^{T2} ; act2b:LOXP:STOP:LOXP:DsRedEx)* 6 dpf fish that was heat shocked at 38°C for 1 hr at 30 hpf and treated with 4-OHT from 31-42 hpf. Fish is stained for insulin (green) and DsRed (red). **G-H)** *Tg(-3.5ubb:CreER^{T2}, myl7:EGFP ; act2b:LOXP:STOP:LOXP:DsRedEx)* fish were treated with 10 µM 4-OHT from 24-42 hpf and stained for insulin (green) and DsRed (red). n = 10-20.

Creation of the *Tg(ins:EGFP-T2A-CreER^{T2})* line

We next generated a tamoxifen-inducible Cre/LoxP system under the control of the insulin promoter in order to label primary beta-cells. In this model, the insulin promoter drives the expression of EGFP and CreER^{T2}, and hence all beta-cells should express EGFP and CreER^{T2} (Figure 2-5A). The *Tg(ins:EGFP-T2A-CreER^{T2})* faithfully labels all beta-cells (Figure 2-5B). We crossed the *Tg(ins:EGFP-T2A-CreER^{T2})* to the existing reporter line *Tg(actb2:LOXP-STOP-LOXP-DsRedEx)* (298) to create the double transgenic *Tg(ins:EGFP-T2A-CreER^{T2} ; actb2:LOXP-STOP-LOXP-DsRedEx)* line. In the absence of 4-OHT, beta-cells would solely express EGFP. In the presence of 4-OHT, beta-cells would express EGFP and DsRed (Figure 2-5A).

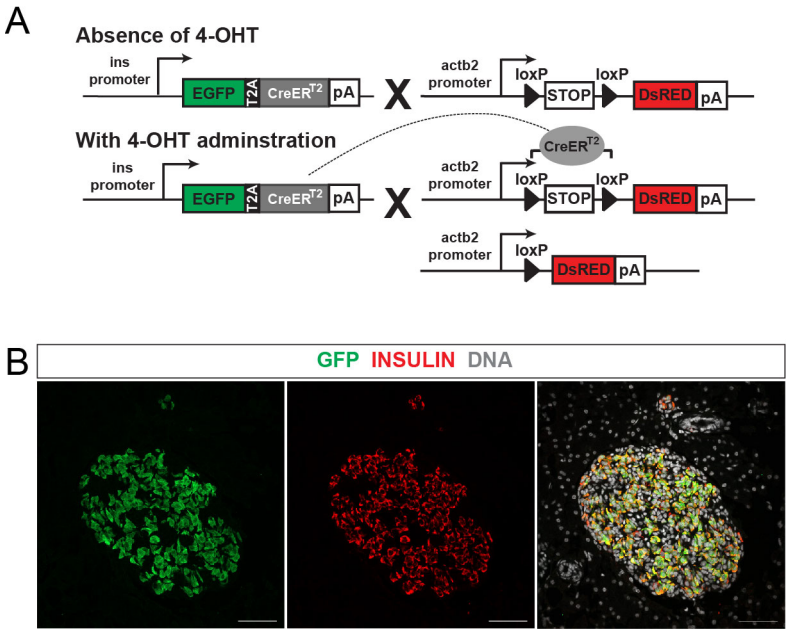

Figure 2-5 The Cre/LoxP-based lineage tracing system for labelling primary and secondary beta-cells

A) Schematic of the *Tg(ins:EGFP-T2A-CreER^{T2} ; actb2:LOXP-STOP-LOXP-DsRedEx)* fish. Administration of 4-OHT will allow for recombination of LoxP sites, thus excising the STOP cassette and allowing for DsRed expression under the ubiquitous *actb2* promoter. **B)** Representative image of an islet from an 8 month old adult *Tg(ins:EGFP-T2A-CreER^{T2})* fish immunostained for GFP (green), insulin (red) and DAPI nuclear stain (DNA; grey). Scale bar = 20 μm.

Primary beta-cells are present in the principal islet in the developing and adult pancreas

To label the primary beta-cells but not the secondary beta-cells with the DsRed label in the *Tg(ins:EGFP-T2A-CreER^{T2} ; actb2:LOXP-STOP-LOXP-DsRedEx)* line, we first determined the ideal time for 4-OHT administration and removal. We administered 4-OHT from 2-8 hpf (6 hours before the onset of insulin expression in the primary beta-cells at 14 hpf). The removal of 4-OHT 6 hours before the appearance of primary beta-cells allowed us to determine if 6 hours was sufficient for drug removal to thereby restrict Cre recombination in beta-cells. We found no DsRed+ beta-cells at 5 dpf, indicating that washing out 4-OHT effectively prevents Cre recombination (Figure 2-6A,B).

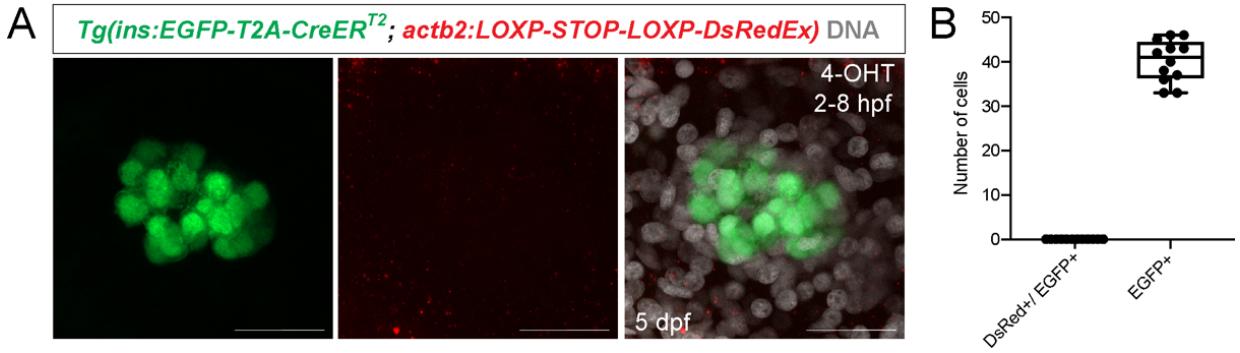

Figure 2-6 Removal of 4-OHT 6 hours before beta-cell appearance does not label beta-cells
A) 4-OHT was administered from 2-8 hpf. Confocal projection of *Tg(ins:EGFP-T2A-CreER^{T2} ; actb2:LOXP-STOP-LOXP-DsRedEx)* fish at 5 dpf ; beta-cells (green). Embryos were stained for DsRed (red) and DAPI nuclear stain (DNA; grey). Scale bar = 20 μm. **B)** The number of DsRed+/EGFP+ and EGFP+ beta-cells in 5 dpf *Tg(ins:EGFP-T2A-CreER^{T2} ; actb2:LOXP-STOP-LOXP-DsRedEx)* fish treated with 4-OHT from 2-8 hpf. Box-and-whisker plots show median, and circles represent individual zebrafish. n = 12.

To label primary beta-cells, we administered 4-OHT from 12 until 42 hpf (approximately 6 hours before the formation of the secondary beta-cells (247)) to *Tg(ins:EGFP-T2A-CreER^{T2} ; actb2:LOXP-STOP-LOXP-DsRedEx)* embryos (Figure 2-7A). In this model, primary beta-cells would express both EGFP and DsRed, while any beta-cell forming after 4-OHT removal

(secondary beta-cells) would solely express EGFP (Figure 2-7B). At 5 dpf, we found 19.4±1.3 primary beta-cells (DsRed+/EGFP+) (Figure 2-7C). The number of primary beta-cells remained static during the first twelve days of development while the number of secondary beta-cells (EGFP+) in the principal islet increased from 5 dpf (17.6±2.4) to 12 dpf (29.7±2.0), a finding similar to a previous report (226) (Figure 2-7C,D). At 30 dpf, we observed a significant increase in the number of primary beta-cells (43.9±4.1) compared to 12 dpf (19.2±1.1) and 5 dpf (19.4±1.3), suggesting that primary beta-cells have the capacity to proliferate during the juvenile stages. (Figure 2-7C,D). In the adult pancreas, we observed primary beta-cells are located in the principal islet (Figure 2-7C,E). The primary beta-cells constitute 6.3±2.1% of the principal islet (Figure 2-7C,E). Interestingly, we observed rare primary (DsRed+) islet cells that do not express EGFP in the principal islet (Figure 2-7C). In our DMSO controls, we observed rare DsRed+ beta-cells (0.8±0.19%) in the principal islet at the adult stages, an indication of leaky CreER^{T2} activation (Figure 2-7C,G) which has been described in other systems (299,311–314).

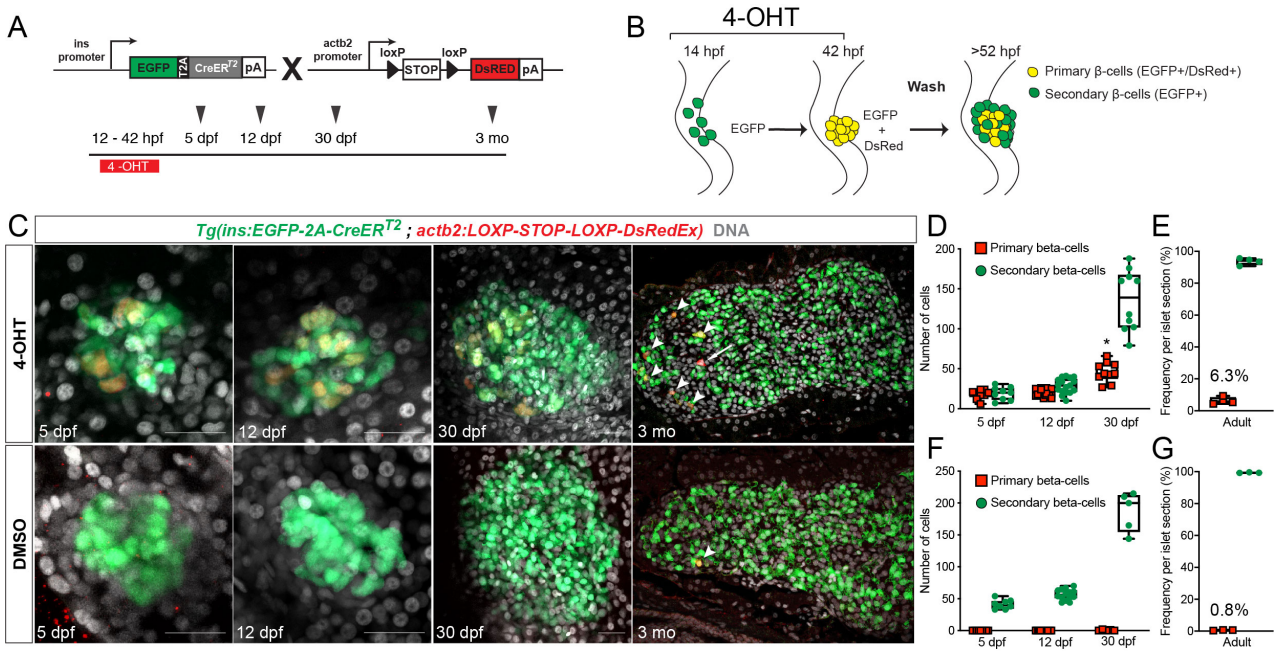

Figure 2-7 Primary beta-cells are present in larval and adult principal islets

A) Experimental timeline for lineage tracing primary and secondary beta-cells in *Tg(ins:EGFP-T2A-CreER^{T2} ; actb2:LOXP-STOP-LOXP-DsRedEx*) fish. 4-OHT was administered from 12-42 hpf in order to label primary beta-cells with DsRed. **B)** Schematic for lineage tracing primary beta-cells. Primary beta-cells appear between 14-24 hpf. By administering 4-OHT from 12-42 hpf, primary beta-cells are labelled with DsRed while secondary beta-cells which appear after 48 hpf would solely express EGFP. **C)** Confocal projections of 4-OHT or DMSO-treated *Tg(ins:EGFP-T2A-CreER^{T2} ; actb2:LOXP-STOP-LOXP-DsRedEx)* fish at 5, 12, and 30 dpf immunostained for DsRed (red) and DAPI nuclear stain (DNA; grey). Scale bar = 20 μm. At 3 months, islets were isolated, sectioned, and immunostained for GFP (green), DsRed (red) and DAPI nuclear stain (DNA; grey). Arrowheads indicate DsRed+/EGFP+ cells. Arrow indicates DsRed+/EGFP- cell. **D)** The number of DsRed+ primary beta-cells (red squares) and secondary beta-cells (green circles) in 4-OHT treated 5, 12, and 30 dpf *Tg(ins:EGFP-T2A-CreER^{T2} ; actb2:LOXP-STOP-LOXP-DsRedEx)* fish. Statistical analysis was performed using a one-way ANOVA with Tukey post-hoc testing. *$p<0.05$ relative to 5 dpf timepoint. **E)** The frequency (%) of DsRed+ primary beta-cells (red squares) and secondary beta-cells (green circles) to total beta-cell number per principal islet section in 4-OHT treated 3 month *Tg(ins:EGFP-T2A-CreER^{T2} ; actb2:LOXP-STOP-LOXP-DsRedEx)* fish. **F)** The number of DsRed+ beta-cells (red squares) and EGFP+ beta-cells (green circles) in DMSO-treated 5, 12, and 30 dpf *Tg(ins:EGFP-T2A-CreER^{T2} ; actb2:LOXP-STOP-LOXP-DsRedEx)* fish. **G)** The frequency (%) of DsRed+ beta-cells (red squares) and EGFP+ beta-cells (green circles) to total beta-cell number per principal islet section in DMSO-treated 3 month old *Tg(ins:EGFP-T2A-CreER^{T2} ; actb2:LOXP-STOP-LOXP-DsRedEx)* fish. Box-and-whisker plots show median, circles and squares represent individual zebrafish. n = 3-17.

Increase in beta-cell number in response to glucose

It has previously been shown that glucose can increase beta-cell number in zebrafish (315,316). We treated *Tg(ins:EGFP-T2A-CreER^{T2} ; actb2:LOXP-STOP-LOXP-DsRedEx*) embryos with 4-OHT from 12-42 hpf to label primary beta-cells with DsRed. We then immersed fish in 0.5% glucose, 2% glucose, or 2% mannitol (osmolarity control) for 8 hrs starting at 6 dpf and quantified primary and secondary beta-cell number at 6.5 dpf (Figure 2-8A). We observed that animals in the 2% glucose bath had a significant increase in the number of beta-cells (51.2±1.6) in comparison to the unfed control (40.5±2.0), 2% mannitol controls (44.0±2.1), and 0.5% glucose bath (44.6±3.6) (Figure 2-8B). This increase was not due to increases in primary beta-cell number as we observed no significant increases in the total number of DsRed+ cells in the 2% glucose bath (20.5±1.2) compared to 0.5% glucose bath (17.0±2.4), unfed control (18.1±0.9), and 2% mannitol

control (18.9±1.9) (Figure 2-8C,D). We observed a significant increase in the number of secondary beta-cells in fish exposed to a 2% glucose bath (30.5±1.5) in comparison to unfed control (22.3±2.0), 0.5% glucose bath (27.6±2.7), and 2% mannitol control (25.1±1.9) (Figure 2-8C,D).

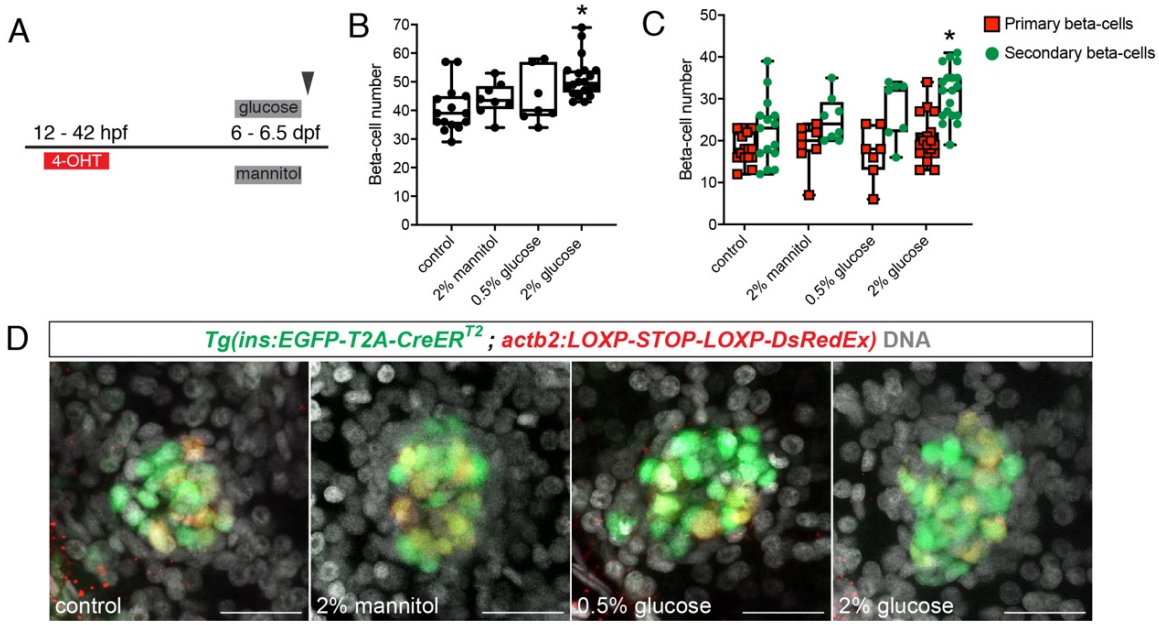

Figure 2-8 Glucose bath from 6-6.5 dpf leads to increases in total beta-cell number
A) Experimental timeline for lineage tracing primary and secondary beta-cells during a 0.5% glucose, 2% mannitol, or 2% glucose bath. 4-OHT was administered from 12 until 42 hpf in order to label primary beta-cells with DsRed. Fish were immersed in control (E3) solution, 0.5% glucose, 2% mannitol, or 2% glucose bath for 8 hrs starting at 6 dpf. Animals were imaged at 6.5 dpf. **B)** The total number of beta-cells in 6.5 dpf *Tg(ins:EGFP-T2A-CreER^{T2} ; actb2:LOXP-STOP-LOXP-DsRedEx)* fish in control solution, 0.5% glucose, 2% mannitol, or 2% glucose bath. **C)** The number of primary beta-cells (red boxes) and secondary beta-cells (green circles) in 6.5 dpf *Tg(ins:EGFP-T2A-CreER^{T2} ; actb2:LOXP-STOP-LOXP-DsRedEx)* fish in control solution, 0.5% glucose, 2% mannitol, or 2% glucose bath. Box-and-whisker plots show median, circles and squares represent individual zebrafish. **B,C)** Statistical analysis was performed using a one-way ANOVA with Tukey post-hoc testing. *p<0.05 relative to control. **D)** Confocal projections of *Tg(ins:EGFP-T2A-CreER^{T2} ; actb2:LOXP-STOP-LOXP-DsRedEx)* fish at 6.5 dpf immunostained for DsRed (red); beta-cells (green), primary beta-cells (red) and DAPI nuclear stain (DNA; grey). Scale bar = 20 μm. n = 7-19.

We questioned if longer exposure to 2% glucose could significantly increase primary beta-cells numbers. We exposed the 4-OHT-treated *Tg(ins:EGFP-T2A-CreER^{T2} ; actb2:LOXP-STOP-*

LOXP-DsRedEx) to a 2% glucose or mannitol bath from 6-8 dpf (Figure 2-9A). At 8 dpf, there is a significant increase in total beta-cell number in response to 2% glucose (58.8 ± 2.2) compared to the control group (50.4±2.3) and 2% mannitol control (47.8±3.3); however, no significant increases in primary beta-cell number were observed between the control group (23.2±0.8), 2% mannitol group (23.2±1.4), or fish immersed in 2% glucose (26.3±2.2), suggesting that 2% glucose does not significantly increase primary beta-cell number during early development (Figure 2-9B-D). We observed a significant increase in the number of secondary beta-cells (32.6±2.3) in fish exposed to a 2% glucose bath in comparison to the control group (27.2±2.4) and 2% mannitol control (24.7±3.5) (Figure 2-9C,D).

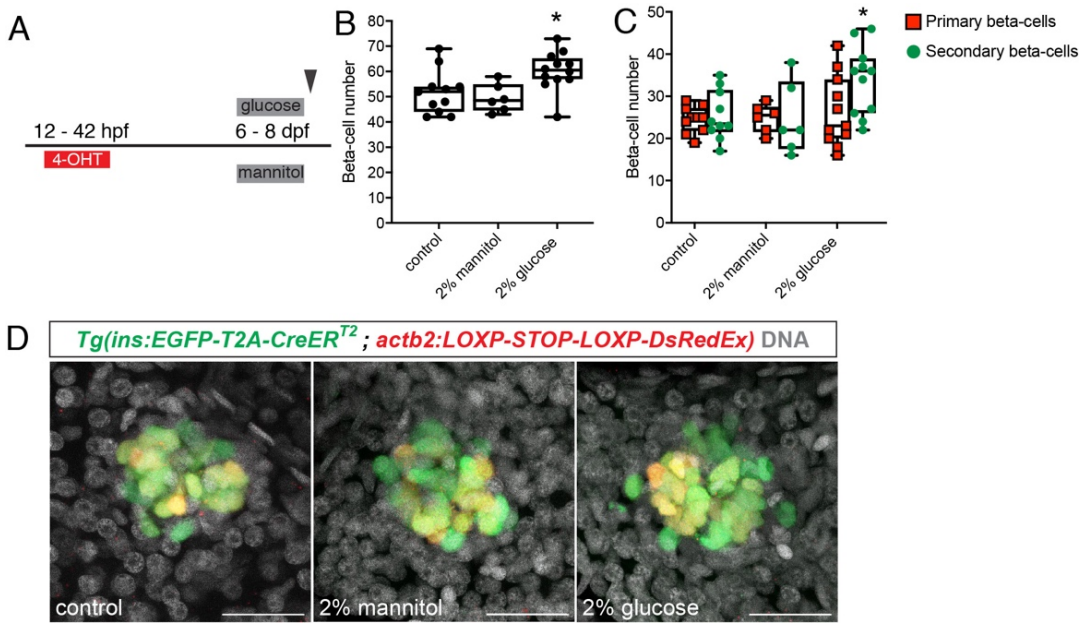

Figure 2-9 Glucose bath from 6-8 dpf leads to increases in total beta-cell number
A) Experimental timeline for lineage tracing primary and secondary beta-cells during a 2% mannitol or 2% glucose bath. 4-OHT was administered from 12-42 hpf in order to label primary beta-cells with DsRed. Fish were immersed in control (E3) solution, 2% mannitol, or 2% glucose bath for 2 days starting at 6 dpf. Animals were imaged at 8 dpf. **B)** The total number of beta-cells in 8 dpf *Tg(ins:EGFP-T2A-CreER^{T2} ; actb2:LOXP-STOP-LOXP-DsRedEx)* fish in control solution, 2% mannitol, or 2% glucose bath. **C)** The number of primary beta-cells (red boxes) and secondary beta-cells (green circles) in 8 dpf *Tg(ins:EGFP-T2A-CreER^{T2} ; actb2:LOXP-STOP-LOXP-DsRedEx)* fish in control solution, 2% mannitol, or 2% glucose bath. Box-and-whisker plots

show median, circles and squares represent individual zebrafish. **B,C)** Statistical analysis was performed using a one-way ANOVA with Tukey post-hoc testing. *p<0.05 relative to control. n = 6-11. **D)** Confocal projections of *Tg(ins:EGFP-T2A-CreER^{T2} ; actb2:LOXP-STOP-LOXP-DsRedEx)* fish at 8 dpf immunostained for DsRed (red); beta-cells (green), primary beta-cells (red) and DAPI nuclear stain (DNA; grey). Scale bar = 20 μm.

Ablation of primary beta-cells does not affect delta-cell or alpha-cell formation

We next sought to determine the effect of primary beta-cell ablation during early development. Using the double transgenic *Tg(ins:nfsB-Flag ; ins:TagRFP)* line, we administered 10 mM MTZ or 0.1% DMSO from 12 hpf until 30 hpf to *Tg(ins:nfsB-Flag ; ins:TagRFP).* In this model, beta-cells expressing the suicide gene *nfsB* would be ablated upon administration of MTZ (282). Because we administered MTZ during the development of primary beta-cells (which arise between 14-24 hpf) and not secondary beta-cells (which arise after 48 hpf), only primary beta-cells would be ablated. We also administered MTZ from 12 hpf until 30 hpf to *Tg(ins:TagRFP)* animals as an additional control (Figure 2-10A). We observed a significant decrease in the number of RFP+ beta-cells at 3 dpf in MTZ-treated *Tg(ins:nfsB-Flag ; ins:TagRFP)* (12.6±1.7) compared to MTZ treated *Tg(ins:TagRFP)* controls (31.5±1.7) and DMSO treated *Tg(ins:nfsB-Flag ; ins:TagRFP)* controls (34.8±1.4) (Figure 2-10B,E). We observed no significant differences in the number of somatostatin+ cells between DMSO-treated *Tg(ins:nfsB-Flag ; ins:TagRFP)* controls, MTZ-treated *Tg(ins:TagRFP)* controls, and beta-cell ablated animals at 3 dpf (28.0±1.8; 26.5±1.2; 22.7±2.1 respectively) or 5 dpf (41.3±2.5; 45.2±3.1; 42.2±3.6 respectively) (Figure 2-10E,F). We also observed no significant differences in the number of glucagon+ cells between DMSO-treated *Tg(ins:nfsB-Flag ; ins:TagRFP)* controls, MTZ-treated *Tg(ins:TagRFP)* controls, and the MTZ-treated *Tg(ins:nfsB-Flag ; ins:TagRFP)* fish at 3 dpf (17.6±2.1; 15.2±1.2; 11.2±2.2 respectively) or 5 dpf (30.6±1.4; 26.8±2.2; 28.2±1.2 respectively) (Figure 2-10D,E). Whole body insulin,

glucagon, and somatostatin expression at 3 dpf exhibited similar results to cell number counts (Figure 2-10C). These results suggest that the ablation of the primary beta-cells does not significantly affect delta-cell or alpha-cell formation.

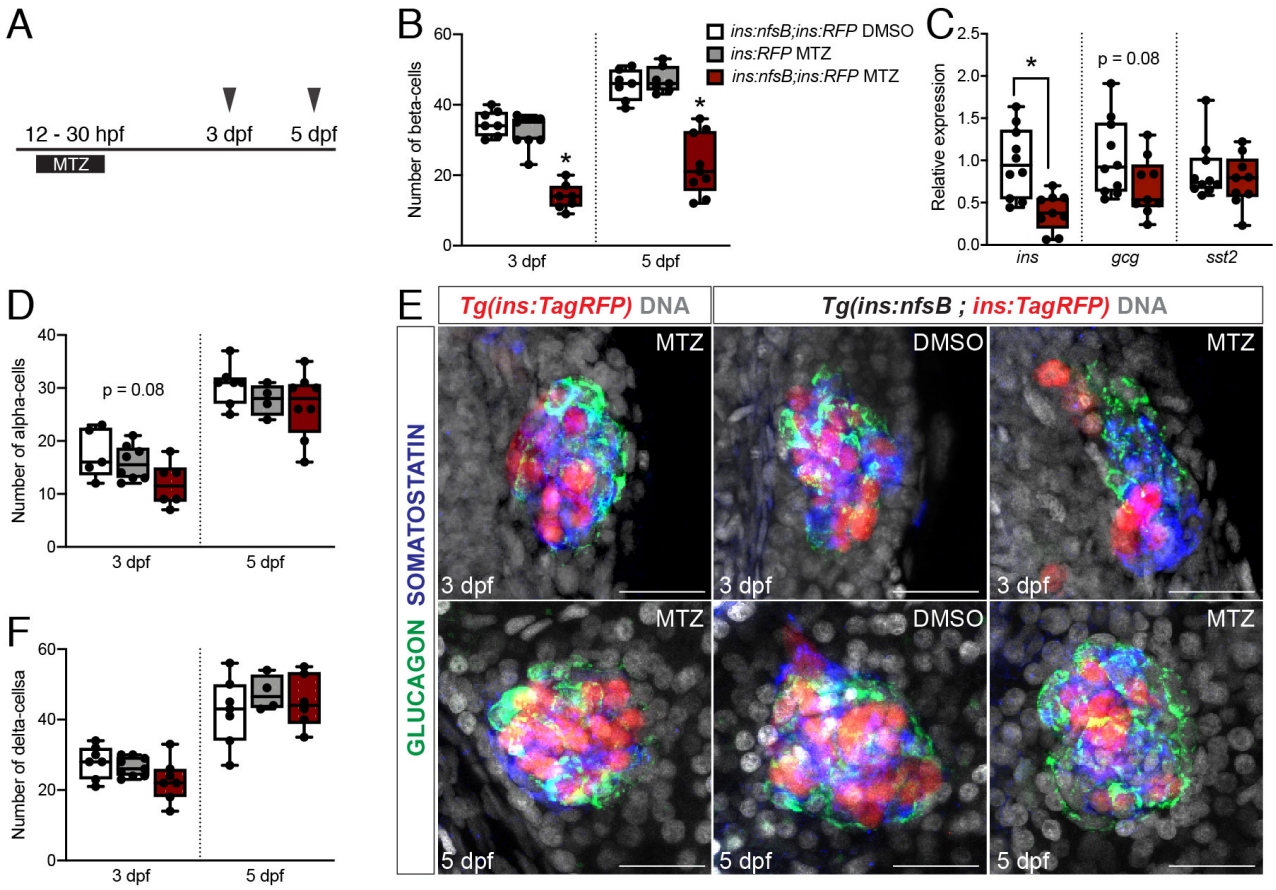

Figure 2-10 Ablation of primary beta-cells does not lead to significant differences in delta- or alpha-cell number at 3 dpf and 5 dpf

A) Experimental timeline for primary beta-cell ablation. Animals were treated with 0.1% DMSO or 10 mM MTZ from 12-30 hpf. Fish were imaged at 3 or 5 dpf. **B)** The total number of beta-cells in MTZ-treated *Tg(ins:nfsB-Flag ; ins:TagRFP)* (abbreviated *ins:nfsB; ins:TagRFP*) beta-cell ablated fish, MTZ-treated *Tg(ins:TagRFP)* control fish, and DMSO-treated *Tg(ins:nfsB; ins:TagRFP)* fish at 3 and 5 dpf. *p<0.05 relative to the DMSO-treated *Tg(ins:nfsB ; ins:TagRFP)*. **C)** Whole body mRNA expression of *ins*, *gcg*, and *sst2* expression at 3 dpf. *p<0.05 relative to control by Student's t-test. **D)** The total number of glucagon-expressing cells in MTZ-treated *Tg(ins:nfsB; ins:TagRFP)* beta-cell ablated fish, MTZ-treated *Tg(ins:TagRFP)* control fish, and DMSO-treated *Tg(ins:nfsB; ins:TagRFP)* fish at 3 and 5 dpf. **E)** Confocal projections of MTZ-treated *Tg(ins:nfsB; ins:TagRFP)* beta-cell ablated fish, MTZ-treated *Tg(ins:TagRFP)* control fish, and DMSO-treated *Tg(ins:nfsB; ins:TagRFP)* fish at 3 and 5 dpf, immunostained for glucagon (green), somatostatin (blue), and DAPI nuclear stain (DNA; grey). Scale bar = 20 μm.

F) The total number of somatostatin-expressing cells in MTZ-treated *Tg(ins:nfsB; ins:TagRFP)* beta-cell ablated fish, MTZ-treated *Tg(ins:TagRFP)* control fish, and DMSO-treated *Tg(ins:nfsB; ins:TagRFP)* fish at 3 and 5 dpf. For **B), D),** and **F)**, statistical analysis was performed using a one-way ANOVA with Tukey post-hoc testing at each timepoint.

Transcriptomes of primary and secondary beta-cells are not different in the adult pancreas

To explore the heterogeneity between beta-cells, we dissected the principal islet in 2.5 month old *Tg(ins:EGFP-T2A-CreER^{T2} ; actb2:LOXP-STOP-LOXP-DsRedEx)* adult fish, which had been treated with 4-OHT from 12-42 hpf to label primary beta-cells DsRed+. We performed fluorescent activated cell sorting (FACS) to isolate EGFP+ beta-cells. Single-cell libraries were generated using a 10× Genomics Chromium single cell 3′ kit. In total, 4,089 single cells were sequenced. Low-quality cells were excluded from analysis using Scater and Seurat. Following this, 3,008 cells were clustered using *k*-nearest neighbor algorithm and visualized using UMAP (Figure 2-11A). Cluster identity was inferred using differentially expressed genes (Figure 2-11H). Insulin was expressed by all cells, and *pdx1* and *neurod1* were detectable in the majority of cells (Figure 2-11B-D). A population of beta-cells had detectable *gcgb* and *sst1.1* expression (Figure 2-11E,F,H). We performed gene enrichment analysis on the 9 clusters to observe if biological functions were upregulated in certain clusters. We observed that clusters 0, 3, 4, and 6 genes are enriched ($p<0.001$) in pathways involved in protein folding responses and stress.

DsRed+ primary beta-cells were not localized in any cluster (Figure 2-11G). We utilized DsRed expression to identify primary beta-cells in our single cell RNA sequencing data set. Approximately 6% of the beta-cells are DsRed+. We then compared the transcriptome of the DsRed+ primary beta-cells and DsRed- cells and found *krt18a.1* and *grn2* were 1.26-fold and 1.24-fold upregulated in the DsRed+ primary beta-cells in comparison to the DsRed- cells. However, qPCR for *krt18a.1* and *grn2* in FACS purified DsRed+/EGFP+ primary and DsRed-/EGFP+

secondary beta-cells indicated no significant differences in gene expression between primary and secondary beta-cells (Figure 2-12A). There were also no significant differences in *ins*, *neurod1*, *pdx1*, or *gck* between primary and secondary beta-cells (Figure 2-12A). These data suggest that there are minimal differences in gene expression between primary and secondary beta-cells.

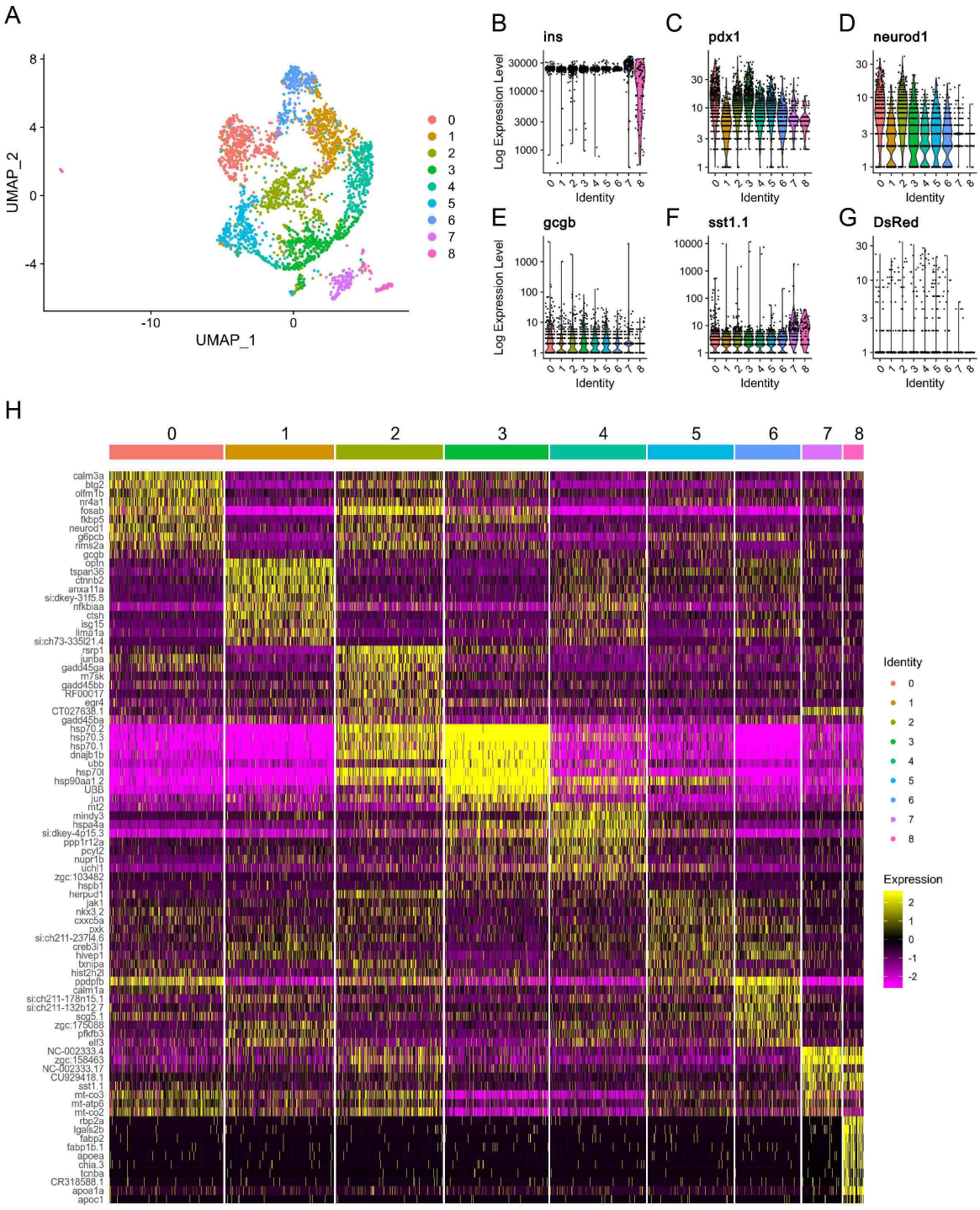

Figure 2-11 Single-cell RNA sequencing analysis of beta-cells from the principal islet
A) UMAP of 9 clusters for all cells positive for EGFP (beta-cells) isolated and dispersed from *Tg(ins:EGFP-T2A-CreER^{T2} ; actb2:LOXP-STOP-LOXP-DsRedEx)* 2.5 month old adult zebrafish that were treated with 4-OHT from 12-42 hpf. **B-G)** Single cell expression of **B)** *insulin,* **C)** *pdx1,*

D) *neurod1,* **E)** *gcgb,* **F)** *sst1.1*, and **G)** *DsRed* across all clusters. **H)** Top ten differentially expressed genes in beta-cell clusters.

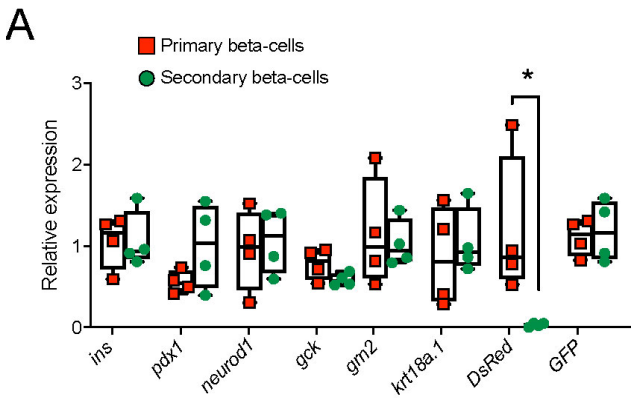

Figure 2-12 Relative expression of beta-cell markers, *grn2,* and *krt18a.1* in isolated DsRed+/EGFP+ primary beta-cells and EGFP+ secondary beta-cells
A) Relative expression of *ins, pdx1, neurod1, gck, grn2, krt18a.1, DsRed* and *GFP* in isolated primary beta-cells (red squares) and secondary beta-cells (green circles) in 3 month old *Tg(ins:EGFP-T2A-CreER^{T2} ; actb2:LOXP-STOP-LOXP-DsRedEx)* zebrafish. *p<0.05 by Student's t-test.

2.4 Discussion

Dorsal derived primary beta-cells and ventral derived secondary beta-cells arise at different timepoints during development and from different precursor pools (226,268). In this study, we sought to characterize the primary beta-cells arising from the dorsal bud and the secondary beta-cells arising from the ventral bud during development and in the adult pancreas.

We established novel transgenic lines to differentially label and ablate primary and secondary beta-cells. However, only our *Tg(ins:EGFP-T2A-CreER^{T2})* line was chosen for our labelling experiments. Given the caveats of the Cre driver lines, we were unable to validate the efficiency of our *Tg(ins:FRT:EGFP:LOXP:IRES:FLP:LOXP:FRT:RFP), Tg(ins:FRT:EGFP:LOXP:IRES:FLP:LOXP:FRT:nfsB-T2A-RFP),* and *Tg(ins:FRT:nfsB-T2A-EGFP:LOXP:IRES:FLP:LOXP:FRT:RFP*) transgenic lines in labelling primary and secondary beta-cells.

The issues regarding the ubiquitous Cre driver lines may be partly due to the use of minimal promoters and random transgene insertion, both of which may cause leaky gene expression. This may explain the results of the *Tg(hsp70l:Cre)* line which exhibited leaky activation of the promoter without heat shock. Leaky expression from the *hsp70l* promoter has also been previously described in other transgenic models (299). Dually inducible systems can significantly reduce leakiness, although transgene expression may still be subject to position-effect variegation (whereby variable changes (silencing) within the transgene can occur among cells of an organism) and position effects, both of which are caveats of random integration(s) of the transgenes which occurs during Tol2 transgenesis (303,304,317). The use of minimal promoters may also affect the ubiquity of expression from the promoter. This may explain the results we observed in the *Tg(hsp70l:mCherry-T2A-CreER^{T2})* and the *Tg(-3.5ubb:CreER^{T2}, myl7:EGFP)* lines. Hence, expression from minimal promoters randomly integrated into the genome may not faithfully recapitulate endogenous expression. In the future, targeted transgene insertion, particularly at the endogenous locus, may mitigate the caveats of random insertions generated via the Tol2 transgenesis method.

While we were unable to utilize our *Tg(ins:FRT:EGFP:LOXP:IRES:FLP:LOXP:FRT:RFP), Tg(ins:FRT:EGFP:LOXP:IRES:FLP:LOXP:FRT:nfsB-T2A-RFP),* and *Tg(ins:FRT:nfsB-T2A-EGFP:LOXP:IRES:FLP:LOXP:FRT:RFP*) transgenic lines, our *Tg(ins:EGFP-T2A-CreER^{T2})* showed more promise as a lineage tracing model. We observed that EGFP expression faithfully recapitulates insulin expression in 8 month old *Tg(ins:EGFP-T2A-CreER^{T2})* adults. Administration of 4-OHT from 12-42 hpf labelled primary beta-cells with DsRed in our *Tg(ins:EGFP-T2A-CreER^{T2} ; actb2:LOXP-STOP-LOXP-DsRedEx)* lineage tracing line. It should be noted that we observed leaky activation of the CreER^{T2} in which 0.8% of adult beta-

cells are labelled without the addition of 4-OHT. The leaky CreER^{T2} activation in the *Tg(ins:EGFP-T2A-CreER^{T2})* transgenic line represents a caveat of this system and interpretation of our results should be made with this limitation in mind.

We found that during the first 12 days of development, primary beta-cell number is stable indicating limited replicative capacity. This is consistent with previous findings (226,269). We observed a significant increase in the number of primary beta-cells at 30 dpf in comparison to 5 and 12 dpf, suggesting that primary beta-cells can proliferate later during development. This increase in primary beta-cells may be the result of the change in diet at 15 dpf, in which we incorporate hatched brine shrimp. A previous study has shown that after a switch to a high calorie diet (hatched brine shrimp) at 15 dpf, beta-cell proliferation increases significantly in comparison to animals that were fed a low calorie diet (316). Given the proliferative response of beta-cells to nutrition, we sought to stimulate beta-cell proliferation at an earlier developmental timepoint by placing beta-cells in a 2% glucose bath. Glucose has been shown to increase beta-cell number in zebrafish larvae (315,316). We did not observe an increase in the number of primary beta-cells after an 8 hr or 48 hr 2% glucose bath, although we observed an increase in the number of secondary beta-cells. These results suggest that a 2% glucose bath cannot significantly increase primary beta-cell number during early development.

In the adult animal, we observed that 6.3% of the principal islet is composed of DsRed+ beta-cells. A proportion of these DsRed+ cells may represent secondary beta-cells that had leaky CreER^{T2} activation at some point during their life cycle. Given that this leaky activation is infrequent (0.8%), the majority of the DsRed+ beta-cells in the 4-OHT-treated *Tg(ins:EGFP-T2A-CreER^{T2} ; actb2:LOXP-STOP-LOXP-DsRedEx)* adult animals represents primary beta-cells. We performed single cell RNA sequencing to characterize the transcriptome of the primary and

secondary beta-cells. We did not identify significant differences in the transcriptional profiles of primary and secondary beta-cells, suggesting that pancreatic origin does not lead to a distinct gene signature in primary and secondary beta-cells in the adult pancreas. While differences in primary and secondary beta-cells have been described at 12 dpf (226), experimental differences in time of sampling (12 dpf and adult) and the experimental models could explain this discrepancy in results. While we did not detect significant differences between transcriptomes in primary and secondary beta-cells, we did observe transcriptional heterogeneity between single beta-cells. Clustering revealed differentially expressed genes between 9 clusters. Gene enrichment analysis revealed that some clusters had upregulated genes involved in protein folding responses and stress. This isn't particularly surprising as it's been previously shown that insulin production itself is a significant stress under basal conditions in beta-cells (318). Differential gene expression between clusters may be due to multiple factors such as cell-to-cell contacts or natural fluctuations in gene expression. For example, the dynamic nature of gene expression at the *Ins2* locus was demonstrated in a live cell imaging study of dispersed primary beta-cells from *Ins2*$^{GFP/+}$ mouse islets, whereby beta-cells showed bursts of GFP (*Ins2* promoter) activity (112). Hence it is possible that the 9 clusters we identified in our data set are not static populations, but rather represent dynamic beta-cell states.

It is still unclear if there is a biological reason for the early appearance of primary beta-cells in the zebrafish. We observed that the ablation of the primary beta-cell population does not lead to any significant changes in delta-cell or alpha-cell number during early pancreas formation, although we observed a trending decrease ($p=0.08$) in the alpha-cells. Interestingly, a previous study found that morpholino knockdown of insulin or blockage of the insulin receptor caused a decrease in the number of glucagon-expressing cells at 3 dpf (319), suggesting some dependence of alpha-cell formation on insulin signalling. Insulin signalling during early mouse endocrine

development has also been shown to play a role in alpha-cell formation. Insulin (*Ins1*$^{-/-}$/*Ins2*$^{-/-}$) deficient neonatal mouse islets display a significant decrease in the relative proportion of glucagon-expressing cells in comparison to *Ins1*$^{+/+}$/*Ins2*$^{+/+}$ controls (320). While we did not observe significant differences in alpha-cell formation at 3 dpf, this may be explained by the appearance of secondary beta-cells after 2 dpf which would not have been ablated in our study. Assessing alpha-cell formation in our model at an early timepoint before the appearance of secondary cells would help clarify if the ablation of primary beta-cells has an effect on early alpha-cell formation. Understanding the role of insulin during islet endocrine formation may be useful to improve the protocols for differentiating human pluripotent stem cells into functional human beta-cells *in vitro*.

In summary, we provide evidence that primary beta-cells are present in the adult principal islet. While transcriptome heterogeneity exists within the principal islet, the primary and secondary beta-cells are transcriptionally similar, indicating that ontogeny and time of formation does not lead to a distinct molecular signature in beta-cells. Our work also establishes a Cre/LoxP lineage tracing tool that will be useful in tracking beta-cells in future studies.

Chapter 3: Vegfa/vegfr2 signalling is necessary for zebrafish islet vessel development, but is dispensable for beta-cell and alpha-cell formation

3.1 Background

The pancreas contains both endocrine and exocrine components. The exocrine pancreas constitutes the majority of the pancreas and produces digestive enzymes which are delivered to the duodenum. The endocrine pancreas consists of the islets of Langerhans that are scattered throughout the exocrine tissue. The primary function of pancreatic islets is to regulate blood glucose levels through the secretion of hormones. The islet consists of 5 endocrine cells types, the insulin secreting beta-cells, glucagon secreting alpha-cells, somatostatin secreting delta-cells, ghrelin secreting epsilon-cells, and the pancreatic polypeptide secreting PP-cells.

Pancreatic islets are highly vascularized. Studies in mice indicate that reciprocal interactions between endothelial cells and islets are important for proper islet development, maturation, and function (69,71). During murine embryogenesis, endothelial cells are important in pancreas specification. The maintenance and induction of key pancreatic transcription factors PDX1 and PTF1A is dependent on signals from aortic endothelial cells, without which pancreas development is severely impaired (69–71). In addition to initiating pancreas morphogenesis, endothelial cells also communicate with mature islet cells. These interactions between islet cells and endothelial cells are primarily mediated by vascular endothelial growth factor-A (VegfA) signalling (80). Lack of islet VegfA in the early murine pancreas or in mature beta-cells results in a significant loss of intra-islet capillaries, impairments in insulin secretion, and glucose intolerance (78–80,321,322).

While the role of endothelial cells on islet development has been well studied in murine models, it is less documented in zebrafish. Zebrafish is an ideal organism to study islet vessel development due to their transparency and rapid *ex-utero* development. Zebrafish pancreas development shares many similarities with mammals suggesting that studies within this system can have broadly relevant insights (236). While it has been previously observed that some insulin-expressing cells still develop in *cloche* mutants which lack endothelial cells (225), signals involved in zebrafish islet vascularization and its relationship with islet development are not completely understood.

In this study, we used a combination of genetic knockdown and pharmaceutical techniques to assess the role of *vegfaa* and *vegfab* in zebrafish islet vessel development and endocrine pancreas formation. We demonstrate that while Vegfaa/Vegfab-Vegfr2 signalling is necessary for proper islet vessel development, it is dispensable for the formation of both beta-cells and alpha-cells.

3.2 Methods

Zebrafish Lines

Adult zebrafish were housed as described in Chapter 2. The following zebrafish lines were used in experiments in Chapter 3: *Tg(fli1a:EGFP)*^{y1} (323) and *Tg(-1.2ins*:*TagRFP)*^{vu514} (315), *Tg(-1.2ins:htBid*$^{TE\text{-}ON}$*)*^{vu524} (280), and *Tg(-1.2ins:H2BmCherry)*^{vu513} (280). Fertilized eggs were collected from adult zebrafish and placed in E3 media (5 mM NaCl, 0.17 mM KCl, 0.33 mM $CaCl_2$•$2H_2O$, 0.33 mM $MgSO_4$) at 28°C in an incubator with a 14 hr light /10 hr dark cycle. After 8 hpf, embryos were treated with 0.003% 1-phenyl-2-thiourea (PTU) in E3 media to inhibit melanin pigment formation.

Morpholino and mRNA Injections

Microinjection was performed using a MM-33 micromanipulator (Sutter Instrument, Novato, CA, USA) and a PicoSpritzer III pressure injector (Parker Hannifin Corp, Pine Brook, NJ, USA). Morpholinos were obtained from GeneTools LLC (Philomath, OR, USA). We injected previously described translation blocking morpholinos into one-cell stage embryos: 10 ng of MO1-vegfaa translation blocking (5′-GTATCAAATAAACAACCAAGTTCAT-3′) (324), 3 ng of MO1-vegfab translation blocking (5'-GGAGCACGCGAACAGCAAAGTTCAT-3') (325); 4.5 ng of MO2-kdr translation blocking (5'-TATGCTCTATTAGATGCCTGTTTAA-3') (325), and 4.5 ng of MO1-kdrl translation blocking (5'-CCGAATGATACTCCGTATGTCAC-3') (326). Our control was a standard scrambled morpholino (5'- CCTCTTACCTCAGTTACAATTTATA-3') injected at 10 ng. All morpholino injections were repeated three independent times. For H2B-BFP mRNA injections, we cloned a T7 promoter upstream of a human histone 2B fused to EBFP2. The pEBFP2-H2B-BFP was a gift from Michael Davidson (Addgene plasmid, 55243). To generate mRNA, we used the mMESSAGE mMACHINE T7 Transcription Kit as per the manufacturer instructions (Life Technologies, AM1344). We injected 100 pg H2B-BFP mRNA into the one cell stage of zebrafish embryos and kept the embryos at 28°C in the dark until imaging.

Chemical Treatments

SU5416 (Sigma-Aldrich, Oakville, ON, Canada S8442) was dissolved in DMSO to 40 mM and stored at -20°C. Embryos were treated with 1 μM SU5416 or 0.1% DMSO in E3 media beginning at 12 hpf up until imaging at 72 hpf or at 72 hpf up until imaging at 96 hpf. The drug solution was refreshed every 24 hrs. To induce secondary islet formation, we administered N-[N-

(3,5-Difluorophenacetyl-L-alanyl)]-S-phenylglycine *t*-Butyl Ester (DAPT) (EMD Millipore, 565770), γ-secretase inhibitor to block Notch signalling. DAPT was dissolved in DMSO to 10 mM and stored at -20°C. The embryos were treated with 20 μM DAPT, 100 μM DAPT, or 1% DMSO in E3 media beginning at 3 dpf until imaging at 4.5 dpf. The embryos were kept at 28°C in the dark until imaging. To induce beta-cell ablation, larvae were treated with doxycycline hyclate (DOX) (Sigma-Aldrich D9891) at 50 μM and tebufenozide (TBF) (EMD Millipore, 31652) at 25 μM at 3 dpf until 5 dpf. Drugs were prepared as previously described (280). The drug solution was refreshed after 24 hrs. The embryos were kept at 28°C in the dark during DOX/TBF administration.

FACS

We used 200 *Tg*(*fli1:EGFP ;ins:TagRFP)* embryos to isolate RFP+ beta-cells at 2 dpf and 3 dpf. The samples were dissociated in 0.25% trypsin at 37°C for 30 min. The cells were filtered with a 40 μm nylon strainer. RFP+ beta-cells were sorted using a BD Influx Cell Sorter (BD Biosciences, Mississauga, ON, Canada). For isolating adult beta-cells, pancreatic tissue was dissected from *Tg*(*ins:TagRFP*) fish and digested as previously described (306). RFP-expressing beta-cells were sorted using BD Influx Cell Sorter (BD Biosciences).

cDNA synthesis and RT-PCR

RNA was isolated from 500-2500 isolated RFP-expressing beta-cells using TRIzol (Invitrogen, Carlsbad, CA, USA). cDNA was prepared using the iScript cDNA synthesis kit (Invitrogen). For RT-PCR of *vegfaa* and *vegfab*, Accuprime Taq DNA Polymerase (Invitrogen) was used, and end products were run on a 1% agarose gel. For qPCR, cDNA was amplified with SsoFast EvaGreen Supermix (BioRad, Richmond, CA, USA) on a CFX96 Touch™ Real–Time PCR Detection System (BioRad). The relative expression of each sample was determined after

normalization to *ef1α*. RT-qPCR controls are described in Chapter 2. Primers for RT-PCR are listed: *vegfaa* forward 5'-AGAAAGAAAACCACTGTGAG-3'; *vegfaa* reverse 5'-AGGAATGTTCTTCCTTAGGT-3'; *vegfab* forward 5'-TGCTGAACACAGTGAATGCCAG-3'; *vegfab* reverse 5'-ACATCCATCTCCAACCACTTCAC-3'; *ef1α* forward 5'-TCAAGGACATCCGTCGTGGTA-3'; *ef1α* reverse 5'-ACAGCAAAGCGACCAAGAGG. Primers for RT-qPCR for *ins*, *pdx1*, *neurod1*, and *ef1α* are listed in Chapter 2 Table 2-3. PCR cycling conditions were as follows: 3-min denaturation step at 95 °C, followed by 40 cycles of denaturation at 95 °C for 15 s, annealing at 55 °C for 15 s, and extension at 72 °C for 25 s.

Immunofluorescence

Zebrafish embryos were anaesthetized with ethyl 3-aminobenzoate methanesulfonate (MS-222, 0.01% w/v) and then fixed with 4% paraformaldehyde overnight at 4°C. Embryos were washed three times with 0.3% Triton X-100 in PBS. The embryos were blocked for 1 hr in PBS with 5% donkey serum (Jackson Immunoresearch Laboratories, West Grove, PA, USA) and 0.3% Triton X-100. Both primary and secondary antibodies were incubated overnight at 4°C. Washes were done with 0.1% Tween/PBS for 30 min three times. Antibodies used were mouse anti-glucagon antibody (1:500, Sigma G2654) and goat anti-mouse Alexa Fluor 647 antibody (1:1000, Life Technologies A21236). Cell nuclei were visualized with 4',6-diamidino-2-phenylindole (DAPI) DNA stain (1:1000, Thermo Fisher Scientific D1306) or TO-PRO™-3 Iodide stain (1:1000, Thermo Fisher Scientific T3605). Samples were mounted in 75% glycerol on concave glass slides (EISCO). All fluorescent images were obtained with a LSM800 Zeiss upright confocal and imaged with a 40X objective. Whole mount tissues were scanned by confocal microscopy. Cell numbers were counted manually. For endothelial cell counts, endothelial cells that were

directly adjacent to islet cells (within 1 μm) were counted. In the DOX/TBF beta-cell ablation experiment, endothelial cells located within the islet or adjacent to alpha-cells (within 1 μm) were counted. The Shapiro–Wilk normality test was used to assess normality of data distribution and when all groups passed the test for normality, a Student's t-test or one-way ANOVA and Tukey post-hoc test were used for statistical analysis for cell counts.

3.3 Results

Endocrine pancreas is highly vascularized

To characterize the formation of islet vessel development, we crossed *Tg(fli1:EGFP)* and *Tg(ins:TagRFP)* zebrafish to create a double transgenic line *Tg(fli1:EGFP; ins:TagRFP)* that labelled the endothelial/hematopoietic cells green and beta-cells red. Beta-cells developed adjacent to vessels at 17 hpf (Figure 3-1A). As early as 40 hpf, endothelial cells were seen within the beta-cell core (Figure 3-1B). At 72 hpf, the primary islet was highly vascularized in comparison to surrounding tissue (Figure 3-1C). At 7 dpf, secondary islets were often observed adjacent to blood vessels (Figure 3-1D).

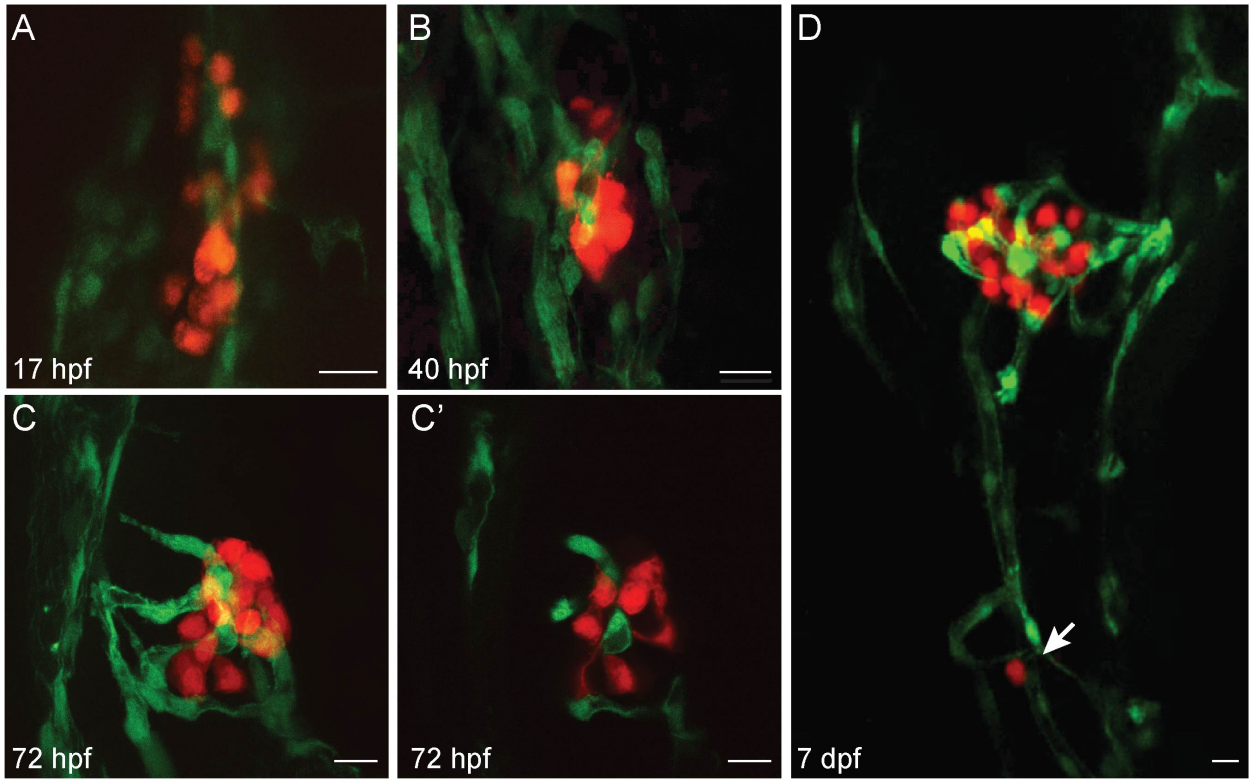

Figure 3-1 The endocrine pancreas develops adjacent to vessels and is highly vascularized
A-C) Confocal projections of the pancreatic islet at 17 hpf, 40 hpf, and 72 hpf in *Tg(fli1:EGFP; ins:TagRFP);* endothelial cells (green) and beta-cells (red). **C'**) Confocal section of projection in **C)**. **D)** Confocal projection of 7 dpf *Tg(fli1:EGFP; ins:TagRFP)* pancreas. Arrow indicates secondary islet. n = 3-8. Scale bar = 10 μm.

Vegf signalling is essential for islet vessel development, but not beta- and alpha- cell formation

To determine if Vegf signalling is required for islet vascularization, we administered a Vegf receptor competitive inhibitor SU5416. *Tg*(*fli1:EGFP; ins:TagRFP*) embryos were treated with SU5416 at 12 hpf until imaging at 72 hpf to assess the development of islet vessels. SU5416 treatment from 12 to 72 hpf reduced islet vessel density (Figure 3-2A-D). This reduction in islet vessels may partially be caused by a failure of the sub-intestinal vein to form which partially gives rise to the pancreatic vessels (327) (Figure 3-3A,B). No significant changes in beta- and alpha-cell

numbers were observed in the SU5416-treated embryos (25.2±2.6; 18.8±2.8) in comparison to the DMSO-treated (27.5±2.5; 19.2±2.0) and untreated wild-type (27.7±2.9; 18.5±2.4) control embryos at 72 hpf (Figure 3-2E,F). Islet architecture was not affected in vessel deficient embryos as the majority of alpha-cells were observed on the islet mantle with beta-cells localized to the islet core in both the control and SU5416-treated embryos (Figure 3-2A-C).

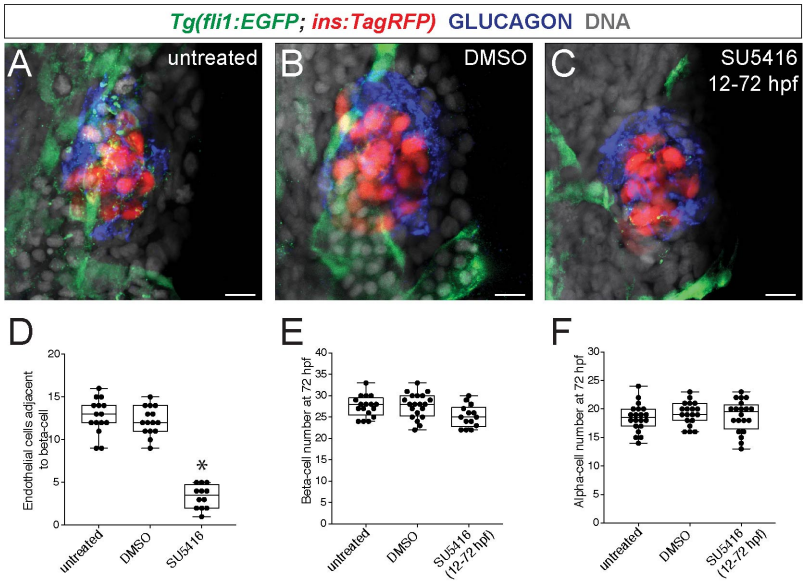

Figure 3-2 Inhibiting Vegf signalling does not affect beta- and alpha-cell formation
A-C) Confocal projections of 72 hpf *Tg(fli1:EGFP; ins:TagRFP)* untreated, DMSO-treated, and SU5416-treated embryos from 12 to 72 hpf; endothelial cells (green), beta-cells (red), and DAPI nuclear stain (DNA; grey). Alpha-cells are labelled with a glucagon (GCG) antibody (blue). **D)** The number of endothelial cells adjacent to beta-cells in untreated, DMSO-treated, and SU5416-treated embryos from 12 to 72 hpf. **E-F)** The number of beta-cells and alpha-cells in *Tg(fli1:EGFP; ins:TagRFP)* untreated, DMSO-treated, and SU5416-treated embryos treated from 12 to 72 hpf. n = 14-20. Statistical analysis was performed using a one-way ANOVA with Tukey post-hoc testing *$p<0.05$ compared to untreated. Box-and-whisker plots show median, and circles represent individual zebrafish. Scale bar = 10 μm.

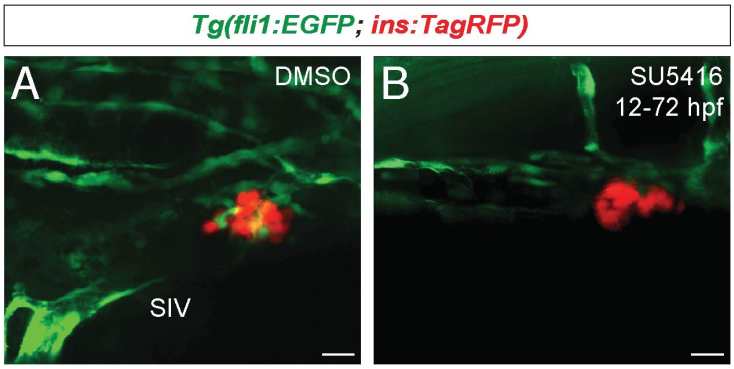

Figure 3-3 Sub-intestinal vein fails to form in SU5416-treated embryos
A-B) Confocal projections of 72 hpf *Tg(fli1:EGFP; ins:TagRFP)* embryos treated with DMSO or SU5416; endothelial cells (green) and beta-cells (red). SIV = sub-intestinal vein. n = 5-7. Scale bar = 20 µm.

To test if continued Vegf signalling is needed to sustain islet vessels, we treated embryos with SU5416 at 72 hpf until imaging at 96 hpf. We observed a reduction of islet vessels suggesting that continued Vegf signalling is necessary to sustain islet vasculature (Figure 3-4A-C). No significant changes in beta-cell numbers were observed in these SU5416-treated embryos (26.3±1.8) in comparison to DMSO-treated and untreated controls (28.5±1.6; 28.7±2.3) (Figure 3-4D).

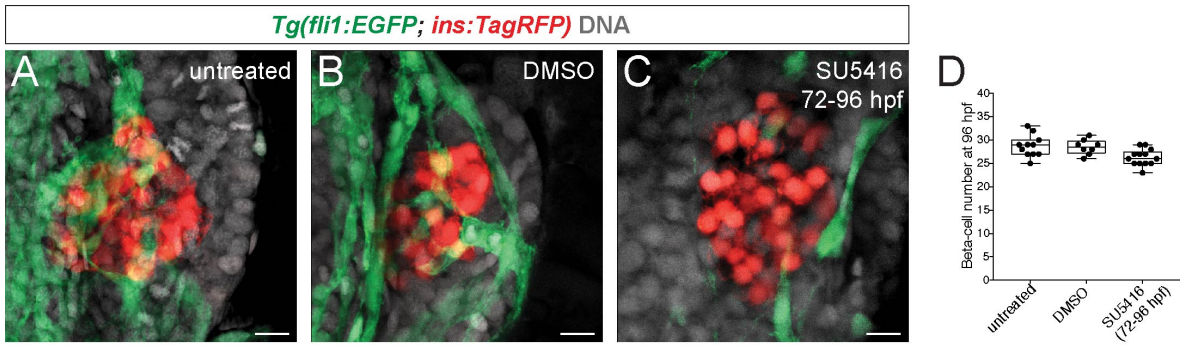

Figure 3-4 Inhibiting Vegf signalling from 72 to 96 hpf does not significantly affect beta-number
A-C) Confocal projections of 96 hpf *Tg(fli1:EGFP; ins:TagRFP)* untreated, DMSO-treated, and SU5416-treated embryos from 72 to 96 hpf; endothelial cells (green), beta-cells (red), and DAPI (DNA; grey). **D)** The number of beta-cells in *Tg(fli1:EGFP; ins:TagRFP)* untreated, DMSO-treated, and SU5416-treated embryos from 72 to 92 hpf. n = 8-13. Box-and-whisker plots show median, and circles represent individual zebrafish. Statistical analysis was performed using a one-way ANOVA with Tukey post-hoc testing. Scale bar = 10 µm.

We also administered SU5416 at 4.5 dpf until imaging at 6 dpf to determine if duct derived secondary islets form in vessel deficient fish. The proportion of fish that developed secondary islets did not change between SU5416-treated (21.4%) and DMSO-treated embryos (25.0%). (Figure 3-5A,B). We also examined secondary islet formation in SU5416-treated embryos given a γ-secretase Notch inhibitor (DAPT), which has been previously shown to stimulate the appearance of secondary islets in zebrafish (227,328). From 3 dpf until 4.5 dpf, we administered DAPT or co-administered DAPT and SU5416 to *Tg(neurod1:GFP)* fish, a transgenic line that marks early pan-endocrine cells, thereby allowing us to capture early secondary islet formation. While there were no significant differences in secondary islet formation in the lower DAPT dose (20 μM) in comparison to untreated and DMSO-treated controls, we did observe a significant increase in the number of secondary islets in fish treated with 100 μM DAPT (Figure 3-5D-J). The addition of SU5416 did not alter the effect of DAPT treatment on secondary islet formation (Figure 3-5D-J). These results suggest that Vegf signalling is dispensable for early secondary islet formation.

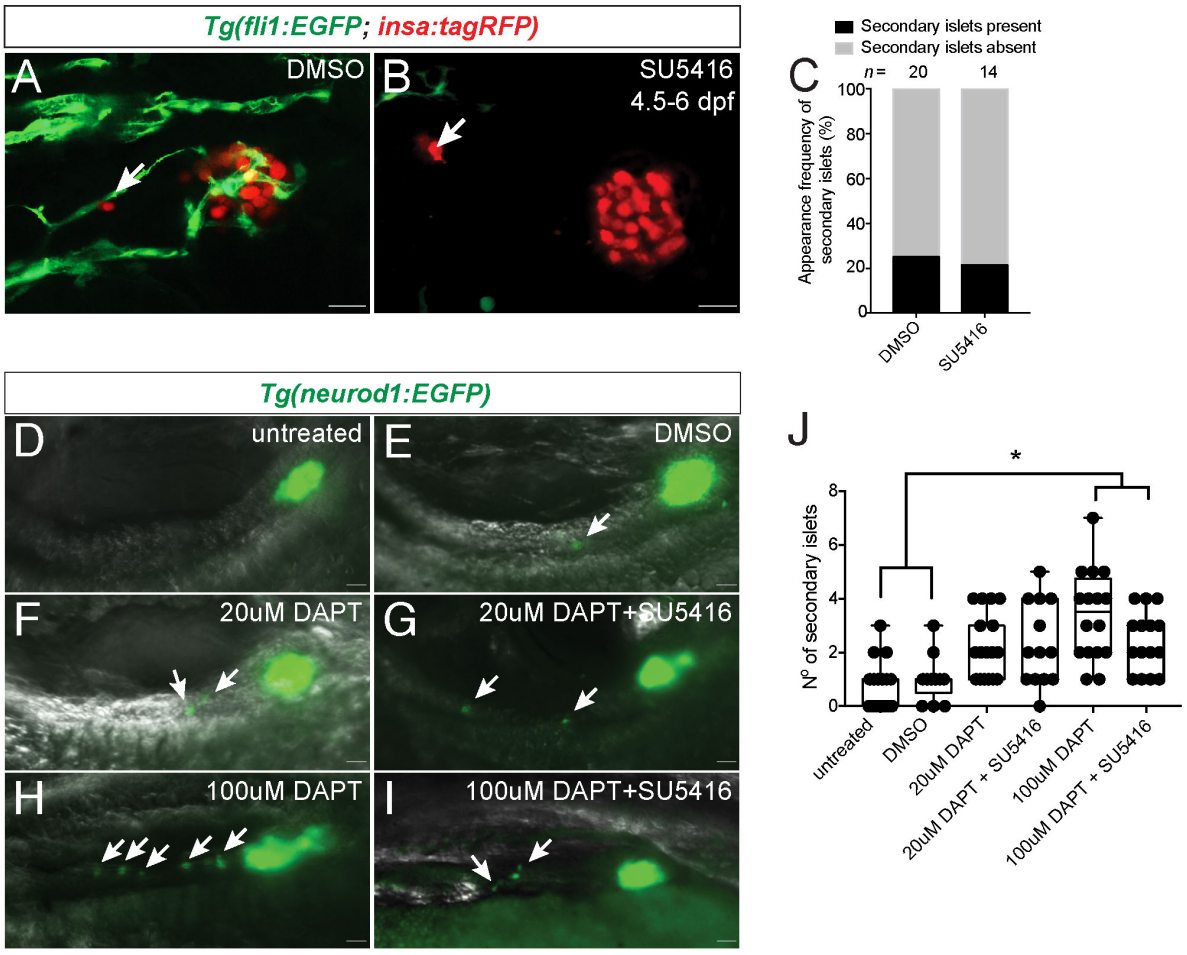

Figure 3-5 Secondary islets form in SU5416-treated fish
A-B) Confocal projections of 6 dpf *Tg(fli1:EGFP; ins:TagRFP)* zebrafish treated with DMSO or SU5416 from 4.5 dpf until 6 dpf. White arrowheads indicate secondary islets; endothelial cells (green) and beta-cells (red). **C)** Frequency of secondary islets in 6 dpf *Tg(fli1:EGFP; ins:TagRFP)* zebrafish treated with DMSO or SU5416 from 4.5 dpf until 6 dpf. n = 14-20. **D-I)** Images of *Tg(neurod1:GFP)* untreated, DMSO-treated, DAPT-treated, or DAPT and SU5416-treated embryos from 3 dpf until 4.5 dpf. White arrowheads indicate secondary islets. **J)** The number of secondary islets in untreated, DMSO-treated, DAPT-treated, or DAPT and SU5416-treated embryos. Box-and-whisker plots show median, and circles represent individual zebrafish. n = 13-19. *p<0.05 by one-way ANOVA and Tukey post-hoc test. Scale bar = 20 μm.

Combined knockdown of *vegfaa* and *vegfab* causes a reduction of islet vessels

To identify potential mediators of signals responsible for islet vascularization, we isolated RFP+ beta-cells from *Tg(ins:TagRFP)* larval fish and adult islets using fluorescence-activated cell

sorting (FACS). We found that *vegfaa* was expressed in beta-cells isolated from fish at 2 dpf and 3 dpf. We also detected *vegfaa* and *vegfab* in adult isolated beta-cells (Figure 3-6A). We next injected previously validated translation blocking morpholinos against *vegfaa* and *vegfab* into *Tg*(*fli1:EGFP; ins:TagRFP)* embryos. In non-injected control zebrafish and those injected with scrambled control morpholinos, we observed greater than 7 endothelial cells adjacent to beta-cells, whereas those animals injected with morpholinos against *vegfaa* had either a mild reduction of islet vessels (between 4-7 endothelial cells adjacent to beta-cells) or a severe reduction of islet vessels (less than 4 endothelial cells adjacent to beta-cells) at 72 hpf (Figure 3-6B,D-F). A small percentage of *vegfab* morpholino knockdown embryos exhibit a mild reduction in islet vessels (Figure 3-6B,G). Combined knockdown of *vegfaa* and *vegfab* (*vegfaa/vegfab*) resulted in a more severe phenotype in comparison to the single knockdown embryos suggesting that both *vegfaa* and *vegfab* are important for islet vessel development (Figure 3-6B,H). In the embryos that demonstrated a reduction or absence of islet vessels in the single *vegfaa* or *vegfab* morpholino knockdown or the double *vegfaa/vegfab* morpholino knockdown, no significant changes in beta-cell numbers were observed in these *vegfaa* (27.0±2.2), *vegfab* (25.7±2.5), and *vegfaa*/*vegfab* (23.3±2.3) morpholino injected embryos in comparison to the scrambled injected or non-injected controls (25.9±2.9; 25.5±3.6) (Figure 3-6C).

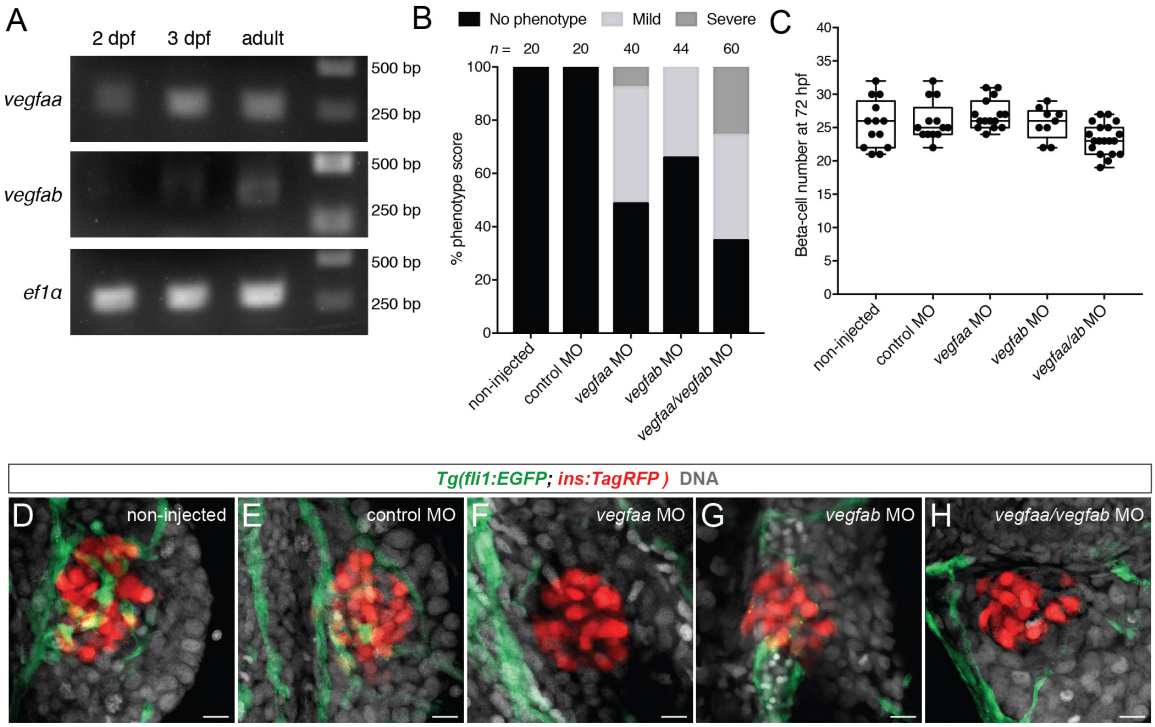

Figure 3-6 Vegfaa and Vegfab are necessary for islet vessel development
A) RT-PCR of *vegfaa* and *vegfab* on sorted 2 dpf, 3 dpf, and adult beta-cells. **B)** Phenotypic score of islet vessels in non-injected, control morpholino, and *vegfaa*, *vegfab*, or *vegfaa/vegfab* morpholino injected *Tg(fli1:EGFP; ins:TagRFP)* embryos. Phenotypes are scored such that no phenotype is comparable to wild-type (more than 7 endothelial cells adjacent to beta-cells), mild phenotype (4-7 endothelial cells adjacent to beta-cells), and severe phenotype (less than 4 endothelial cells adjacent to beta-cells). **C)** The number of beta-cells in 72 hpf *Tg(fli1:EGFP; ins:TagRFP)* control and morpholino injected embryos. In the *vegfaa*, *vegfab*, and *vegfaa/ab* morpholino injected embryos, only the embryos that demonstrated a reduction or absence of islet vessels were counted. n = 9-21. Box-and-whisker plots show median, and circles represent individual zebrafish. Statistical analysis was performed using a one-way ANOVA with Tukey post-hoc testing. **D-H)** Confocal projections of **D)** non-injected, **E)** scrambled injected, **F)** *vegfaa*, **G)** *vegfab*, or **H)** *vegfaa/ab* morpholino injected embryos at 72 hpf; endothelial cells (green), beta-cells (red), and DAPI (DNA; grey). Scale bar = 10 μm.

Combined knockdown of *kdr* and *kdrl* causes a reduction of islet vessels

We also assessed the role of *kdr* and *kdrl*, the primary receptors of VegfA in zebrafish. We found that single morpholino knockdown of either *kdr* or *kdrl* in *Tg(fli1:EGFP; ins:TagRFP)* zebrafish did not affect islet vessels (Figure 3-7A,C-G). However, double knockdown of *kdr* and *kdrl* resulted in a reduction of islet vessels (Figure 3-7A,G). In the *kdr/kdrl* injected embryos that

demonstrated a reduction in islet vessels, no significant changes in beta-cell numbers were observed (25.5±2.9) in comparison to the scrambled and non-injected controls (27.4±2.6; 27.4±2.7) (Figure 3-7B).

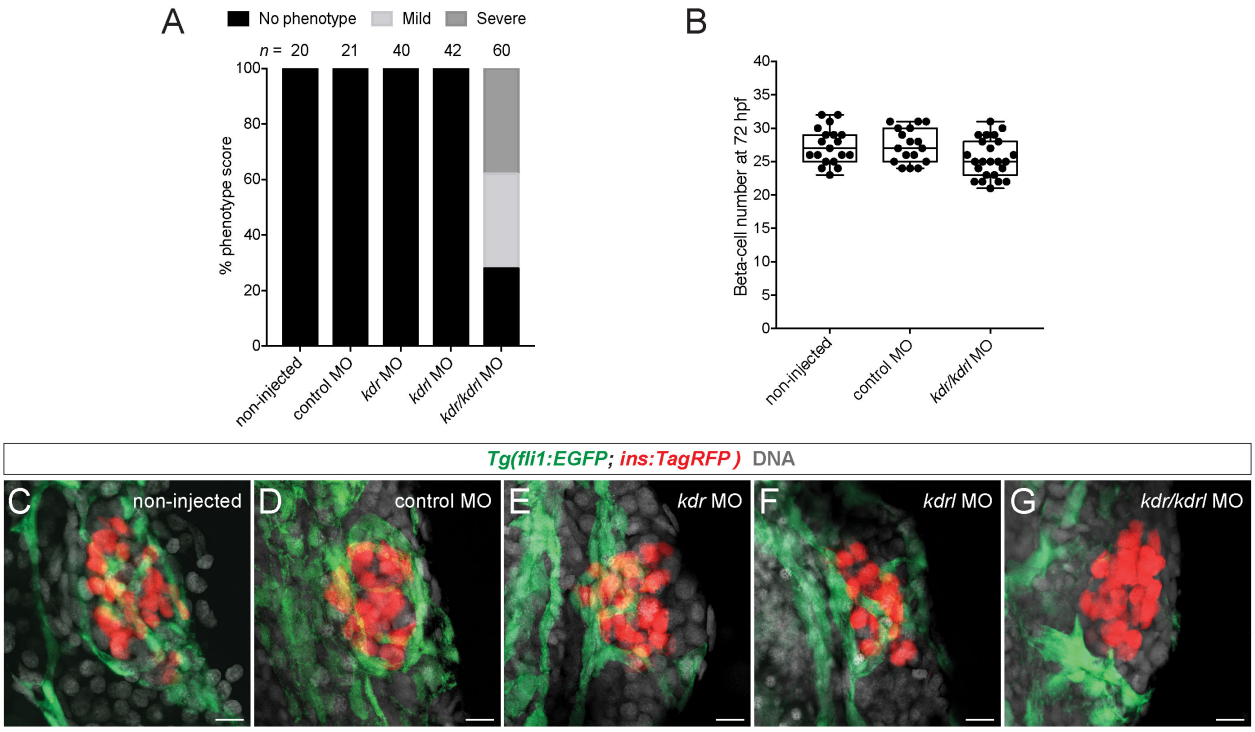

Figure 3-7 Vegfr2 receptor knockdown leads to disruptions in islet vessel development
A) Phenotypic score of islet vessels in non-injected, control morpholino, and *kdr*, *kdrl*, or *kdr/kdrl* morpholino injected *Tg(fli1:EGFP; ins:TagRFP)* embryos. **B)** The number of beta-cells in 72 hpf *Tg(fli1:EGFP; ins:TagRFP)* control and morpholino injected embryos. In the *kdr/kdrl* morpholino injected embryos, only the embryos that demonstrated a reduction or absence of islet vessels were counted. Box-and-whisker plots show median, and circles represent individual zebrafish. n = 17-24. Statistical analysis was performed using a one-way ANOVA with Tukey post-hoc testing. **C-G)** Confocal projections of **C)** non-injected, **D)** control injected, **E)** *kdr*, **F)** *kdrl*, or **G)** *kdr/kdrl* morpholino injected embryos at 72 hpf; endothelial cells (green), beta-cells (red), and DAPI (DNA; grey). Scale bar = 10 µm.

To determine if beta-cells originating from the dorsal and ventral pancreatic bud form in vessel deficient fish, we performed a previously described label-retaining cell assay to mark dorsal pancreatic bud derived beta-cells (226). In this assay, H2B-EBFP mRNA is injected into one cell stage embryos. The H2B-EBFP protein is diluted by cell division, but cells that are quiescent retain

the label (226). The beta-cells originating from the dorsal pancreatic bud have been previously described to be quiescent by 24 hpf and retain the label (H2B-EBFP^{+}) (226). Ventral bud derived beta-cells arise later in development after multiple rounds of progenitor proliferation and consequently the ventral bud derived beta-cells do not retain the label (H2B-EBFP^{-}). We found that both dorsal bud derived (H2B-EBFP^{+}) and ventral bud derived beta-cells (H2B-EBFP^{-}) were present in the *kdr/kdrl* injected embryos (Figure 3-8A-C). Together, these results suggest that Vegfaa/Vegfab-Vegfr2 signalling is necessary for islet vascularization but not required for beta-cell formation regardless of the origin of the beta-cells.

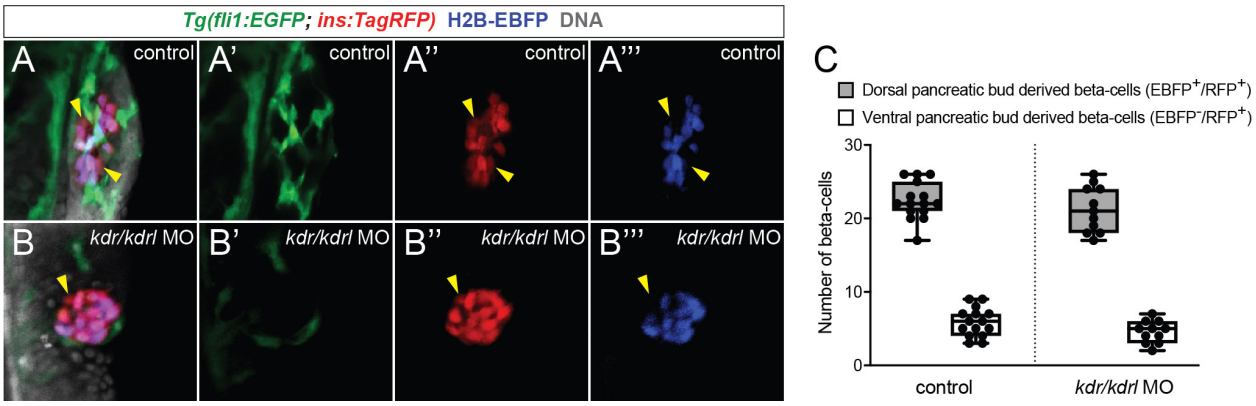

Figure 3-8 Beta-cells derived from the dorsal and ventral pancreatic bud are present in *kdr/kdrl* injected zebrafish

A-B''') Confocal projections of 72 hpf *Tg(fli1:EGFP; ins:TagRFP)* embryos **A-A''')** injected with H2B-EBFP mRNA or **B-B''')** co-injected with H2B-EBFP mRNA and *kdr/kdrl* morpholino; endothelial cells (green), beta-cells (red), dorsal pancreatic bud derived beta-cells (blue), and TO-PRO-3 nuclear stain (DNA; grey). Yellow arrowheads indicate beta-cells derived from the ventral pancreatic bud (H2B-EBFP^{-}/RFP^{+}). **C)** The number of beta-cells derived from the dorsal pancreatic bud (H2B-EBFP2^{+}/RFP^{+}) and ventral pancreatic bud (H2B-EBFP^{-}/RFP^{+}) at 72 hpf. Box-and-whisker plots show median, and circles represent individual zebrafish. n = 11-15. A Student's t-test was performed to assess statistical significance in the number of dorsally-derived beta-cells or the number of ventrally-derived beta-cells between control and *kdr/kdrl* knockdown animals.

To determine if islet vessels influenced beta-cell maturation, we used FACS to isolate RFP+ *Tg(fli1:EGFP; ins:TagRFP)* beta-cells from scrambled injected controls and *kdr/kdrl*

morpholino knockdown embryos at 72 hpf. Expression of *insulin (ins)* was significantly downregulated in vessel deficient embryos in comparison to scrambled injected controls (Figure 3-9A) but levels of beta-cell maturation genes *pdx1* and *neurod1* were not significantly altered (Figure 3-9B,C).

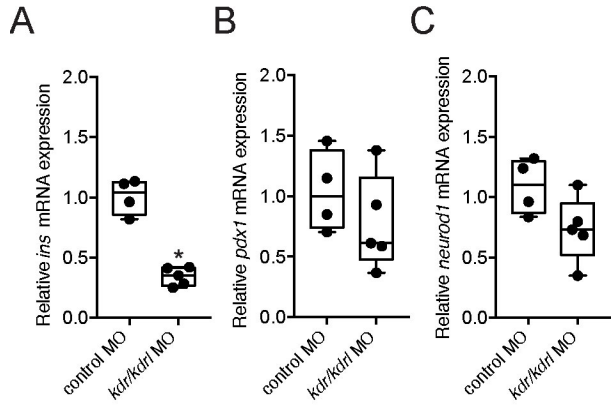

Figure 3-9 Relative expression of *ins, pdx1, and neurod1* in isolated beta-cells from vessel deficient fish
Relative expression of **A)** *ins,* **B)** *pdx1*, and **C)** *neurod1* in isolated beta-cells of control injected and *kdr/kdrl* morpholino injected *Tg(fli1:EGFP; ins:TagRFP)* embryos at 72 hpf. All values were normalized to *ef1α*. *p<0.05 by Student's t-test.

A reduction of islet vessels is observed following beta-cell ablation

To determine if endothelial cells undergo changes during beta-cell ablation, we crossed the following double transgenic line *Tg(-1.2ins:htBid*$^{TE\text{-}ON}$*; -1.2ins:H2BmCherry)* (280) to *Tg(fli1:EGFP)* to create the triple transgenic line *Tg(-1.2ins:htBid*$^{TE\text{-}ON}$*; -1.2ins:H2BmCherry; fli1:EGFP)*. In this transgenic, the proapoptotic protein tBID is expressed under the control of the tetracycline- and ecdysone-inducible system which upon addition of DOX and TBF results in ablation of beta-cells (280). We administered DOX and TBF (DOX/TBF) at 3 dpf until 5 dpf. We observed a significant decrease in the number of beta-cells following DOX/TBF administration at all timepoints in comparison to their DMSO-treated controls (Figure 3-10A-H). There is no significant decrease in alpha-cell numbers in the DOX/TBF-treated fish in comparison to their

timepoint matched DMSO-treated controls (Figure 3-10I). We also observed a significant decrease in the number of endothelial cells at 5 dpf in the DOX/TBF-treated fish in comparison to DMSO-treated controls (Figure 3-10A-C,J). However, there is no significant difference in the number of endothelial cells at 8 dpf or 11 dpf in DOX/TBF-treated fish in comparison to their timepoint matched DMSO-treated controls (Figure 3-10D-G,J). These results suggest a decrease in the number of islet endothelial cells after beta-cell destruction, but revascularization of the islet during beta-cell regeneration.

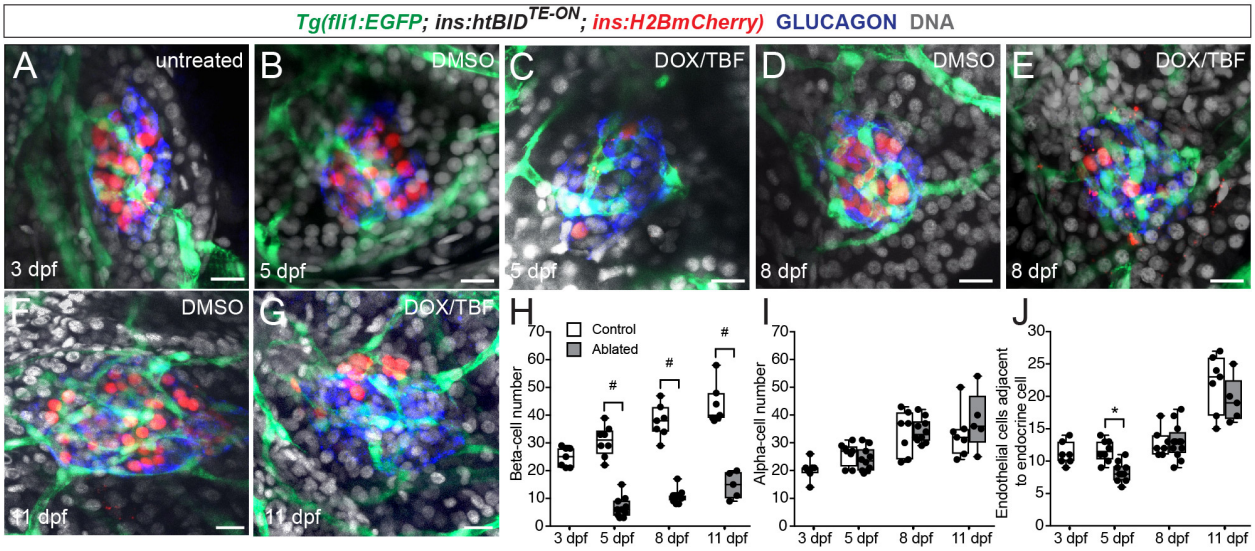

Figure 3-10 The number of islet endothelial cells decreases after beta-cell ablation
A-G) Confocal projections of **A)** 3 dpf, **B)** 5 dpf control, **C)** 5 dpf beta-cell ablated fish, **D)** 8 dpf control, **E)** 8 dpf beta-cell ablated fish, **F)** 11 dpf control, **G)** 11 dpf beta-cell ablated *Tg(-1.2ins:htBid*$^{TE\text{-}ON}$*; -1.2ins:H2BmCherry; fli1:EGFP*) fish ; endothelial cells (green), beta-cells (red), glucagon (blue) and DAPI (DNA; grey). Scale bar = 10 µm. **H-J)** The number of **H)** beta-cells, **I)** alpha-cells, and **J)** endothelial cells during beta-cell ablation and regeneration in *Tg(-1.2ins:htBid*$^{TE\text{-}ON}$*; -1.2ins:H2BmCherry; fli1:EGFP*) fish treated with either DMSO (control) or DOX/TBF (beta-cell ablated) from 3-5 dpf. Box-and-whisker plots show median, and circles represent individual zebrafish. n = 5-12. Student's t-test was conducted between the control and ablated groups at the same timepoint. $^{*,\#}p<0.05$.

3.4 Discussion

In this study, we explored the angiogenic factors responsible for zebrafish islet vessel

development and the effect of endothelial cells on pancreatic endocrine formation and maturation. Beta-cells develop adjacent to blood vessels. Endothelial cells can be found within the islet as early as 40 hpf. The formation of beta-cells adjacent to endothelial cells is similarly observed in murine models where the pancreatic epithelium forms adjacent to embryonic endothelial cells (69). Administration of the Vegf inhibitor SU5416 from 12 to 72 hpf caused a significant reduction of endothelial cells within the islet, although no significant changes in beta- and alpha-cell numbers were observed. Our results are consistent with previous studies which have observed the formation of insulin-expressing cells in vessel deficient *cloche* zebrafish mutants (225). No significant changes in the number of secondary islets were found in SU5416-treated fish from 4.5 until 6 dpf in comparison to control fish, suggesting that Vegf signalling is also dispensable for early secondary islet formation. Our results differ from murine pancreatic specification which is dependent on signals from the endothelial cells (69,71), suggesting species differences in pancreas specification.

We found that treatment of zebrafish embryos with Vegf competitive inhibitor SU5416 from 72 hpf to 96 hpf after the islet vessels have been established leads to a decrease in islet vessels, suggesting that continuous Vegf signalling is needed to sustain islet vessels. This finding is consistent with observations in murine islets that Vegf signalling is the primary mediator of islet vessel formation and maintenance (79,80).

To determine which Vegf angiogenic factors are responsible for zebrafish islet vessel development, we performed RT-PCR and found that both *vegfaa* and *vegfab* are expressed in the beta-cells as early as 2 dpf, suggesting the recruitment of endothelial cells early on during islet development. Combined knockdown of *vegfaa* and *vegfab* caused a more severe phenotype in the reduction of islet vessels in 72 hpf embryos in comparison to the single knockdown of *vegfaa* or

vegfab. This may reflect partial redundancy between *vegfaa* and *vegfab*, as has been suggested for intestinal vessel development (325,329). Despite the reduction of islet vessels in *vegfaa/vegfab* knockdown animals, there were no significant changes in beta-cell numbers between the vessel deficient and control islets. Similarly, double knockdown of the primary VegfA receptors, *kdrl* and *kdr*, resulted in a similar loss of islet vessels, but there were no significant changes in beta-cell numbers in *kdr/kdrl* knockdown animals in comparison to controls. Single knockdown of *kdr* or *kdrl* did not significantly reduce islet vessels suggesting possible overlapping roles between the two receptors. These data are consistent with a previous report which found a more severe phenotype in intestinal vessel development when *kdrl*^{um19} mutants were also injected with a *kdr* morpholino in comparison to *kdrl*^{um19} mutants or *kdr* morpholino knockdown animals (329). Together, these results suggest that VegfA/Vegfr2 signalling is necessary for islet vascularization but not required for beta-cell formation. In the vessel deficient embryos, we observed a decrease in *ins* mRNA expression in comparison to control animals, suggesting that islet hormone expression is influenced by Vegfa/Vegfr2 signalling. Similarly, in *VegfA* deficient mouse islets, a decrease in insulin expression has also been reported (330). This reduction in insulin expression in the murine *VegfA* deficient islets is believed to be due to the absence of a vascular basement membrane which promotes insulin gene expression (330).

In mice, *VegfA* inactivation during early development results in severe islet hypovascularization and significantly reduces beta-cell mass as a consequence of a decrease in beta-cell proliferation during postnatal stages (322). While we did not observe any significant differences in beta-cell number between vessel deficient and control zebrafish at 72 hpf, this discrepancy may reflect the fact that beta-cell neogenesis and not proliferation is the main mechanism of beta-cell formation during zebrafish embryonic stages (226,251). At 72 hpf, the

majority of the islet is composed of quiescent dorsal bud derived beta-cells (110,226). Thus, any putative changes in beta-cell proliferation would be undetected in our zebrafish model during early pancreas development. While there may be a decrease in beta-cell proliferation and mass during later stages of zebrafish pancreas development, an islet cell specific *vegfA* knockout zebrafish model may be needed to assess this as *vegfaa/ab* and *kdr/kdrl* knockdown models develop pericardial edema and die after 72 hpf, and SU5416 application in larval fish (after 72 hpf) for over 52 hours causes high rates of lethality (data not shown).

Oxygen accessibility may also lead to the species differences during pancreas development in vascular deficient models. In the murine pancreas, oxygen levels affect endocrine cell differentiation (75). Embryos from pregnant rats exposed to a hypoxic environment (8% O_2) prior to the secondary endocrine transition have significantly blunted endocrine differentiation in comparison to embryos from the control pregnant rats exposed to a normoxic environment (21% O_2) (75). *In vitro,* increasing oxygen levels (21%, 60%, and 80%) leads to the induction of endocrine hormone expression in cultured E13.5 rat pancreatic explants in a concentration-dependent manner (75). As mammalian embryos require a functional cardiovascular system to bring oxygen to tissues, a lack of endothelial cells creates a hypoxic environment and consequently negatively affects endocrine pancreas differentiation. In contrast, given that zebrafish develop *ex-utero*, the embryos are in a normoxic milieu (331). Hence, an avascular environment does not lead to hypoxia during early zebrafish development and may explain the formation of endocrine cells despite the lack of endothelial cells in our zebrafish models. Future studies controlling the ambient oxygen content could reveal its role during early endocrine cell formation in the zebrafish.

We also observed a decrease in islet endothelial cells after beta-cell destruction and revascularization of the islet during beta-cell regeneration. This is unlikely due to a bystander

affect as alpha-cell number is not significantly reduced in beta-cell ablated fish compared to control fish, but rather this may indicate changes in vasculature organization during beta-cell ablation. In the adult zebrafish pancreas, changes in islet vasculature after beta-cell destruction and during regeneration have been reported (224). In other tissues, revascularization of the damaged tissue occurs quickly after insult (332,333). In cardiomyocytes, this fast revascularization is essential in the regeneration process as it promotes cell proliferation (332). Whether islet endothelial cells are needed for beta-cell regeneration is unknown. Future studies addressing beta-cell regeneration in an avascular islet environment may reveal novel mechanisms for beta-cell renewal. In addition, identifying beta-cell transcriptome changes during beta-cell regeneration and during beta-cell development in an avascular environment could elucidate the role of endothelial cells in beta-cell formation and renewal.

In summary, the present study demonstrates that Vegfaa/Vegfab-Vegfr2 signalling is dispensable for beta- and alpha-cell neogenesis, although blocking Vegfaa/Vegfab-Vegfr2 signalling decreases insulin expression. Our study has identified Vegfaa and Vegfab as potential mediators for islet vessel development. These findings may have implications in zebrafish beta-cell regeneration studies, as we observed changes in islet vasculature during beta-cell destruction and regeneration. Interfering with Vegfaa/Vegfab-Vegfr2 signalling during beta-cell regeneration may provide insight into mechanisms required for the endogenous expansion of beta-cell mass in zebrafish following beta-cell ablation.

Chapter 4: Contribution of a non-beta-cell source during beta-cell regeneration but not beta-cell maintenance in zebrafish

4.1 Background

There have been significant efforts to understand the mechanism of beta-cell regeneration in the hope to stimulate endogenous beta-cell renewal to treat and potentially cure diabetes. The regeneration of beta-cells may be accomplished through beta-cell replication, differentiation of progenitor/stem cells (beta-cell neogenesis), or transdifferentiation from differentiated non-beta-cells. To date, most of the methods to study beta-cell regeneration have utilized chemically-induced or surgically-induced beta-cell ablation rodent models (133–135,141,147,152–156). Young rodents show significant increases in beta-cell mass over time after chemical or surgical induced beta-cell ablation. Most studies attribute this increase in beta-cell mass to increases in beta-cell proliferation (133–135,139,152), and a few studies have reported transdifferentiation of non-beta-cells (159,160) and beta-cell neogenesis (141,147,197) to contribute to beta-cell regeneration under extreme beta-cell loss. While rodents show some ability for regeneration, this capacity diminishes in older animals (110). This is mostly attributed to the age dependent decline in beta-cell proliferation which is the main mechanism of murine beta-cell maintenance (107,135,136). Interestingly, young adult zebrafish (less than 12 months old) have a robust capacity for beta-cell regeneration without the need for insulin therapy as they can rapidly normalize blood glucose within a week and regenerate beta-cell mass within three weeks after beta-cell ablation (218,219). Regeneration in older zebrafish has yet to be explored. The mean age of laboratory zebrafish is 36 months (334) but decreases in physical activity and a degeneration of

skeletal muscle is seen as early as 15 months and 12 months respectively (334–336). Differences in the rate of fin regeneration are observed between 4 month and 18 month old animals (337). Whether there are differences in the rate of beta-cell regeneration with respect to age is unknown. Pancreas development is similar between zebrafish and mammals; hence, elucidating the mechanisms of zebrafish beta-cell regeneration may reveal potential avenues for beta-cell renewal in the mammalian model.

The exact mechanisms of adult zebrafish beta-cell regeneration are still unclear. Upon STZ-mediated beta-cell ablation, an increase in peri-islet proliferation has been observed (219). Studies using a genetic cell ablation system in which beta-cells expressing the nitroreductase *nfsB* suicide gene undergo cell death upon addition of metronidazole (MTZ) have suggested non-beta-cell sources to contribute to beta-cell regeneration (218,283,295). Lineage tracing of alpha-cells during beta-cell ablation in larval fish has shown that a small contribution of alpha-cells can transdifferentiate into insulin-expressing cells (283,294). The number of *nkx6.1*-expressing ductal cells that express insulin is significantly increased during adult beta-cell regeneration (295) and *Sox9b* homozygous mutant larval zebrafish, which have impaired ductal development, exhibit blunted beta-cell regeneration (248), suggesting the contribution of ductal cells to beta-cell renewal. Lineage tracing of a specialized type of ductal cell, the centroacinar cell (CAC), has shown that 43% of new beta-cells that arise during beta-cell regeneration originate from CACs in adult zebrafish (218). The role of beta-cell proliferation in regenerative conditions is not clear. EdU labelling after beta-cell ablation reveals an increase in EdU+ beta-cells although it is unclear if these proliferating cells represent proliferation of pre-existing beta-cells or their precursors (218). The role of beta-cell proliferation in the maintenance of adult beta-cell mass under physiological conditions is also unclear as lineage tracing of the beta-cells has yet to be conducted

under normal conditions. In this study, we sought to characterize islet morphology under physiological and regenerative conditions, investigate the main mechanism of beta-cell maintenance in the zebrafish, and determine the contribution of non-beta-cells to beta-cell regeneration in the zebrafish.

4.2 Method

Zebrafish Lines

Zebrafish were housed as previously described in Chapter 2. The following zebrafish lines were used un this Chapter: *Tg(-1.2ins:TagRFP)*^{vu514} (315), *Tg(ins:EGFP)*^{jh3} (282), *Tg(gcga:EGFP)*^{ia1} (257), *Tg(actb2:LOXP-STOP-LOXP-DsRedEx)*^{sd5} (298), *Tg(ins:PhiYFP,Eco.-nfsB,sst2:CFP)*^{jh33} *(abbreviated Tg(ins:YFP-nfsB,sst2:CFP)* (218), *Tg(ins:nfsB-Flag,cryaa:mCherry)* ^{s950}, and *Tg(ins:EGFP-T2A-CreER*^{T2}*)* which we generated in Chapter 2. Genotyping of the *Tg(actb2:LOXP-STOP-LOXP-DsRedEx)* line was done as previously described in Chapter 2.

Chemical Treatments

(Z)-4-Hydroxytamoxifen (4-OHT) (Sigma-Aldrich, Oakville, ON, Canada, H7904) dissolved in DMSO to 10 mM and stored at -20°C. Adult zebrafish were treated with 1.0 μM 4-OHT or 0.1% DMSO. Fish were kept from light for 14 hrs, after which animals were transferred to fresh fish water and fed once. Animals were subjected to this regimen for 3 consecutive days. For metronidazole (MTZ) (Sigma-Aldrich, M3761) treatment, adult fish were incubated in 0.25, 0.5, 1.0 or 2.5 mM MTZ or 0.1% DMSO. Fish were kept from light for 14 hrs, and subsequently

transferred to fresh fish water and fed once. Animals were subjected to this regimen for 2 consecutive days. Day 0 post treatment was defined as the first day of treatment.

FACS and qPCR

To isolate EGFP+ beta-cells, we dissected the principal islet from 5 month and 20 month old *Tg(ins:EGFP)* adult fish. 2 pancreata were combined for each sample point. The samples were digested as described in Chapter 2. EGFP+ beta-cells were sorted using a BD Influx Cell Sorter (BD Biosciences, Mississauga, ON, Canada). RNA was isolated from 3000-6000 isolated GFP-expressing beta-cells using TRIzol (Invitrogen, Carlsbad, CA, USA). cDNA was prepared using the iScript cDNA synthesis kit (Invitrogen). cDNA was amplified with SsoFast EvaGreen Supermix (BioRad, Richmond, CA, USA) on a CFX96 Touch™ Real–Time PCR Detection System (BioRad). The relative expression of each gene was determined after normalization to *ef1α*. RT-qPCR controls are described in Chapter 2. Primers for RT-qPCR are listed in Table 4.1. PCR cycling conditions were as follows: 3-min denaturation step at 95°C, followed by 40 cycles of denaturation at 95°C for 15 s, annealing at 55°C for 15 s, and extension at 72°C for 25 s.

Table 4-1 RT-qPCR primer sequences

Gene	Forward Primer	Reverse Primer	Accession
ef1α	TCAAGGACATCCGTCGTGGTA	ACAGCAAAGCGACCAAGAGG	NM_131263
insulin	TCTGCTTCGAGAACAGTGTG	GGAGAGCATTAAGGCCTGTG	NM_131056
pdx1	GGGCGCGAGATGTATTTGTTGA	CAAATCTCACACGCACGCATG	NM_131443
neurod1	TCATGCTTTCCTCGCTGTATGACT	CCACGAAGGGCATGAAACTATCA	NM_130978
gck	ATCCTCATGGTGGACCAA	ATCACCAACCTCGGAGC	NM_001045385
nkx2.2a	TCAGCTGAAGGTTCCGGAGATTTT	CGACAATCCTTATACTAGATGGCTCG	NM_131422

glut2	TGTGCTGTGGCCATGAC	CCAGGTCCGATCTCAAAG AA	NM_001042721

Immunofluorescence

For immunostaining whole mount larval zebrafish, immunofluorescence was performed as previously described in Chapter 2. Antibodies used were mouse anti-somatostatin (1:250, Beta-cell Consortium, AB1985) and goat anti-mouse Alexa Fluor 647 antibody (1:1000, Life Technologies A21236). Cell nuclei were visualized with 4′,6-diamidino-2-phenylindole (DAPI) DNA stain (1:1000, Thermo Fisher Scientific D1306). Samples were mounted in 75% glycerol on concave glass slides (EISCO). All fluorescent images were obtained with a LSM800 Zeiss upright confocal and imaged with a 40X objective. Whole mount tissues were scanned by confocal microscopy. Cell numbers were counted manually.

For paraffin embedded sections, the pancreata were dissected out of fish using fine tip needles and fixed in 4% paraformaldehyde overnight at 4°C. Tissues were transferred to 70% ethanol for long-term storage before paraffin embedding and sectioning (5 µm thickness; Wax-It Histology Services, Vancouver, Canada). The sections were immunostained as previously described in Chapter 2. The following primary antibodies were used in this Chapter: guinea-pig anti-insulin (1:250, DAKO, A0564), mouse anti-insulin (1:100, Cell Signalling Technologies, 8138S), rabbit anti-glucagon (1:250, Abcam, ab92517), mouse anti-somatostatin (1:250, Beta-cell Consortium, AB1985), rabbit anti-somatostatin (1:500, ABclonal, A9274), mouse anti-EGFP (1:100, Millipore Sigma, MAB3580), rabbit anti-DsRed (1:200, Clontech, 632496), and mouse anti-PCNA (1:10, Abcam, ab29). The following day slides were washed and incubated with appropriate Alexa Fluor antibodies (1:1000, Life Technologies) for 1 hr at room temperature before mounting with VECTASHIELD Hard Set Mounting Medium with DAPI (Vector

Laboratories, Burlingame, CA, H-1500). All fluorescent images were obtained with a LSM800 Zeiss upright confocal and imaged with a 40X objective. Pancreatic sections were cut 20 to 50 μm apart and at least 5 sections per animal were used in quantification. We used ImageJ to calculate endocrine cell area of each cell type by outlining islet size (based on nuclear clustering) and quantifying immunoreactive area within the islet. In lineage tracing experiments, cell numbers were counted manually in a double-blind experiment.

Glucose Measurements

Fasting blood glucose measurements were taken in the morning. Adult fish were fasted for 24 hrs, anaesthetized in 0.01% w/v MS-222, and decapitated by cutting cleanly through the pectoral girdle and severing the heart as previously described (338). Whole blood was analyzed immediately with a FreeStyle Lite (Abbot) glucose meter by applying a test strip directly to the cardiac blood.

Statistics

The Shapiro–Wilk normality test was used to assess normality of data distribution. Upon passing the test for normality, data was subjected to Student's t-test or one-way ANOVA with Tukey post-hoc test for multiple comparisons. When one or more groups failed the test for normality, we used the nonparametric Kruskal-Wallis test with Dunn's multiple comparisons test.

4.3 Results

Adult zebrafish islets contain a high proportion of beta-cells and delta-cells

In order to characterize islet morphology, we isolated pancreata from 4 month old and 18 month old *Tg(ins:TagRFP)* adult zebrafish. We stained for insulin, glucagon, and somatostatin to

characterize beta-, alpha-, and delta-cell endocrine islet proportions, respectively. We observed no significant differences in glucagon+, insulin+, and somatostatin+ cell proportions in young (4 month old) and middle-aged (18 month old) adult fish. In 4 month and 18 month old fish, beta-cells and delta-cells constitute the vast majority of the islet (4 mo: 42.4±8.5%; 49.6±4.0%; 18 mo: 37.0±0.5%; 48.6±1.4% respectively) (Figure 4-1A,D-F). Alpha-cells comprise approximately 14% of the islet. Alpha-cells are located on the islet mantle as well as in the islet core in apparently bigger islets (greater than 200 islet cells within one section). In smaller islets, alpha-cells are primarily localized to the islet mantle (Figure 4-1A). The embryonic and larval zebrafish islets at 3 and 9 dpf were also observed to have high proportions of delta cells (19.4±1.0%; 33.4±1.9%) and beta-cells (52.1±2.1%; 43.5±2.0%) which are found within the islet core while alpha-cells are predominantly on the islet mantle (Figure 4-1G-H). We stained for PCNA in the 4 month and 18 month old zebrafish. We observed very low PCNA+ beta-, alpha-, and delta-cells in 4 month and 18 month old adult zebrafish (Figure 4-1B). We also observed a small percentage of polyhormonal cells in 4 month and 18 month old adult zebrafish (0.8±0.3%; 0.9±0.2%) (Figure 4-1A,I). The majority of these polyhormonal cells (>70%) were somatostatin and insulin co-positive cells. In both the 4 month old and 18 month old adult pancreas, single endocrine cells were often observed adjacent to pancreatic ducts, which has been proposed to be a niche for endocrine progenitor cells (218).

To determine if beta-cells from young and older adult zebrafish exhibit differential expression of beta-cell maturation markers, we performed qPCR on isolated EGFP+ beta-cells from 5 month and 20 month old *Tg(ins:EGFP).* We observed no significant differences in the

expression of *ins, glut2, neurod1, pdx1*, *gck,* and *nkx2.2a* in the 5 month and 20 month old zebrafish (Figure 4-1J), which is consistent with a previous report (271).

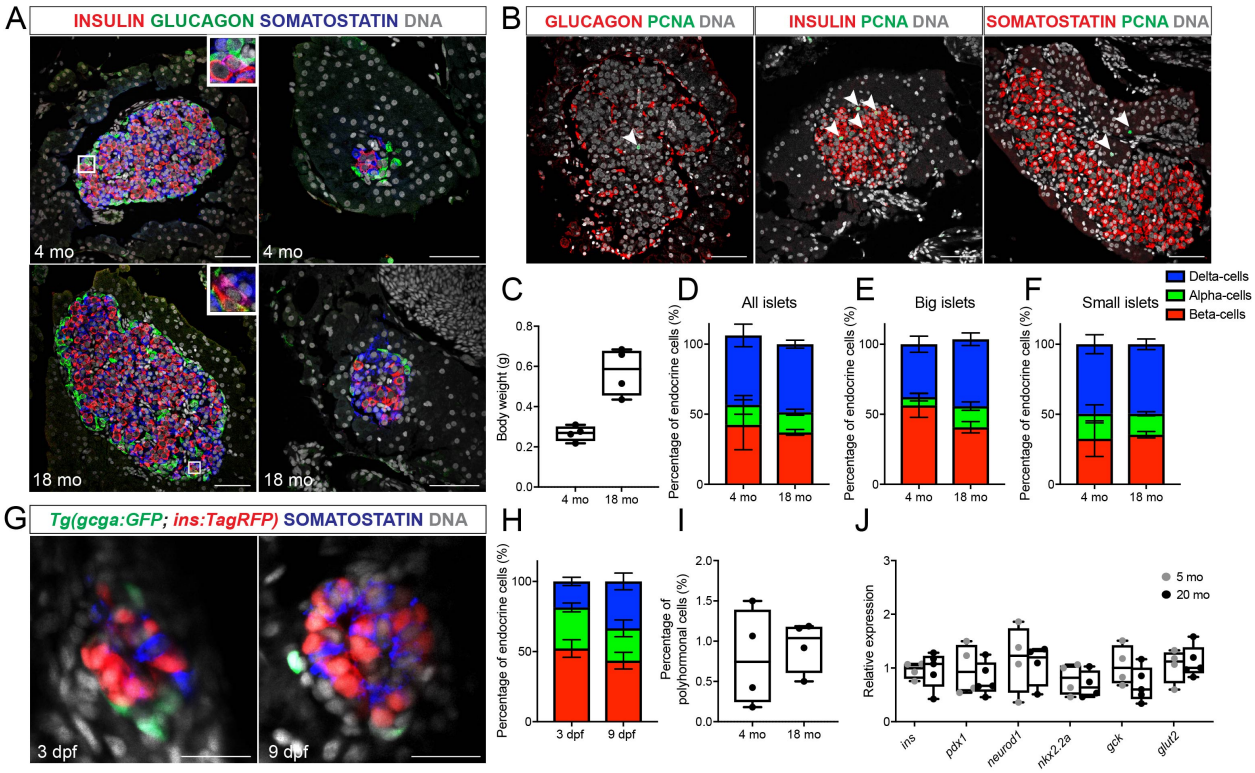

Figure 4-1 Zebrafish islets have a high proportion of beta-cells and delta-cells
A-B) Representative images of islets from 4 month (4 mo) and 18 month old (18 mo) *Tg(ins:TagRFP)* zebrafish immunostained for **A)** insulin (red), glucagon (green), somatostatin (blue), and DAPI nuclear stain (DNA; grey) ; or **B)** proliferative cell nuclear antigen (PCNA) (green), DAPI nuclear stain (DNA; grey), and glucagon, insulin, or somatostatin (red). Scale bar = 20 µm. **C)** Body weight of 4 month and 18 month old *Tg(ins:TagRFP)* zebrafish. **D-F)** Relative islet contribution of insulin, glucagon, and somatostatin-expressing cells in 4 month and 18 month old *Tg(ins:TagRFP)* zebrafish in **E)** big islets (bigger than 200 cells per section) or **F)** small islets (less than 50 cells per section). n = 4. **G)** Confocal projections of *Tg(gcga:EGFP ; ins:TagRFP)* immunostained for somatostatin (blue) and DAPI nuclear stain (DNA; grey). **H)** Relative islet contribution of insulin, glucagon, and somatostatin-expressing cells in 3 and 9 days post fertilization (dpf) *Tg(gcga:GFP ; ins:TagRFP)* zebrafish. n = 4. **I)** Percentage of polyhormonal cells in 4 month and 18 month old *Tg(ins:TagRFP)* pancreata. **J)** Relative expression of *ins, pdx1, neurod1, nkx2.2a, gck,* and *glut2* in isolated beta-cells from 5 month (grey circles) and 20 month (black circles) old *Tg(ins:EGFP)* zebrafish. For each gene, statistical analysis was performed using a Student's t-test. n = 4-5.

Beta-cell regeneration occurs in 4 month old and 17 month old zebrafish

Next, we sought to characterize the islets during beta-cell regeneration. We first attempted to use the *Tg(-1.2ins:htBid$^{TE\text{-}ON}$,cryaa:DsRed)* (280) transgenic line. We administered 50 µM doxycycline and 25 µM tebufenozide, similar concentrations that we used to ablate beta-cells in larval animals in Chapter 3, for 2 days overnight. However, there was minimal elevation in fasting blood glucose levels (75±8.1 mg/dl) at 3 dpa and some animals displayed hemorrhaging. We therefore decided to use the *nfsB*/MTZ ablation system which has previously been used in adult beta-cell ablation studies (218,219). In this transgenic, the *nfsB* gene which encodes for the nitroreductase enzyme is expressed by the beta-cells. Upon addition of MTZ, *nfsB*-expressing cells convert the drug to a cytotoxic compound resulting in the selective ablation of *nfsB*-expressing beta-cells. We immersed *Tg(ins:YFP-nfsB,sst2:CFP)* 4 month old adult fish in 0.25, 0.5, 1.0 or 2.5 mM MTZ overnight for 2 days to determine the optimal concentration for beta-cell ablation. We observed that 2.5 mM MTZ led to reliable ablation of beta-cells as determined by elevated fasting blood glucose readings (Figure 4-2A).

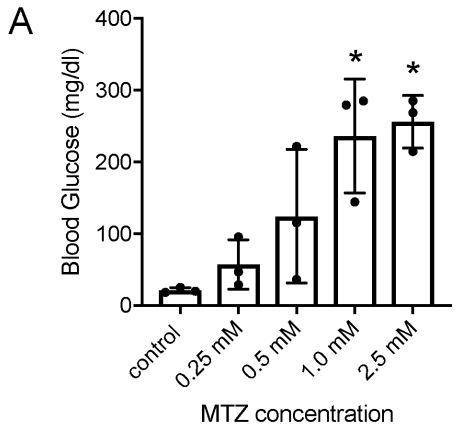

Figure 4-2 MTZ dose response curve in *Tg(ins:YFP-nfsB,sst2:CFP)* adult zebrafish
A) Fasting blood glucose levels at 3 days post ablation from *Tg(ins:YFP-nfsB,sst2:CFP)* 3 month old adult zebrafish treated with 0.25, 0.5, 1.0, or 2.5 mM of MTZ. MTZ was administered overnight for 2 days in water. Day 0 is defined as first day of treatment. Fasting blood glucose

readings were taken 3 days after initial MTZ administration. Statistical analysis was performed using a one-way ANOVA with Tukey post-hoc testing. *$p<0.05$ in comparison to control. n = 3.

We administered 2.5 mM of MTZ or DMSO in the water to 4 month and 17 month old *Tg(ins:YFP-nfsB,sst2:CFP)* animals overnight for 2 days in order to ablate beta-cells and harvested tissues at 0, 3, 5, 7, and 14 days post ablation (dpa) (Figure 4-3A). We also administered 2.5 mM 4 month and 16 month old MTZ to wild-type AB (WT) fish as an additional control.

In MTZ-treated 4 month and 17 month old *Tg(ins:YFP-nfsB,sst2:CFP)* zebrafish, we observed a significant increase in fasting blood glucose levels at 3, 5, and 7 dpa (195±12.0 mg/dl; 68.6±7.7 mg/dl ; 36.6±4.4 mg/dl) in comparison to the *Tg(ins:YFP-nfsB,sst2:CFP)* DMSO control (22.7±6.3 mg/dl) and MTZ-treated WT controls (average 22.0±6.7 mg/dl) (Figure 4-3B). Fasting blood glucose in *Tg(ins:YFP-nfsB,sst2:CFP)* zebrafish at 14 dpa (38.3±6.0 mg/dl) was not statistically significant in comparison to controls (22.7±1.8 mg/dl) (Figure 4-3B). The percentage of insulin+ islet area was significantly decreased at 3, 5, 7, and 14 dpa (10.3±1.5%; 14.1±2.1%; 25.9±3.2%; 30.4±2.3%) in comparison to the control animals (41.4±1.9%) (Figure 4-3C,D). However, the insulin+ islet area was significantly increased at 7 and 14 dpa (25.9±3.2%; 30.4±2.3%) in comparison to 3 dpa (10.3±1.5%) (Figure 4-3C,D), suggesting beta-cell renewal in the beta-cell ablated adult animals. This is consistent with previous findings in adult zebrafish (218,219). We observed a trending increase in insulin+/somatostatin+ co-expressing cells during beta-cell regeneration (Figure 4-3E). PCNA staining revealed no significant differences in somatostatin+ cell proliferation at any time point during beta-cell regeneration (Figure 4-3F-G). We observed no significant differences in insulin+ islet area, fasting blood glucose levels, somatostatin+/insulin+ cells, or proliferative somatostatin+ cells between 4 month and 17 month

old zebrafish during beta-cell ablation and regeneration (Figure 4-3B-G), suggesting that older and younger zebrafish have the same capacity for beta-cell renewal.

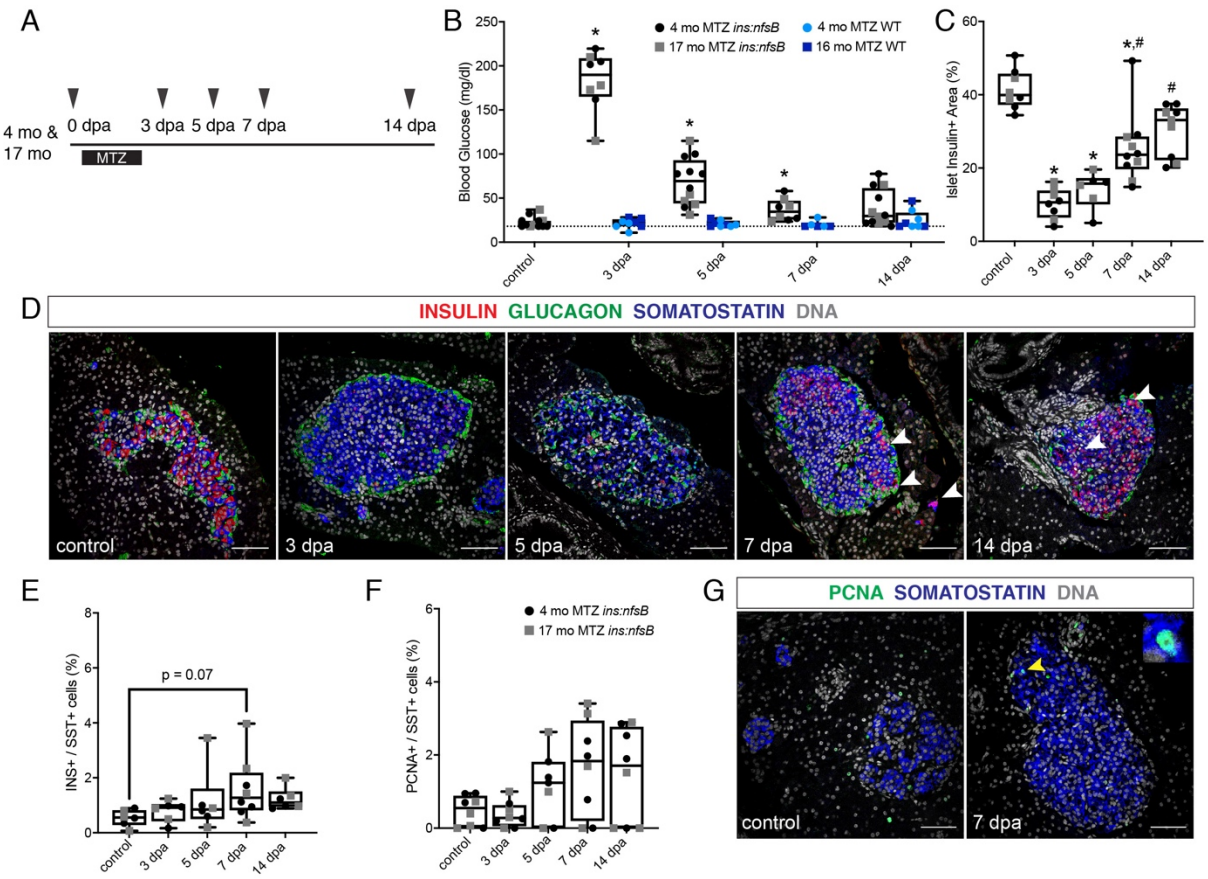

Figure 4-3 Beta-cell regeneration occurs in 4 month and 17 month old zebrafish
A) Experimental timeline of beta-cell ablation in 4 month and 17 month old *Tg(ins:YFP-nfsB,sst2:CFP)* (abbreviated *ins:nfsB)*. 2.5 mM MTZ was applied for 2 days. Tissues were harvested 0 (control), 3, 5, 7, and 14 days post ablation (dpa). **B)** Fasting blood glucose of MTZ-treated 4 month and 17 month old *Tg(ins:YFP-nfsB,sst2:CFP)* or 4 month and 16 month old WT zebrafish at 0 (control), 3, 5, 7, and 14 dpa. Statistical analysis was performed using a one-way ANOVA with Tukey post-hoc testing. *p<0.05 relative to control. Dotted grey is the limit of detection of the glucose meter. **C)** Insulin+ area in MTZ-treated 4 month and 17 month old MTZ treated *Tg(ins:YFP-nfsB,sst2:CFP).* *p<0.05 relative to control, #p<0.05 relative to 3 dpa**. D)** Representative images of islets immunostained for insulin (red), glucagon (green), somatostatin (blue), and DAPI nuclear stain (DNA; grey) from *Tg(ins:YFP-nfsB,sst2:CFP)* at 0 (control), 3, 5, 7, and 14 dpa. Percentage of **E)** insulin, somatostatin co-positive cells and **F)** PCNA, somatostatin co-positive cells at 0, 3, 5, 7, and 14 dpa. Statistical analysis was performed using a one-way ANOVA with Tukey post-hoc testing. **G)** Representative images of islets immunostained for

PCNA (green), somatostatin (blue), and DAPI nuclear stain (DNA; grey) from *Tg(ins:YFP-nfsB,sst2:CFP)* at 0, 3, 5, 7, and 14 dpa. Box-and-whisker plots show median, and black circles represent 4 month old *Tg(ins:YFP-nfsB,sst2:CFP)* zebrafish, grey squares represent 17 month old *Tg(ins:YFP-nfsB,sst2:CFP)* zebrafish, light blue circles represent 4 month old MTZ-treated control, dark blue squares represent 16 month old MTZ-treated WT control. Scale bar = 20 μm.

Beta-cell proliferation is the main mechanism of beta-cell maintenance in the adult zebrafish pancreas

Next, we sought to determine if beta-cell proliferation was the main mechanism of beta-cell maintenance in the adult zebrafish. We crossed the *Tg(ins:EGFP-T2A-CreER^{T2})* transgenic line to the established *Tg(actb2:LOXP-STOP-LOXP-DsRedEx*) (298) line to generate the following double transgenic *Tg(ins:EGFP-T2A-CreER^{T2} ; actb2:LOXP-STOP-LOXP-DsRedEx)* (Figure 4-4A). In this double transgenic animal, beta-cells express EGFP and CreER^{T2}. Upon addition of 4-OHT, CreER^{T2} will recombine LoxP sites allowing for the expression of DsRed under the control of the ubiquitous *actin beta 2 (actb2)* promoter. In this system, beta-cells are heritably labelled with DsRed upon the addition of 4-OHT, and consequently beta-cells derived from pre-existing DsRed+ beta-cells would retain the DsRed label. Beta-cells arising from a non-beta-cell source would not express the DsRed label. If beta-cell proliferation is the main mechanism of beta-cell maintenance in the adult zebrafish pancreas, we would expect the frequency of DsRed+ beta-cells to remain constant as the animal ages. If a non-beta-cell source contributes to beta-cell maintenance, we would expect a dilution in the frequency of DsRed+ beta-cells (Figure 4-4B).

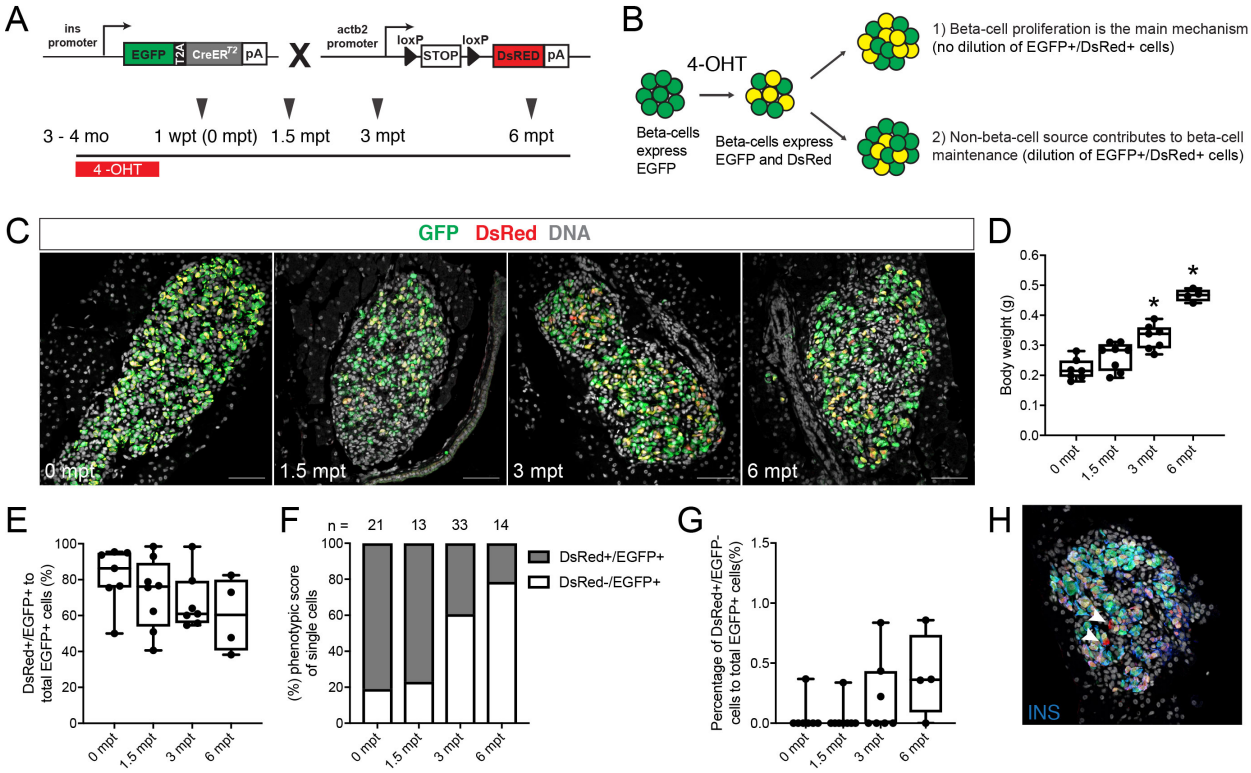

Figure 4-4 Lineage tracing of adult beta-cells

A) Experimental timeline for lineage tracing pre-existing beta-cells in *Tg(ins:EGFP-T2A-CreER^{T2} ; actb2:LOXP-STOP-LOXP-DsRedEx)* transgenic adult zebrafish. Animals were immersed in water that contained 1.0 µM 4-OHT overnight for 3 days. Tissue was harvested 1 week (1 wpt) or 1.5, 3, or 6 months post 4-OHT treatment (mpt). **B)** Predictions for different models of beta-cell maintenance. In this example, the initial labelling efficiency of beta-cells is 50%. After 4-OHT treatment, 50% of beta-cells will express DsRed. Maintenance of beta-cell mass by self-duplication predicts that the fraction of labelled beta-cells remains constant at 50%. Contribution of non-beta-cells to beta-cell maintenance would lead to a gradual decrease in the fraction of labelled beta-cells (less than 50%). **C)** Representative images of islets immunostained for GFP (green), DsRed (red), and DAPI nuclear stain (DNA; grey) from *Tg(ins:EGFP-T2A-CreER^{T2} ; actb2:LOXP-STOP-LOXP-DsRedEx)* fish at 1 week (0 mpt), 1.5, 3, and 6 mpt. Scale bar = 20 µm. **D)** Body weight in *Tg(ins:EGFP-T2A-CreER^{T2} ; actb2:LOXP-STOP-LOXP-DsRedEx)* fish at 0, 1.5, 3, and 6 mpt. **E)** Proportion of labelled (DsRed+) beta-cells at 0, 1.5, 3, and 6 mpt. Cell numbers were counted manually in a double blind experiment. **F)** Frequency of DsRed-/EGFP+ single cells at 0, 1.5, 3, and 6 mpt. n = the number of single cells counted in animals in **E)**. **G)** Percentage of DsRed+/EGFP- cells at 0, 1.5, 3, and 6 mpt. Box-and-whisker plots show median, and circles represent individual zebrafish. For **D**) and **E**), statistical analysis was performed using a one-way ANOVA with Tukey post-hoc testing. *p<0.05 relative to 0 mpt. n = 4-8. For **G**), statistical analysis was performed using a Kruskal-Wallis test with a Dunn's multiple comparisons test. **H)** Representative image of an islet immunostained with DsRed (red), GFP (green), insulin (blue) and DAPI nuclear stain (DNA; grey) in a 3 mpt *Tg(ins:EGFP-T2A-CreER^{T2} ; actb2:LOXP-STOP-LOXP-DsRedEx).* White arrowheads point to DsRed+/EGFP-/INS- cells.

We administered 1.0 μM 4-OHT in the water to 4 month old adult *Tg(ins:EGFP-T2A-CreER^{T2} ; actb2:LOXP-STOP-LOXP-DsRedEx)* fish for 3 days in order to label the beta-cells DsRed+. We sacrificed fish 1 week, 1.5 month (5.5 months old), 3 months (7 months old), and 6 months (10 months old) post 4-OHT treatment (mpt) (Figure 4-4A). During this time, there are significant increases in body weight (Figure 4-4D, Figure 4-5B) and principal islet size (Figure 4-5A,C). We observed no significant changes in the percentage of DsRed+ beta-cells at 0 mpt (81.0±6.2%), 1.5 mpt (68.3±6.4%), 3 mpt (68.2±6.5%) and 6 mpt (60.3±10.4%) (Figure 4-4C,E). These results suggest that beta-cell proliferation is the main mechanism of beta-cell maintenance in the adult. However, we observed an increase in the frequency of unlabelled (DsRed-) single beta-cells over time (Figure 4-4F), suggesting the appearance of *de novo* single beta-cells from non-beta-cells. The appearance of single beta-cells is infrequent in the adult zebrafish pancreas. We also observed rare DsRed+/EGFP-/insulin- cells within islets (Figure 4-4G,H).

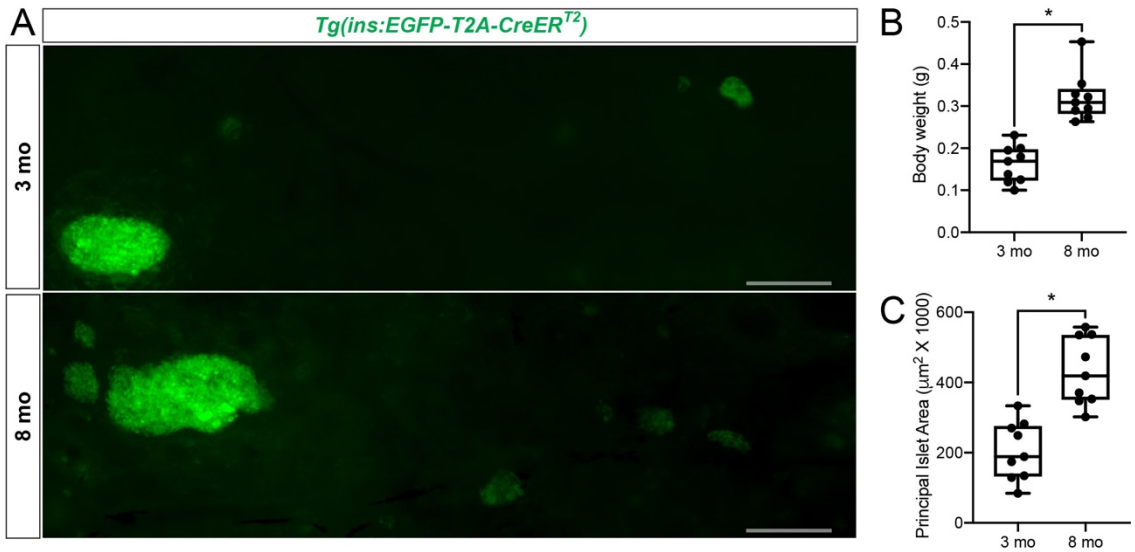

Figure 4-5 Principal islet size in 3 month and 8 month old zebrafish.
A) Images of dissected pancreata in 3 month old (3 mo) and 8 month old (8 mo) *Tg(ins:EGFP-T2A-CreER^{T2})* zebrafish. Scale bar = 500 μm. **B)** Body weight and **C)** principal islet area in

Tg(ins:EGFP-T2A-CreER^{T2}) animals at 3 month and 8 month old zebrafish. Box-and-whisker plots show median, and circles represent individual zebrafish. *p<0.05 by Student's t-test. n = 9.

Non-beta-cell source contributes to beta-cell renewal after >90% beta-cell ablation

To determine the contribution of a non-beta-cell source during beta-cell regeneration, we crossed the *Tg(ins:EGFP-T2A-CreER^{T2} ; actb2:LOXP-STOP-LOXP-DsRedEx)* line to the *Tg(ins:nfsB-Flag ,cryaa:mCherry)* line. We immersed 3 month old adult *Tg(ins:EGFP-T2A-CreER^{T2} ; actb2:LOXP-STOP-LOXP-DsRedEx ; ins:nfsB-Flag,cryaa:mCherry)* fish in 1.0 μM 4-OHT in the water for 3 days in order to label the beta-cells DsRed+ (Figure 4-6A,B). One week after 4-OHT administration, we immersed fish in 2.5 mM MTZ overnight for 2 days to ablate beta-cells. We collected tissues at 0 (control) 3, 7, 14, and 21 dpa. We observed a significant increase in fasting blood glucose of MTZ-treated fish at 3 dpa (289.6±24.2 mg/dl) compared to all other timepoints (Figure 4-6C). We observed a significant decrease in the percentage of insulin+ islet area at 3, 7, and 14 dpa (2.3±1.4%; 17.8±2.0%; 30.2±4.6% respectively), but not at 21 dpa (31.9±5.3%) in comparison to the 0 dpa control animals (43.5±5.3%) (Figure 4-6D,F). We observed a significant dilution in the percentage of insulin+/DsRed+ beta-cells at 7, 14 and 21 dpa (0.3±0.3%; 0.6±0.4%; 0.5±0.5%) in comparison to 0 dpa control fish (47.8±6.0%) (Figure 4-6E). These results suggest a non-beta-cell source contributes to beta-cell regeneration.

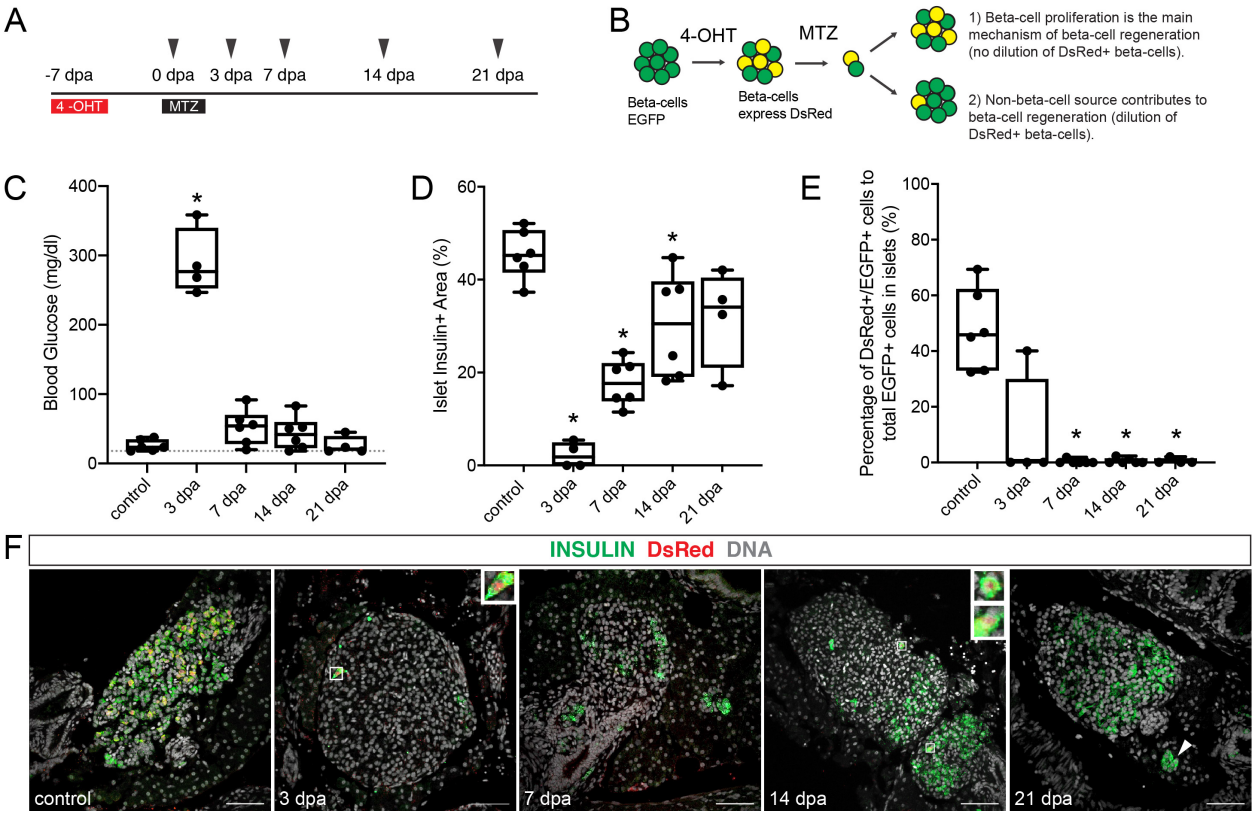

Figure 4-6 Lineage tracing of adult beta-cells during regeneration

A) Experimental timeline for lineage tracing of regenerated beta-cells from *Tg(ins:EGFP-T2A-CreER^{T2} ; actb2:LOXP-STOP-LOXP-DsRedEx ; ins:nfsB-Flag,cryaa:mCherry)* transgenic zebrafish. Fish were immersed in 1.0 µM 4-OHT water overnight for 3 days. Four days after 4-OHT treatment, fish were immersed in 2.5 mM MTZ water overnight for 2 days. Tissues were harvested at 0 (control), 3, 7, 14, and 21 days post ablation (dpa). **B)** Predictions for different models of regenerated beta-cells. In this example, the initial labelling efficiency of beta-cells is 50%. After 4-OHT administration, 50% of beta-cells will express DsRed. Upon 2.5 mM MTZ administration, >90% of the beta-cells will be ablated. If regenerated beta-cells arise solely from pre-existing beta-cells, the fraction of labelled beta-cells remains constant at 50%. Contribution of non-beta-cells to regenerated beta-cell mass would lead to a gradual decrease in the fraction of labelled beta-cells (less than 50%). **C)** Fasting blood glucose, **D)** insulin+ area, and **E)** the proportion of labelled (DsRed+) beta-cells in *Tg(ins:EGFP-T2A-CreER^{T2} ; actb2:LOXP-STOP-LOXP-DsRedEx ; ins:nfsB-Flag, cryaa:mCherry)* at 0, 3, 7, 14, and 21 dpa. Box-and-whisker plots show median, and circles represent individual zebrafish. For **C)** and **D)**, statistical analysis was performed using a one-way ANOVA with Tukey post-hoc testing. For **E)**, statistical analysis was performed using a Kruskal-Wallis test with a Dunn's multiple comparisons test. *$p<0.05$ relative to control (0 dpa). n = 4-6. Grey dotted line in **C)** indicates the limit of detection of the glucose meter. **F)** Representative image of islets immunostained with DsRed (red), insulin (green), and DAPI nuclear stain (DNA; grey) from *Tg(ins:EGFP-T2A-CreER^{T2} ; actb2:LOXP-STOP-LOXP-DsRedEx ; ins:nfsB-Flag,cryaa:mCherry)* animals of 0, 3, 7, 14, and 21 dpa.

4.4 Discussion

In this Chapter, we characterized islet morphology and investigated the sources of new beta-cells under physiological and regenerative conditions in the adult zebrafish. We observed that islet endocrine composition does not significantly change in larval, young (4 month old) and middle-aged (18 month old) zebrafish islets. At all ages, we observed high proportions of delta-cells (up to 50%) in the islet. This islet composition is significantly different to rodents and humans, in which delta-cells occupy 2-11% of the total adult endocrine islet (296,339). The metabolic and physiological implications of the high proportion of pancreatic delta-cells have yet to be explored in the zebrafish. In mice, inhibiting delta-cell differentiation by knocking out *Hhex* during pancreas development does not lead to significant changes in beta-cell number (340). Conditional knockout of *Hhex* in adulthood also does not lead to significant alterations in beta-cell or alpha-cell number, but mice exhibit enhanced insulin and glucagon release in response to stimuli (340), highlighting somatostatin's role in inhibiting both insulin and glucagon secretion. Given the high proportions of delta-cells in the zebrafish, it would be interesting to observe the phenotype after delta-cell ablation during early development and conditional ablation of the delta-cells in the adult zebrafish. These studies would provide insights into the role of delta-cells in the zebrafish islet.

We observed alpha-cells on the islet mantle and the islet core of larger islets in the zebrafish. This is similar to human islet morphology in which alpha-cells are also found in the islet core in larger islets, while smaller islets have alpha-cells located on the islet mantle (342–344). *In vivo* imaging of zebrafish secondary islets, which emerge from the ductal epithelium, have been shown to migrate to the principal islet (345). This migration and subsequent clustering of islets could subsequently give rise to alpha-cells within the islet core. Given the differences in islet

architecture between mammals and zebrafish, it would be interesting to probe beta-cell synchrony in response to glucose in adult zebrafish islets. Adult mouse beta-cells, which are located in the islet core, display islet-wide Ca^{2+} synchrony in response to glucose, whereas the Ca^{2+} synchrony of adult human beta-cells is localized to subpopulations (341). These differences between mouse and human beta-cell synchrony is thought to be attributed to differences in islet architecture as human islets have beta-cells and alpha-cells that are found within the islet core (342–344). Whether the presence of delta-cells and alpha-cells in the islet core in the adult zebrafish islet leads to localized Ca2+ synchrony has yet to be fully explored.

We also observed a small proportion of polyhormonal cells in the adult zebrafish islets. In the developing mammalian pancreas, polyhormonal cells can be observed, but they are rarely found in adult mammals under normal physiological conditions (346,347). In our findings, we observed that the majority of polyhormonal endocrine cells in the adult are insulin, somatostatin co-positive. We also observed a trending increase in the number of insulin, somatostatin co-positive cells during beta-cell regeneration. Whether these cells represent immature cells or represent cells transitioning between the delta- and beta-cell identities is currently unclear. Lineage tracing of delta-cells during beta-cell regeneration and under physiological conditions would determine if delta-cells contribute to beta-cell expansion and renewal.

Like rodents, beta-cell proliferation is low in adult zebrafish (1%) (251,271). However, we observed that as the zebrafish ages, beta-cell expansion in the adult stage is primarily mediated by beta-cell proliferation under normal physiological conditions. These results are consistent with mammalian studies which report proliferation as the main mechanism of beta-cell maintenance in the adult islet (135). However, this does not rule out the possibility of a non-beta-cell source contributing to beta-cell mass. In our beta-cell lineage tracing experiment under normal

physiological conditions, we observed increases in single unlabelled (new) beta-cells. Interestingly, previous studies have suggested a subset of pancreatic progenitor cells in the zebrafish adult pancreas which reside on or adjacent to the pancreatic ducts (295,306). In one study, up to 5% of *nkx6.1*-expressing ductal cells also express insulin in the adult pancreas under physiological conditions (295). However, whether these insulin+ cells on the duct represent ductal-to-beta-cell transdifferentiation or general ductal cell plasticity is unclear. Future studies which lineage trace ductal cells under physiological conditions would provide clarity on ductal cell contribution to beta-cell maintenance.

In our beta-cell lineage tracing experiment under normal physiological conditions, we also observed rare DsRed+/EGFP-/INS- cells. There is no significant increase in the number of DsRed+/GFP-/INS- overtime. It is unclear if these cells represent dedifferentiated beta-cells or beta-cells that have transient lower insulin gene activity. In mice, bursts of transcriptional activity under the *Ins1* and *Ins2* promoter have been described, indicating the dynamic nature of gene transcription in the beta-cell (94,111,112). Assessing the transcriptional profile of these DsRed+/EGFP-/INS- cells through single cell RNA sequencing would provide an unbiased and thorough characterization of these cells.

While we observed that beta-cell proliferation is the primary mechanism of beta-cell expansion in the adult zebrafish, we found that it is not the main mechanism in >90% beta-cell ablation. Lineage tracing of adult beta-cells revealed that a non-beta-cell source contributes to beta-cell renewal. This non-beta-cell source may represent other pancreatic endocrine cells, acinar, or ductal cells. Previous studies have suggested the contribution of ductal cells to beta-cell regeneration (248,295,306). For example, *Sox9b* mutant larval zebrafish, which have defective ductal development, displayed significantly reduced beta-cell regeneration in comparison to

control fish (248), suggesting the role of ductal cells to beta-cell renewal. Another study utilizing *Tg(nkx6.1:GFP)* adult zebrafish found significantly higher numbers of GFP+ ductal cells expressing insulin during beta-cell regeneration (11%) compared to control animals (5%) (295), suggesting possible transdifferentiation of ductal cells into insulin-expressing cells. More recently, lineage tracing of centroacinar cells (CACs), a specialized type of ductal cell located at the center of the acinus at the duct terminus, showed that 43% of insulin+ cells at 10 days post MTZ treatment originate from CACs (218). CACs also show a significant increase in proliferation during beta-cell renewal (218). Whether CACs are the sole contributor of beta-cell renewal in zebrafish is still unclear. CACs are also found in the rodent pancreas, located at the proximal tips of the pancreatic ductal tree and have been proposed to be pancreatic progenitor cells (348–350). Similar to zebrafish CACs, rodent CACs express *Sox9* and are Notch responsive (65,218,227,248,350,351); however, ductal/CAC contribution in mammalian pancreatic injury models is controversial. While some studies have reported increases in ductal cell proliferation (140,141) and increases in the frequency of insulin+ and PDX1+ cells on pancreatic ducts after pancreatic injury (139,197,352), lineage tracing of ducts/CACs using *Sox9* (65), *Hes1* (68), *Hnf1b* (67), or *Muc1* (200) promoters have shown no significant contribution of ductal tissue to beta-cell renewal. It is worth noting that some studies had low labelling efficiencies (20-40%) (67,68,200); as such, the contribution of ductal cells during beta-cell regeneration could be overlooked in these mammalian studies.

While we did not observe a significant increase in glucagon+/insulin+ or somatostatin+/insulin+ area during beta-cell regeneration, we cannot rule out the possibility that new beta-cells are also generated from these cell types. Studies have reported transdifferentiation of alpha-cells into beta-cells during beta-cell regeneration in larval zebrafish (283,294), suggesting that alpha-cells are a potential cell source for new beta-cells. It is possible that the extent of beta-cell ablation

and the age of ablation (larval vs ductal) may impact the type of regenerative mechanism(s) utilized. In mice, delta-to-beta-cell transdifferentiation is exhibited in diphtheria toxin mediated beta-cell ablation in 2 week old neonatal mice (159), but not 2 month old adult mice which exhibit alpha-to-beta-cell transdifferentiation (160), suggesting that age is a factor in determining cell plasticity. Lineage tracing of the various different islet endocrine cells, ductal cells, and acinar cells will help clarify the cell sources responsible for zebrafish beta-cell renewal at different ages. Future studies should also explore the mechanism of beta-cell regeneration under different extents of beta-cell ablation as regenerative mechanisms may differ in complete and partial beta-cell ablation models. It would also be interesting to probe the cell types responsible for the increase in beta-cell mass under diet induced obesity in adult zebrafish (288). While lineage tracing can help determine the cell sources that contribute to beta-cell regeneration and the associated increase in beta-cell mass in response to nutrition, low labelling efficiencies (due to low Cre recombination efficiency, low-level Cre or marker expression from minimal promoters, and/or heterogeneity in promoter activity), leaky expression or activation of Cre, and/or dynamic changes in transcription can complicate interpretations of lineage tracing experiments. In addition, marker genes, such as GFP, can cause gene expression changes or cell cytotoxicity (353,354), which in turn can affect biological mechanisms. These important caveats should be kept in mind while interpreting our and other lineage tracing results. Despite these caveats, lineage tracing has proven to be a powerful technique for tracking cells *in vivo* and dissecting roles of different cell types during development and regeneration. Understanding the cell sources in variable regenerative conditions will provide insight into the mechanism(s) of beta-cell regeneration in zebrafish and may provide insight into possible cell sources that may be activated in beta-cell regeneration in mammals.

Chapter 5: Conclusion

5.1 Research findings

As the number of diabetes cases continues to grow, the economic burden associated with their medical care increases as well. Insulin therapy is a lifesaving treatment, although this therapy does not address the underlying pathology: the lack of adequate beta-cell number or function. Replacement or regeneration of beta-cells could offer a cure that allows for optimal glycemic control. In this thesis, we utilized zebrafish as a model to explore beta-cell biology and regeneration.

First, we characterized beta-cells arising from different ontogenies. Previous research has indicated that different precursor populations give rise to the dorsal and ventral pancreatic buds (226,268). Furthermore, a previous study has identified transcriptional differences between beta-cells derived from the dorsal and ventral pancreatic buds early in development (226,267). However, the relative contribution of the beta-cells arising from dorsal and ventral buds to overall adult beta-cell mass is unclear, and whether transcriptional differences exist between these two populations in the adult animal is unknown. We first undertook the development of a novel transgenic line, *Tg(ins:EGFP-T2A-CreER^{T2})*. By crossing our line with the existing *Tg(actb2:LOXP-STOP-LOXP-DsRedEx)*, we were able to heritably label beta-cells. A small amount of leaky activation of CreER^{T2} was observed. While it wasn't completely unexpected as leaky transport of the CreER^{T2} fusion protein to the nucleus has been described in different systems (299,311–314), it is a caveat of our lineage tracing system that should be kept in mind while interpreting our results. Dorsally-derived beta-cells arise first (thus we term primary beta-cells) in development. With our Cre/LoxP lineage tracing model, we determined that the primary beta-cells give rise to a small proportion of beta-cells in the adult pancreatic principal islet. Beta-cells derived

from the ventral pancreatic bud (termed secondary beta-cells) arise later in development and constitute the majority of beta-cell mass in the adult. While there are transcriptional differences between beta-cells in the adult pancreas, the transcriptional profiles of primary and secondary beta-cells are similar. This finding suggests that ontogeny does not dictate a distinct beta-cell transcriptional profile.

We next sought to characterize the angiogenic factors important in islet vascularization and the role of endothelial cells in beta-cell development. We found that *Vegfaa* and *Vegfab* are expressed in beta-cells and that inhibiting VegfA/vegfr2 signalling using genetic (morpholino) or pharmaceutical means does not lead to significant differences in beta-cell or alpha-cell formation. We interestingly observed that the number of endothelial cells decreases after beta-cell ablation, but the islet becomes revascularized during beta-cell regeneration. During heart and fin regeneration, new vessels appear at the damaged site, and this revascularization is necessary for tissue regeneration (332,333). Hence, the role of vascularization during beta-cell ablation and regeneration warrants further investigation.

In the final experiments of this thesis, we characterized islet morphology in physiological and regenerative conditions as well as identified new sources of beta-cells under physiological and regenerative conditions via lineage tracing of the beta-cells which has not previously been conducted in the adult zebrafish. Beta-cells and delta-cells constitute the majority of islet mass, and islet morphology looks similar in control and regenerated islets. Utilizing the Cre/LoxP lineage tracing tool we developed in Chapter 2, we lineage traced pre-existing adult beta-cells. Like rodents, beta-cell maintenance in zebrafish adult stages is primarily mediated through beta-cell proliferation. However, in >90% beta-cell destruction, a non-beta-cell source is the primary contributor of new beta-cells. This is consistent with studies that have suggested that ductal cells

contribute to adult beta-cell regeneration (218,295). Our studies highlight some key differences in delta-cell islet proportions between mammals and zebrafish. Our studies also highlight the regenerative ability of the zebrafish organism and give insight into the mechanism of beta-cell renewal. Understanding the regenerative mechanism(s) in zebrafish may lead to the development of new therapeutic targets to promote regeneration of new beta-cells in mammals, which will ultimately bring hope to the cure of diabetes.

5.2 Key limitations

The work presented in this thesis has various caveats including methodology and model systems. These limitations are discussed within each chapter. Here we outline two general limitations. The first limitation is the use of transgenic models. In our studies, the transgenic models used were generated using the Tol2 transposon method, in which the transgene is placed into a Tol2 transposon vector to facilitate random genomic integration(s) of the transgene (303,304). The regulatory environment at the site of integration can influence the expression of the transgenic reporter leading to mosaic patterns of transgene expression, otherwise known as position effects. Position effects may explain the lack of ubiquity in the *Tg(-3.5ubb:CreER^{T2}, myl7:EGFP)* and *Tg(hsp701:mCherry-T2A-CreER^{T2}*) Cre driver lines tested in Chapter 2. In addition, off-target expression involving neighboring endogenous genes can also be a caveat of random transgene insertion (355). Given that most, if not all, applications want controlled temporal and spatial regulation of introduced transgenes, random transgene integration(s) and position effects can provide major obstacles. The use of insulators within the transgene can help prevent chromosomal position effects and block distal enhancer activity (356). Targeted transgene integration can also allow for better control of specific reporter expression. PhiC31 integrase

method has the potential to limit variability of position effects (317) and alternative methods such as CRISPR/Cas9 that allow genetic modification to be targeted to genomic locations have been developed (357–360). For example, CRISPR/Cas9 has allowed for successful EGFP reporter integration into both targeted *pax2a* alleles in zebrafish, thus allowing real-time visualization of target gene expression (358). Knock-ins can also be advantageous as expression would be faithfully recapitulated at the endogenous locus, whereas transgenics often involve the use of minimal promoters. Thus, gene integration at a targeted locus may mitigate substantial variation in expression patterns and provide more faithful recapitulation of gene expression. Despite the aforementioned challenges of using the Tol2 system to generate transgenic models, mapping out transgene insertions, outbreeding to create sublines with single copies of the transgene, and thorough and continuous characterization of transgenic lines can help to ensure tissue specific activity.

The second limitation we would like to address is the use of zebrafish. Zebrafish are a powerful model to probe basic cell biology and regeneration. While zebrafish pancreas development is similar to mammalian pancreas development, key differences in the transcriptional cascade and morphological development have been identified (236,237,239). Hence, it is important that interspecies conclusions be made with caution. For example, our results indicate that the dorsal pancreatic bud which gives rise to the primary beta-cells do not constitute the majority of islet cell mass. In contrast, the dorsal pancreas constitutes the majority of the pancreas in mammals (118,119). Moreover, the dorsal pancreatic bud in zebrafish solely gives rise to pancreatic endocrine cells, while the dorsal bud in mammals give rise to endocrine and exocrine tissue (236,237,239), suggesting that the dorsal pancreatic bud may not be analogous between mammals and zebrafish. It should also be acknowledged that there are experimental challenges of

the zebrafish model system. The size of larval zebrafish do not allow for blood collection; albeit, measurement of whole organism free glucose provides a reliable alternative method (252,361). Repeated blood glucose measurements in the adult is challenging (362), and the limited amount of blood do not allow for assessment of plasma hormone levels in individual animals. Despite these experimental challenges, the rapid organ development and remarkable ability of tissue regeneration make the zebrafish a powerful model to study pancreas development and renewal. As more sophisticated tools are made available to zebrafish research, this model system will help provide insights to new key pathways relevant to normal physiology and metabolic diseases such as diabetes.

5.3 Future directions

The studies outlined in this thesis have been focused on the development of Cre/LoxP lineage tracing line and understanding fundamental aspects of zebrafish beta-cell biology and regeneration including understanding possible differences in beta-cells that arise from different ontogenies, the effect of islet vessel deficiency during early endocrine development, and the primary cell sources in beta-cell maintenance and regeneration. While this work has answered some basic questions in zebrafish beta-cell biology and renewal, a number of avenues of investigation remain to be explored.

5.3.1 Further investigation of zebrafish beta-cell heterogeneity

While we did not observe distinct transcriptional profiles between primary and secondary beta-cells, our single cell RNA sequencing data indicates transcriptional heterogeneity between beta-cells. Exploring these populations may yield important insights into beta-cell transitional

states and beta-cell heterogeneity in the adult zebrafish. For example, our data indicates that some beta-cells have detectable glucagon and somatostatin expression. In Chapter 4, we observed polyhormonal cells, most of which were somatostatin, insulin co-positive cells. In our lineage tracing experiments in Chapter 4, we also observed the existence of DsRed+, but EGFP- and insulin-negative cells, suggesting dynamic gene expression or possible islet cell plasticity. Future studies analyzing genes implicated in alpha-cell and delta-cell identity in the insulin, glucagon-expressing cells and the insulin, somatostatin-expressing cells in our single cell RNA sequencing data set may provide better understanding of the transcriptional profile of these polyhormonal cells. Lineage tracing of alpha-cells and delta-cells in the adult animals under physiological conditions may also provide detail into adult endocrine cell plasticity during physiological conditions.

5.3.2 Determining the role of delta-cells in the zebrafish

In Chapter 4, we observed a vast number of delta-cells within the islet (up to 50%). We also observed somatostatin+ single cells scattered throughout the exocrine pancreas. This is vastly different from mammalian islet morphology in which delta-cells make 2-11% of the islet. The physiological implications of delta-cells in zebrafish islet development and regeneration, normal islet function, and glucagon and insulin secretion are not known. Inhibiting delta-cell differentiation or ablating pancreatic delta-cells during development and in the adult islet would allow us to better characterize the role of pancreatic delta-cells during endocrine formation and maintenance.

We also observed that delta-cells are interspersed among beta-cells within the islet core. Given the importance of beta-cell connections in proper insulin secretion, it would be interesting

to tandemly observe calcium signalling in delta-cells and beta-cells in response to various stimuli. The generation of a *Tg(sst2:RCaMP)* line, in which the somatostatin promoter drives a red genetically encoded calcium indicator (GECI) as a readout of calcium regulated somatostatin secretion and the subsequent crossing of this line to the existing *Tg(ins:GCaMP)* line (269) in which the insulin promoter drives a green GECI, may provide interesting observations into calcium regulated somatostatin and insulin secretion. Given the transparency and *ex-utero* development of the zebrafish, this model offers a unique advantage to observe calcium oscillations in delta-cells and beta-cells *in vivo.*

5.3.3 Assessing the role of vasculature in beta-cell biology and beta-cell regeneration

In Chapter 3, we observed that islet vasculature is significantly decreased after beta-cell ablation. This observation is supported by a separate report which observed islet vasculature reorganization upon beta-cell ablation and regeneration in adult zebrafish (224). In other tissues, revascularization during organ regeneration has been reported and is necessary for tissue regeneration (332,333). Hence, the role of vasculature in beta-cell regeneration warrants further investigation. Disruption of islet Vegfaa and Vegfab signalling during beta-cell ablation and regeneration will help discern the role of vasculature in beta-cell renewal. This can be achieved by conditional islet specific *vegfaa*/*vegfab* knockout studies, or by creating a dominant negative *vegfaa* and/or *vegfab* under the control of an islet specific promoter. Decreases in islet vasculature in a conditional model would allow us to determine the role that vasculature plays during beta-cell regeneration. Such a model would also be useful in future studies probing the role of vasculature in beta-cell biology in adult zebrafish.

Hypervascularization experiments under physiological and regenerative conditions involving the overexpression of *vegfaa* under a pancreatic or an islet specific promoter may also prove to be insightful in dissecting the role of vasculature during zebrafish beta-cell regeneration. In mice, short term overexpression of *Vegfa* in adult beta-cells, resulted in islet hypervascularization, increased beta-cell proliferation, and protection from alloxan mediated beta-cell death (87). Whether an increase in islet vasculature can play a protective role in *nfsB*/MTZ-mediated beta-cell death or enhance beta-cell regeneration in zebrafish is unknown. Overall, the role of islet vessels during zebrafish beta-cell regeneration is poorly understood and should be the topic of future studies. Understanding the role of vasculature during zebrafish beta-cell renewal may help drive our understanding of beta-cell regeneration in mammals.

5.3.4 Further investigation of the cell sources for beta-cell renewal under physiological stressors

Previous beta-cell regeneration studies have implicated ductal/centroacinar cells and alpha-cells as sources for new beta-cells in regeneration (218,248,294,295,363). Our results in Chapter 4 support this as our lineage tracing studies indicate that proliferation of pre-existing beta-cells after >90% beta-cell ablation in adult zebrafish is rare, if at all, contributes to the increase in beta-cell mass during regeneration. These data suggest that a non-beta-cell source is contributing to beta-cell renewal. Lineage tracing of ductal cells, acinar cells, and non-beta islet cells will be crucial to understand the cell types involved in beta-cell regeneration. Furthermore, lineage tracing of beta-cells under different extents of beta-cell ablation may also yield important insights into the regenerative mechanism(s) used after extreme (>90%) and partial (~50%) beta-cell ablation. It is possible that the regenerative mechanism activated is contingent on the extent of ablation. For example, under extreme beta-cell loss in mice, beta-cell neogenesis and transdifferentiation have

been reported (147,159,160). It would also be of interest to understand the regenerative mechanism(s) at different ages extending from the zebrafish larval stage and at various adult ages. While our studies indicate that the capacity for beta-cell regeneration does not change between 4 month old and 17 month old zebrafish, it is possible that the regenerative mechanisms may vary between ages. After extreme beta-cell loss, young mice exhibit delta-to-beta-cell transdifferentiation while older mice exhibit alpha-to-beta-cell transdifferentiation (159,160), suggesting cell plasticity may be age-dependent. Lineage tracing of different pancreatic cell types during beta-cell regeneration in larval fish and adult fish at various adult ages should be explored. It would also be interesting to determine the extent of beta-cell regeneration in older (>2 years old) fish. In mice, regeneration is restricted in older mice as there is an age dependent decline in proliferation, which is the main mechanism of beta-cell maintenance and regeneration (110). While beta-cell proliferation does not seem to be the main mechanism of beta-cell regeneration in zebrafish, it is possible that regenerative mechanisms in zebrafish may also be age dependent. In fin regeneration, slight differences in fin outgrowth are observed between young (4 month) and old (1.5 years old) animals when examined in the late regeneration stages (337). Understanding the factors that influence zebrafish beta-cell renewal will be critical next steps in beta-cell regeneration studies.

Determining new cell sources in type 2 diabetes zebrafish models would also be of interest to the field. *Tg(ins:EGFP)* fish that are overfed (6 times daily than the standard 2 times daily) exhibit increases in GFP+ fluorescent area (288), and overnutrition has been shown to increase beta-cell mass in larval fish (316,364). Lineage tracing of beta-cells in overnutrition and type 2 diabetes models could yield important insights into zebrafish beta-cell biology and regeneration.

5.3.5 Dissecting the mechanisms that promote and hinder beta-cell regeneration

The factors that cause beta-cell renewal are not known. In mammals, glycemic control has been proposed to be an important factor in beta-cell regeneration after STZ-mediated beta-cell destruction and pancreatectomy (194,365). In zebrafish, organ regeneration is impaired in response to hyperglycemia, which can be achieved by multiple STZ injections or immersing zebrafish in glucose during the recovery process (275,366). It is possible that a hyperglycemic environment may also blunt zebrafish beta-cell regeneration. Immersing zebrafish in a glucose bath during the beta-cell regeneration process would help determine if hyperglycemia affects the capacity of beta-cell renewal. Single cell RNA sequencing of beta-cells during various stages of the regenerative process may also yield a better understanding of the genes involved in regeneration. Such studies will allow for a comprehensive examination of transcriptional changes and may provide insights into the genes and mechanisms that are important in beta-cell regeneration in mammals.

5.4 Concluding thoughts

There have been considerable developments to improve glycemic control in patients with diabetes including advancements in insulin therapy and diabetes medications. However, many of these methods still provide suboptimal glucose control, and insulin injections and constant glucose monitoring can be a burden in patients with diabetes. Islet transplantation shows significant therapeutic promise; however, this therapy is hampered by the lack of available islets. While hPSCs can provide an unlimited source of insulin-producing cells, the precise developmental cascades that turn human pancreatic progenitor cells into fully functional endocrine cells are still being discovered. Stimulation or activation of endogenous beta-cell regeneration is an alternative strategy to replace beta-cell loss in patients with diabetes; however, these mechanisms are still

relatively unclear in the mammalian system. Given the similarity in pancreas development, the zebrafish model has the potential to unveil new understandings of beta-cell development, biology, and regeneration.

This current thesis has clarified some basic biological questions regarding zebrafish beta-cell biology and renewal. Furthermore, we developed and characterized a novel zebrafish transgenic line *Tg(ins:EGFP-T2A-CreER^{T2})* which will be valuable in Cre mediated conditional labelling during beta-cell physiological and regenerative conditions. A better understanding of the cell types that contribute to zebrafish beta-cell regeneration may allow for the development of beta-cell regenerative strategies in humans. It is hoped that the findings presented in this thesis can contribute a better understanding of beta-cell biology and regeneration in order to improve beta-cell replacement strategies for diabetes.

Bibliography

1. International Diabetes Federation. International Diabetes Federation. [Internet]. IDF DIABETES ATLAS - 8TH EDITION. 2017. Available from: http://www.diabetesatlas.org
2. Centers for Disease Control and Prevention. National Diabetes Statistics Report [Internet]. Atlanta, GA; 2017. Available from: https://www.cdc.gov/diabetes/
3. Dupuis J, Langenberg C, Prokopenko I, Saxena R, Soranzo N, Jackson AU, Wheeler E, Glazer NL, Bouatia-Naji N, Gloyn AL, Lindgren CM, Mägi R, Morris AP, Randall J, Johnson T, Elliott P, Rybin D, Thorleifsson G, Steinthorsdottir V, et al. New genetic loci implicated in fasting glucose homeostasis and their impact on type 2 diabetes risk. Nat Genet. 2010;42(2):105–16.
4. Zhang C, Qi L, Hunter DJ, Meigs JB, Manson JAE, Van Dam RM, Hu FB. Variant of transcription factor 7-like 2 (TCF7L2) gene and the risk of type 2 diabetes in large cohorts of U.S. women and men. Diabetes. 2006;55(9):2645–8.
5. Willcox A, Richardson SJ, Bone AJ, Foulis AK, Morgan NG. Analysis of islet inflammation in human type 1 diabetes. Clin Exp Immunol. 2009;155(2):173–81.
6. Bingley PJ. Clinical applications of diabetes antibody testing. J Clin Endocrinol Metab. 2010;95(1):25–33.
7. Barrett JC, Clayton DG, Concannon P, Akolkar B, Cooper JD, Erlich HA, Julier C, Morahan G, Nerup J, Nierras C, Plagnol V, Pociot F, Schuilenburg H, Smyth DJ, Stevens H, Todd JA, Walker NM, Rich SS, Consortium TT 1 DG. Genome-wide association study and meta-analysis find that over 40 loci affect risk of type 1 diabetes. Nat Genet. 2009;41(6):703–7.
8. Latres E, Finan DA, Greenstein JL, Kowalski A, Kieffer TJ. Navigating two roads to glucose normalization in diabetes: automated insulin delivery devices and cell therapy. Cell Metab. 2019;29(3):545–63.
9. Allen N, Gupta A. Current diabetes technology: Striving for the artificial pancreas. Diagnostics. 2019;9(1):E31.
10. Shapiro AM, Lakey JR, Ryan EA, Korbutt GS, Toth E, Warnock GL, Kneteman NM, Rajotte RV. Islet transplantation in seven patients with type 1 diabetes mellitus using a glucocorticoid-free immunosuppressive regimen. N Engl J Med. 2000;343(4):230–8.
11. Shapiro AMJ, Pokrywczynska M, Ricordi C. Clinical pancreatic islet transplantation. Nat Rev Endocrinol. 2017;13(5):268–77.
12. Borg DJ, Bonifacio E. The use of biomaterials in islet transplantation. Curr Diab Rep. 2011;11(5):434–44.
13. Ernst AU, Wang LH, Ma M. Islet encapsulation. J Mater Chem B. 2018;6(42):6705–22.
14. Groot Nibbelink M, Skrzypek K, Karbaat L, Both S, Plass J, Klomphaar B, van Lente J, Henke S, Karperien M, Stamatialis D, van Apeldoorn A. An important step towards a prevascularized islet microencapsulation device: in vivo prevascularization by combination of mesenchymal stem cells on micropatterned membranes. J Mater Sci Mater Med. 2018;29(11):1–10.
15. D'Amour KA, Bang AG, Eliazer S, Kelly OG, Agulnick AD, Smart NG, Moorman MA, Kroon E, Carpenter MK, Baetge EE. Production of pancreatic hormone-expressing endocrine cells from human embryonic stem cells. Nat Biotechnol. 2006;24(11):1392–

401.
16. Kroon E, Martinson LA, Kadoya K, Bang AG, Kelly OG, Eliazer S, Young H, Richardson M, Smart NG, Cunningham J, Agulnick AD, D'Amour KA, Carpenter MK, Baetge EE. Pancreatic endoderm derived from human embryonic stem cells generates glucose-responsive insulin-secreting cells in vivo. Nat Biotechnol. 2008;26(4):443–52.
17. Rezania A, Bruin JE, Riedel MJ, Mojibian M, Asadi A, Xu J, Gauvin R, Narayan K, Karanu F, O'Neil JJ, Ao Z, Warnock GL, Kieffer TJ. Maturation of human embryonic stem cell-derived pancreatic progenitors into functional islets capable of treating pre-existing diabetes in mice. Diabetes. 2012;61(8):2016–29.
18. Velazco-Cruz L, Song J, Maxwell KG, Goedegebuure MM, Augsornworawat P, Hogrebe NJ, Millman JR. Acquisition of Dynamic Function in Human Stem Cell-Derived β Cells. Stem Cell Reports. 2019;12(2):351–65.
19. Rezania A, Bruin JE, Arora P, Rubin A, Batushansky I, Asadi A, O'Dwyer S, Quiskamp N, Mojibian M, Albrecht T, Yang YHC, Johnson JD, Kieffer TJ. Reversal of diabetes with insulin-producing cells derived in vitro from human pluripotent stem cells. Nat Biotechnol. 2014;32(11):1121–33.
20. Pagliuca FW, Millman JR, Gürtler M, Segel M, Van Dervort A, Ryu JH, Peterson QP, Greiner D, Melton DA. Generation of functional human pancreatic β cells in vitro. Cell. 2014;159(2):428–39.
21. Oram RA, Jones AG, Besser REJ, Knight BA, Shields BM, Brown RJ, Hattersley AT, McDonald TJ. The majority of patients with long-duration type 1 diabetes are insulin microsecretors and have functioning beta cells. Diabetologia. 2014;57(1):187–91.
22. Oram RA, McDonald TJ, Shields BM, Hudson MM, Shepherd MH, Hammersley S, Pearson ER, Hattersley AT, Sanders T, Tiley S, Gellatly E, Beall L, Shepherd B, Colhune H, Colclough K, Ellard S. Most people with long-duration type 1 diabetes in a large population-based study are insulin microsecretors. Diabetes Care. 2015;38(2):323–8.
23. Davis AK, DuBose SN, Haller MJ, Miller KM, DiMeglio LA, Bethin KE, Goland RS, Greenberg EM, Liljenquist DR, Ahmann AJ, Marcovina SM, Peters AL, Beck RW, Greenbaum CJ. Prevalence of detectable c-peptide according to age at diagnosis and duration of type 1 diabetes. Diabetes Care. 2015;38(3):476–81.
24. Yu MG, Keenan HA, Shah HS, Frodsham SG, Pober D, He Z, Wolfson EA, D'Eon S, Tinsley LJ, Bonner-Weir S, Pezzolesi MG, King GL. Residual beta cell function and monogenic variants in long-duration type 1 diabetes patients. J Clin Invest. 2019;130(6):1–12.
25. Meier JJ, Bhushan A, Butler AE, Rizza RA, Butler PC. Sustained beta cell apoptosis in patients with long-standing type 1 diabetes: Indirect evidence for islet regeneration? Diabetologia. 2005;48(11):2221–8.
26. Willcox A, Richardson SJ, Bone AJ, Foulis AK, Morgan NG. Evidence of increased islet cell proliferation in patients with recent-onset type 1 diabetes. Diabetologia. 2010;53(9):2020–8.
27. Butler AE, Janson J, Bonner-Weir S, Ritzel R, Rizza R, Butler PC. Beta-cell deficit and increased beta-cell apoptosis in humans with type 2 diabetes. Diabetes. 2003;52(1):102–10.
28. Matveyenko AV, Butler PC. Relationship between β-cell mass and diabetes onset. Diabetes, Obes Metab. 2008;10(SUPPL. 4):23–31.

29. Rahier J, Guiot Y, Goebbels RM, Sempoux C, Henquin JC. Pancreatic beta-cell mass in European subjects with type 2 diabetes. Diabetes Obes Metab. 2008;10 Suppl 4(7):32–42.
30. Butler AE, Dhawan S, Hoang J, Cory M, Zeng K, Fritsch H, Meier JJ, Rizza RA, Butler PC. α-Cell deficit in obese type 2 diabetes, a minor role of α-Cell dedifferentiation and degranulation. J Clin Endocrinol Metab. 2016;101(2):523–32.
31. Brennan J, Lu CC, Norris DP, Rodriguez TA, Beddington RSP, Robertson EJ. Nodal signalling in the epiblast patterns the early mouse embryo. Nature. 2001;411(6840):965–9.
32. Weinstein DC, Ruiz i Altaba A, Chen WS, Hoodless P, Prezioso VR, Jessell TM, Darnell JJ. The winged-helix transcription factor HNF-3 beta is required for notochord development in the mouse embryo. Cell. 1994;78(4):575–88.
33. Ang SL, Rossant J. HNF-3 beta is essential for node and notochord formation in mouse development. Cell. 1994;78(4):561–74.
34. Kanai-Azuma M, Kanai Y, Gad JM, Tajima Y, Taya C, Kurohmaru M, Sanai Y, Yonekawa H, Yazaki K, Tam PPL, Hayashi Y. Depletion of definitive gut endoderm in Sox17-null mutant mice. Development. 2002;129(10):2367–79.
35. Zorn AM, Wells JM. Vertebrate Endoderm Development and Organ Formation. Annu Rev Cell Dev Biol. 2009;25(1):221–51.
36. Stafford D, Prince VE. Retinoic acid signaling is required for a critical early step in zebrafish pancreatic development. Curr Biol. 2002;12(14):1215–20.
37. Chen Y, Pan FC, Brandes N, Afelik S, Sölter M, Pieler T. Retinoic acid signaling is essential for pancreas development and promotes endocrine at the expense of exocrine cell differentiation in Xenopus. Dev Biol. 2004;271(1):144–60.
38. Hebrok M, Kim SK, Melton DA. Notochord repression of endodermal sonic hedgehog permits pancreas development. Genes Dev. 1998;12(11):1705–13.
39. Wells JM, Melton DA. Early mouse endoderm is patterned by soluble factors from adjacent germ layers. Development. 2000;127(8):1563–72.
40. Tiso N, Filippi A, Pauls S, Bortolussi M, Argenton F. BMP signalling regulates anteroposterior endoderm patterning in zebrafish. Mech Dev. 2002;118(1–2):29–37.
41. Martín M, Gallego-Llamas J, Ribes V, Kedinger M, Niederreither K, Chambon P, Dollé P, Gradwohl G. Dorsal pancreas agenesis in retinoic acid-deficient Raldh2 mutant mice. Dev Biol. 2005;284(2):399–411.
42. Kim SK, Hebrok M, Li E, Oh SP, Schrewe H, Harmon EB, Lee JS, Melton DA. Activin receptor patterning of foregut organogenesis. Genes Dev. 2000;14(15):1866–71.
43. Deutsch G, Jung J, Zheng M, Lóra J, Zaret KS. A bipotential precursor population for pancreas and liver within the embryonic endoderm. Development. 2001;128(6):871–81.
44. Gannon M, Herrera PL, Wright CVE. Mosaic Cre-mediated recombination in pancreas using the pdx-1 enhancer/promoter. Genesis. 2000;26(2):143–4.
45. Gu G, Dubauskaite J, Melton DA. Direct evidence for the pancreatic lineage: NGN3+ cells are islet progenitors and are distinct from duct progenitors. Development. 2002;129(10):2447–57.
46. Jonsson J, Carlsson L, Edlund T, Edlund H. Insulin-promoter-factor 1 is required for pancreas development in mice. Nature. 1994;371(6498):606–9.
47. Offield MF, Jetton TL, Labosky PA, Ray M, Stein RW, Magnuson MA, Hogan BL, Wright CV. PDX-1 is required for pancreatic outgrowth and differentiation of the rostral duodenum. Development. 1996;122(3):983–95.

48. Stoffers DA, Zinkin NT, Stanojevic V, Clarke WL, Habener JF. Pancreatic agenesis attributable to a single nucleotide deletion in the human IPF1 gene coding sequence. Nat Genet. 1997;15(1):106–10.
49. Gittes GK. Developmental biology of the pancreas: A comprehensive review. Dev Biol. 2009;326(1):4–35.
50. Godlewski G, Gaubert J, Cristol-Gaubert R, Radi M, Baecker V, Travo P, Prudhomme M, Prat-Pradal D. Moving and fusion of the pancreatic buds in the rat embryos during the embryonic period (carnegie stages 13-17) by a three-dimensional computer-assisted reconstruction. Surg Radiol Anat. 2011;33(8):659–64.
51. Villasenor A, Chong DC, Cleaver O. Biphasic Ngn3 expression in the developing pancreas. Dev Dyn. 2008;237(11):3270–9.
52. Gradwohl G, Dierich A, LeMeur M, Guillemot F. Neurogenin3 Is Required for the Development of the Four Endocrine Cell Lineages of the Pancreas. Proc Natl Acad Sci U S A. 2000;97(4):1607–11.
53. Rubio-Cabezas O, Jensen JN, Hodgson MI, Codner E, Ellard S, Serup P, Hattersley AT. Permanent neonatal diabetes and enteric anendocrinosis associated with biallelic mutations in NEUROG3. Diabetes. 2011;60(4):1349–53.
54. Teitelman G, Alpert S, Polak JM, Martinez A, Hanahan D. Precursor cells of mouse endocrine pancreas coexpress insulin, glucagon and the neuronal proteins tyrosine hydroxylase and neuropeptide Y, but not pancreatic polypeptide. Development. 1993;118(4):1031–9.
55. Herrera PL, Huarte J, Sanvito F, Meda P, Orci L, Vassalli JD. Embryogenesis of the murine endocrine pancreas; early expression of pancreatic polypeptide gene. Development. 1991;113(4):1257–65.
56. Upchurch BH, Aponte GW, Leiter AB. Expression of peptide YY in all four islet cell types in the developing mouse pancreas suggests a common peptide YY-producing progenitor. Development. 1994;120(2):245–52.
57. Herrera PL. Adult insulin- and glucagon-producing cells differentiate from two independent cell lineages. Development. 2000;127(11):2317–22.
58. Pictet RL, Clark WR, Williams RH, Rutter WJ. An ultrastructural analysis of the developing embryonic pancreas. Dev Biol. 1972;29(4):436–67.
59. Zhou Q, Law AC, Rajagopal J, Anderson WJ, Gray PA, Melton DA. A multipotent progenitor domain guides pancreatic organogenesis. Dev Cell. 2007;13(1):103–14.
60. Schaffer AE, Freude KK, Nelson SB, Sander M. Nkx6 transcription factors and Ptf1a function as antagonistic lineage determinants in multipotent pancreatic progenitors. Dev Cell. 2010;18(6):1022–9.
61. Jennings RE, Berry AA, Kirkwood-Wilson R, Roberts NA, Hearn T, Salisbury RJ, Blaylock J, Hanley KP, Hanley NA. Development of the human pancreas from foregut to endocrine commitment. Diabetes. 2013;62(10):3514–22.
62. Salisbury RJ, Blaylock J, Berry AA, Jennings RE, De Krijger R, Hanley KP, Hanley NA. The window period of NEUROGENIN3 during human gestation. Islets. 2014;6(3).
63. Jeon J, Correa-Medina M, Ricordi C, Edlund H, Diez JA. Endocrine cell clustering during human pancreas development. J Histochem Cytochem. 2009;57(9):811–24.
64. Chintinne M, Stangé G, Denys B, In ’T Veld P, Hellemans K, Pipeleers-Marichal M, Ling Z, Pipeleers D. Contribution of postnatally formed small beta cell aggregates to functional

beta cell mass in adult rat pancreas. Diabetologia. 2010;53(11):2380–8.
65. Kopp JL, Dubois CL, Schaffer AE, Hao E, Shih HP, Seymour PA, Ma J, Sander M. Sox9+ ductal cells are multipotent progenitors throughout development but do not produce new endocrine cells in the normal or injured adult pancreas. Development. 2011;138(4):653–65.
66. Inada A, Nienaber C, Katsuta H, Fujitani Y, Levine J, Morita R, Sharma A, Bonner-Weir S. Carbonic anhydrase II-positive pancreatic cells are progenitors for both endocrine and exocrine pancreas after birth. Proc Natl Acad Sci U S A. 2008;105(50):19915–9.
67. Solar M, Cardalda C, Houbracken I, Martín M, Maestro MA, De Medts N, Xu X, Grau V, Heimberg H, Bouwens L, Ferrer J. Pancreatic exocrine duct cells give rise to insulin-producing β cells during embryogenesis but not after birth. Dev Cell. 2009;17(6):849–60.
68. Kopinke D, Brailsford M, Shea JE, Leavitt R, Scaife CL, Murtaugh LC. Lineage tracing reveals the dynamic contribution of Hes1+ cells to the developing and adult pancreas. Development. 2011;138(3):431–41.
69. Lammert E, Cleaver O, Melton D. Induction of pancreatic differentiation by signals from blood vessels. 2001;294(5542):564–7.
70. Jacquemin P, Yoshitomi H, Kashima Y, Rousseau GG, Lemaigre FP, Zaret KS. An endothelial-mesenchymal relay pathway regulates early phases of pancreas development. Dev Biol. 2006;290(1):189–99.
71. Yoshitomi H, Zaret KS. Endothelial cell interactions initiate dorsal pancreas development by selectively inducing the transcription factor Ptf1a. Development. 2004;131(4):807–17.
72. Krapp A, Knöfler M, Ledermann B, Bürki K, Berney C, Zoerkler N, Hagenbüchle O, Wellauer PK. The bHLH protein PTF1-p48 is essential for the formation of the exocrine and the correct spatial organization of the endocrine pancreas. Genes Dev. 1998;12(23):3752–63.
73. Kawaguchi Y, Cooper B, Gannon M, Ray M, MacDonald RJ, Wright CVE. The role of the transcriptional regulator Ptf1a in converting intestinal to pancreatic progenitors. Nat Genet. 2002;32(1):128–34.
74. Shah SR, Esni F, Jakub A, Paredes J, Lath N, Malek M, Potoka DA, Prasadan K, Mastroberardino PG, Shiota C, Guo P, Miller KA, Hackam DJ, Burns RC, Tulachan SS, Gittes GK. Embryonic mouse blood flow and oxygen correlate with early pancreatic differentiation. Dev Biol. 2011;349(2):342–9.
75. Heinis M, Simon MT, Ilc K, Mazure NM, Pouysségur J, Scharfmann R, Duvillié B. Oxygen tension regulates pancreatic beta-cell differentiation through hypoxia-inducible factor 1alpha. Diabetes. 2010;59(3):662–9.
76. Magenheim J, Ilovich O, Lazarus A, Klochendler A, Ziv O, Werman R, Hija A, Cleaver O, Mishani E, Keshet E, Dor Y. Blood vessels restrain pancreas branching, differentiation and growth. Development. 2011;138(21):4743–52.
77. Pierreux CE, Cordi S, Hick AC, Achouri Y, Ruiz de Almodovar C, Prévot PP, Courtoy PJ, Carmeliet P, Lemaigre FP. Epithelial: Endothelial cross-talk regulates exocrine differentiation in developing pancreas. Dev Biol. 2010;347(1):216–27.
78. Reinert RB, Cai Q, Hong JY, Plank JL, Aamodt K, Prasad N, Aramandla R, Dai C, Levy SE, Pozzi A, Labosky PA, Wright CVE, Brissova M, Powers AC. Vascular endothelial growth factor coordinates islet innervation via vascular scaffolding. Development. 2014;141(7):1480–91.

79. Lammert E, Gu G, McLaughlin M, Brown D, Brekken R, Murtaugh LC, Gerber HP, Ferrara N, Melton DA. Role of VEGF-A in vascularization of pancreatic islets. Curr Biol. 2003;13(12):1070–4.
80. Brissova M, Shostak A, Shiota M, Wiebe PO, Poffenberger G, Kantz J, Chen Z, Carr C, Jerome WG, Chen J, Baldwin HS, Nicholson W, Bader DM, Jetton T, Gannon M, Powers AC. Pancreatic islet production of vascular endothelial growth factor-A is essential for islet vascularization, revascularization, and function. Diabetes. 2006;55(11):2974–85.
81. Kaido T, Yebra M, Cirulli V, Montgomery AM. Regulation of human β-cell adhesion, motility, and insulin secretion by collagen IV and its receptor α1β1. J Biol Chem. 2004;279(51):53762–9.
82. Piper K, Brickwood S, Turnpenny LW, Cameron IT, Ball SG, Wilson DI, Hanley NA. Beta cell differentiation during early human pancreas development. J Endocrinol. 2004;181(1):11–23.
83. Meier JJ, Köhler CU, Alkhatib B, Sergi C, Junker T, Klein HH, Schmidt WE, Fritsch H. β-cell development and turnover during prenatal life in humans. Eur J Endocrinol. 2010;162(3):559–68.
84. Brissova M, Shostak A, Fligner CL, Revetta FL, Washington MK, Powers AC, Hull RL. Human islets have fewer blood vessels than mouse islets and the density of islet vascular structures is increased in type 2 diabetes. J Histochem Cytochem. 2015;63(8):637–45.
85. Takahashi Y, Sekine K, Kin T, Takebe T, Taniguchi H. Self-condensation culture enables vascularization of tissue fragments for efficient therapeutic transplantation. Cell Rep. 2018;23(6):1620–9.
86. Pepper AR, Pawlick R, Bruni A, Wink J, Rafiei Y, O'Gorman D, Yan-Do R, Gala-Lopez B, Kin T, MacDonald PE, Shapiro AMJ. Transplantation of human pancreatic endoderm cells reverses diabetes post transplantation in a prevascularized subcutaneous site. Stem Cell Reports. 2017;8(6):1689–700.
87. De Leu N, Heremans Y, Coppens V, Van Gassen N, Cai Y, D'Hoker J, Magenheim J, Salpeter S, Swisa A, Khalaileh A, Arnold C, Gradwohl G, Van De Casteele M, Keshet E, Dor Y, Heimberg H. Short-term overexpression of VEGF-A in mouse beta cells indirectly stimulates their proliferation and protects against diabetes. Diabetologia. 2014;57(1):140–7.
88. Kehm R, König J, Nowotny K, Jung T, Deubel S, Gohlke S, Schulz TJ, Höhn A. Age-related oxidative changes in pancreatic islets are predominantly located in the vascular system. Redox Biol. 2018;15:387–93.
89. Almaça J, Molina J, Arrojo E Drigo R, Abdulreda MH, Jeon WB, Berggren PO, Caicedo A, Nam HG. Young capillary vessels rejuvenate aged pancreatic islets. Proc Natl Acad Sci. 2014;111(49):17612–7.
90. Hogan MF, Liu AW, Peters MJ, Willard JR, Rabbani Z, Bartholomew EC, Ottley A, Hull RL. Markers of islet endothelial dysfunction occur in male B6.BKS(D)-leprdb/J mice and may contribute to reduced insulin release. Endocrinology. 2017;158(2):293–303.
91. Farack L, Golan M, Egozi A, Dezorella N, Bahar Halpern K, Ben-Moshe S, Garzilli I, Tóth B, Roitman L, Krizhanovsky V, Itzkovitz S. Transcriptional heterogeneity of beta cells in the intact pancreas. Dev Cell. 2019;48(1):115-125.e4.
92. Lorenzo PI, Fuente-Martín E, Brun T, Cobo-Vuilleumier N, Jimenez-Moreno CM, G. Herrera Gomez I, López Noriega L, Mellado-Gil JM, Martin-Montalvo A, Soria B,

Gauthier BR. PAX4 defines an expandable β-cell subpopulation in the adult pancreatic islet. Sci Rep. 2015;5:15672.
93. Bader E, Migliorini A, Gegg M, Moruzzi N, Gerdes J, Roscioni SS, Bakhti M, Brandl E, Irmler M, Beckers J, Aichler M, Feuchtinger A, Leitzinger C, Zischka H, Sattler RW, Jastroch M, Tschöp M, Machicao F, Staiger H, et al. Identification of proliferative and mature β-cells in the islets of langerhans. Nature. 2016;535(7612):430–4.
94. Szabat M, Luciani DS, Piret JM, Johnson JD. Maturation of adult β-cells revealed using a Pdx1/ insulin dual-reporter lentivirus. Endocrinology. 2009;150(4):1627–35.
95. Jetton TL, Magnuson MA. Heterogeneous expression of glucokinase among pancreatic beta cells. Proc Natl Acad Sci U S A. 1992;89(7):2619–23.
96. Jörns A, Tiedge M, Lenzen S. Nutrient-dependent distribution of insulin and glucokinase immunoreactivities in rat pancreatic beta cells. Virchows Arch. 1999;434(1):75–82.
97. Smukler SR, Arntfield ME, Razavi R, Bikopoulos G, Karpowicz P, Seaberg R, Dai F, Lee S, Ahrens R, Fraser PE, Wheeler MB, van der Kooy D. The adult mouse and human pancreas contain rare multipotent stem cells that express insulin. Cell Stem Cell. 2011;8(3):281–93.
98. Karaca M, Castel J, Tourrel-Cuzin C, Brun M, Géant A, Dubois M, Catesson S, Rodriguez M, Luquet S, Cattan P, Lockhart B, Lang J, Ktorza A, Magnan C, Kargar C. Exploring functional β-cell heterogeneity in vivo using PSA-NCAM as a specific marker. PLoS One. 2009;4(5):e5555.
99. Hermann M, Pirkebner D, Draxl A, Berger P, Untergasser G, Margreiter R, Hengster P. Dickkopf-3 is expressed in a subset of adult human pancreatic beta cells. Histochem Cell Biol. 2007;127(5):513–21.
100. Dorrell C, Schug J, Canaday PS, Russ HA, Tarlow BD, Grompe MT, Horton T, Hebrok M, Streeter PR, Kaestner KH, Grompe M. Human islets contain four distinct subtypes of β cells. Nat Commun. 2016;7:11756.
101. Van De Winkel M, Pipeleers D. Autofluorescence-activated cell sorting of pancreatic islet cells: purification of insulin-containing B-cells according to glucose-induced changes in cellular redox state. Biochem Biophys Res Commun. 1983;114(2):835–42.
102. Wang J, Baimbridge KG, Brown JC. Glucose- and acetylcholine-induced increase in intracellular free Ca2+ in subpopulations of individual rat pancreatic beta-cells. Endocrinology. 1992;131(1):146–52.
103. Kiekens R, In't Veld P, Mahler T, Schuit F, Van De Winkel M, Pipeleers D. Differences in glucose recognition by individual rat pancreatic B cells are associated with intercellular differences in glucose-induced biosynthetic activity. J Clin Invest. 1992;89(1):117–25.
104. Van Schravendijk CF, Kiekens R, Pipeleers DG. Pancreatic beta cell heterogeneity in glucose-induced insulin secretion. J Biol Chem. 1992;267(30):21344–8.
105. Qiu WL, Zhang YW, Feng Y, Li LC, Yang L, Xu CR. Deciphering pancreatic islet β cell and α cell maturation pathways and characteristic features at the single-cell level. Cell Metab. 2017;25(5):1194-1205.e4.
106. Katsuta H, Aguayo-Mazzucato C, Katsuta R, Akashi T, Hollister-Lock J, Sharma AJ, Bonner-Weir S, Weir GC. Subpopulations of GFP-marked mouse pancreatic β-cells differ in size, granularity, and insulin secretion. Endocrinology. 2012;153(11):5180–7.
107. Teta M, Long SY, Wartschow LM, Rankin MM, Kushner JA. Very slow turnover of beta-cells in aged adult mice. Diabetes. 2005;54(9):2557–67.

108. Rankin MM, Kushner JA. Adaptive β-cell proliferation is severely restricted with advanced age. Diabetes. 2009;58(6):1365–72.
109. Aguayo-Mazzucato C, van Haaren M, Mruk M, Lee TB, Crawford C, Hollister-Lock J, Sullivan BA, Johnson JW, Ebrahimi A, Dreyfuss JM, Van Deursen J, Weir GC, Bonner-Weir S. β cell aging markers have heterogeneous distribution and are induced by insulin resistance. Cell Metab. 2017;25(4):898-910.e5.
110. Tschen SI, Dhawan S, Gurlo T, Bhushan A. Age-dependent decline in beta-cell proliferation restricts the capacity of beta-cell regeneration in mice. Diabetes. 2009;58(6):1312–20.
111. Szabat M, Pourghaderi P, Soukhatcheva G, Verchere CB, Warnock GL, Piret JM, Johnson JD. Kinetics and genomic profiling of adult human and mouse β-cell maturation. Islets. 2011;3(4):175–87.
112. Modi H, Skovsø S, Ellis C, Krentz NAJ, Zhao YB, Cen H, Noursadeghi N, Panzhinskiy E, Hu X, Dionne DA, Xuan S, Huising MO, Kieffer TJ, Lynn FC, Johnson JD. Ins2 gene bursting activity defines a mature β-cell state. bioRxiv. 2019;702589.
113. Laybutt DR, Preston AM, Åkerfeldt MC, Kench JG, Busch AK, Biankin AV, Biden TJ. Endoplasmic reticulum stress contributes to beta cell apoptosis in type 2 diabetes. Diabetologia. 2007;50(4):752–63.
114. Talchai C, Xuan S, Lin HV, Sussel L, Accili D. Pancreatic β cell dedifferentiation as a mechanism of diabetic β cell failure. Cell. 2012;150(6):1223–34.
115. Spijker HS, Song H, Ellenbroek JH, Roefs MM, Engelse MA, Bos E, Koster AJ, Rabelink TJ, Hansen BC, Clark A, Carlotti F, de Koning EJ. Loss of β-cell identity occurs in type 2 diabetes and is associated with islet amyloid deposits. Diabetes. 2015;64(8):2928–38.
116. Cinti F, Bouchi R, Kim-Muller JY, Ohmura Y, Sandoval PR, Masini M, Marselli L, Suleiman M, Ratner LE, Marchetti P, Accili D. Evidence of β-cell dedifferentiation in human type 2 diabetes. J Clin Endocrinol Metab. 2016;101(3):1044–54.
117. Johnston NR, Mitchell RK, Haythorne E, Pessoa MP, Semplici F, Ferrer J, Piemonti L, Marchetti P, Bugliani M, Bosco D, Berishvili E, Duncanson P, Watkinson M, Broichhagen J, Trauner D, Rutter GA, Hodson DJ. Beta cell hubs dictate pancreatic islet responses to glucose. Cell Metab. 2016;24(3):389–401.
118. Baetens D, Malaisse-Lagae F, Perrelet A, Orci L. Endocrine pancreas: three-dimensional reconstruction shows two types of islets of langerhans. Science. 1979;206(4424):1323–5.
119. Trimble ER, Renold AE. Ventral and dorsal areas of rat pancreas: islet hormone content and secretion. Am J Physiol. 1981;240(4):E422-7.
120. Ellenbroek JH, Töns HA, de Graaf N, Loomans CJ, Engelse MA, Vrolijk H, Voshol PJ, Rabelink TJ, Carlotti F, de Koning EJ. Topologically heterogeneous beta cell adaptation in response to high-fat diet in mice. PLoS One. 2013;8(2):e56922.
121. Orci L, Malaisse-Lagae F, Baetens D, Perrelet A. Pancreatic-polypeptide-rich regions in human pancreas. Lancet. 1978;2(8101):1200–1.
122. Gersell DJ, Gingerich RL, Greider MH. Regional distribution and concentration of pancreatic polypeptide in the human and canine pancreas. Diabetes. 1979;28(1):11–5.
123. Ahlgren U, Pfaff SL, Jessell TM, Edlund T, Edlund H. Independent requirement for ISL1 in formation of pancreatic mesenchyme and islet cells. Nature. 1997;385(6613):257–60.
124. Neuhuber WL. Vagal afferent fibers almost exclusively innervate islets in the rat pancreas as demonstrated by anterograde tracing. J Auton Nerv Syst. 1989;29(1):13–8.

125. Trimble ER, Halban PA, Wollheim CB, Renold AE. Functional differences between rat islets of ventral and dorsal pancreatic origin. J Clin Invest. 1982;69(2):405–13.
126. Wang X, Misawa R, Zielinski MC, Cowen P, Jo J, Periwal V, Ricordi C, Khan A, Szust J, Shen J, Millis JM, Witkowski P, Hara M. Regional differences in islet distribution in the human pancreas - preferential beta-cell loss in the head region in patients with type 2 diabetes. PLoS One. 2013;8(6):e67454.
127. Bosco D, Orci L, Meda P. Homologous but not heterologous contact increases the insulin secretion of individual pancreatic B-cells. Exp Cell Res. 1989;184(1):72–80.
128. Pipeleers D, in't Veld PI, Maes E, Van De Winkel M. Glucose-induced insulin release depends on functional cooperation between islet cells. Proc Natl Acad Sci U S A. 1982;79(23):7322–5.
129. Wojtusciszyn A, Armanet M, Morel P, Berney T, Bosco D. Insulin secretion from human beta cells is heterogeneous and dependent on cell-to-cell contacts. Diabetologia. 2008;51(10):1843–52.
130. van der Meulen T, Donaldson CJ, Cáceres E, Hunter AE, Cowing-Zitron C, Pound LD, Adams MW, Zembrzycki A, Grove KL, Huising MO. Urocortin3 mediates somatostatin-dependent negative feedback control of insulin secretion. Nat Med. 2015;21(7):769–76.
131. Rodriguez-Diaz R, Abdulreda MH, Formoso AL, Gans I, Ricordi C, Berggren PO, Caicedo A. Innervation patterns of autonomic axons in the human endocrine pancreas. Cell Metab. 2011;14(1):45–54.
132. Bonner Weir S, Trent DF, Weir GC. Partial pancreatectomy in the rat and subsequent defect in glucose-induced insulin release. J Clin Invest. 1983;71(6):1544–53.
133. Lee CS, De León DD, Kaestner KH, Stoffers DA. Regeneration of pancreatic islets after partial pancreatectomy in mice does not involve the reactivation of neurogenin-3. Diabetes. 2006;55(2):269–72.
134. Peshavaria M, Larmie BL, Lausier J, Satish B, Habibovic A, Roskens V, Larock K, Everill B, Leahy JL, Jetton TL. Regulation of pancreatic beta-cell regeneration in the normoglycemic 60% partial-pancreatectomy mouse. Diabetes. 2006;55(12):3289–98.
135. Dor Y, Brown J, Martinez OI, Melton DA. Adult pancreatic beta-cells are formed by self-duplication rather than stem-cell differentiation. Nature. 2004;429(6987):41–6.
136. Teta M, Rankin MM, Long SY, Stein GM, Kushner JA. Growth and regeneration of adult beta cells does not involve specialized progenitors. Dev Cell. 2007;12(5):817–26.
137. Plachot C, Movassat J, Portha B. Impaired beta-cell regeneration after partial pancreatectomy in the adult Goto-Kakizaki rat, a spontaneous model of type II diabetes. Histochem Cell Biol. 2001;116(2):131–9.
138. Brockenbrough JS, Weir GC, Bonner-Weir S. Discordance of exocrine and endocrine growth after 90% pancreatectomy in rats. Diabetes. 1988;37(2):232–6.
139. Misfeldt AA, Costa RH, Gannon M. β-cell proliferation, but not neogenesis, following 60% partial pancreatectomy is impaired in the absence of FoxM1. Diabetes. 2008;57(11):3069–77.
140. Li W-C, Rukstalis JM, Nishimura W, Tchipashvili V, Habener JF, Sharma A, Bonner-Weir S. Activation of pancreatic-duct-derived progenitor cells during pancreas regeneration in adult rats. J Cell Sci. 2010;123(16):2792–802.
141. Bonner-Weir S, Baxter LA, Schuppin GT, Smith FE. A second pathway for regeneration of adult exocrine and endocrine pancreas: A possible recapitulation of embryonic

development. Diabetes. 1993;42(12):1715–20.
142. Berrocal T, Luque AÁ, Pinilla I, Lassaletta L. Pancreatic regeneration after near-total pancreatectomy in children with nesidioblastosis. Pediatr Radiol. 2005;35(11):1066–70.
143. Watanabe H, Saito H, Rychahou PG, Uchida T, Evers BM. Aging is associated with decreased pancreatic acinar cell regeneration and phosphatidylinositol 3-kinase/Akt activation. Gastroenterology. 2005;128(5):1391–404.
144. Gargani S, Thévenet J, Yuan JE, Lefebvre B, Delalleau N, Gmyr V, Hubert T, Duhamel A, Pattou F, Kerr-Conte J. Adaptive changes of human islets to an obesogenic environment in the mouse. Diabetologia. 2013;56(2):350–8.
145. Téllez N, Vilaseca M, Martí Y, Pla A, Montanya E. β-Cell dedifferentiation, reduced duct cell plasticity, and impaired β-cell mass regeneration in middle-aged rats. Am J Physiol Metab. 2016;311(3):E554–63.
146. Menge BA, Tannapfel A, Belyaev O, Drescher R, Müller C, Uhl W, Schmidt WE, Meier JJ. Partial pancreatectomy in adult humans does not provoke β-cell regeneration. Diabetes. 2008;57(1):142–9.
147. Xu X, D'Hoker J, Stangé G, Bonné S, De Leu N, Xiao X, Van De Casteele M, Mellitzer G, Ling Z, Pipeleers D, Bouwens L, Scharfmann R, Gradwohl G, Heimberg H. β cells can be generated from endogenous progenitors in injured adult mouse pancreas. Cell. 2008;132(2):197–207.
148. Rankin MM, Wilbur CJ, Rak K, Shields EJ, Granger A, Kushner JA. β-cells are not generated in pancreatic duct ligation-induced injury in adult mice. Diabetes. 2013;62(5):1634–45.
149. Xiao X, Chen Z, Shiota C, Prasadan K, Guo P, El-Gohary Y, Paredes J, Welsh C, Wiersch J, Gittes GK. No evidence for β cell neogenesis in murine adult pancreas. J Clin Invest. 2013;123(5):2207–17.
150. Rossini AA, Like AA, Chick WL, Appel MC, Cahill GF. Studies of streptozotocin-induced insulitis and diabetes. Proc Natl Acad Sci. 1977;74(6):2485–9.
151. Lenzen S. The mechanisms of alloxan- and streptozotocin-induced diabetes. Diabetologia. 2008;51(2):216–26.
152. Wang RN, Bouwens L, Klöppel G. Beta-cell proliferation in normal and streptozotocin-treated newborn rats: site, dynamics and capacity. Diabetologia. 1994;37(11):1088–96.
153. Jörns A, Klempnauer J, Tiedge M, Lenzen S. Recovery of pancreatic β cells in response to long-term normoglycemia after pancreas or islet transplantation in severely streptozotocin diabetic adult rats. Pancreas. 2001;23(2):186–96.
154. Fernandes A, King LC, Guz Y, Stein R, Wright CVE, Teitelman G. Differentiation of new insulin-producing cells is induced by injury in adult pancreatic islets. Endocrinology. 1997;138(4):1750–62.
155. Yin D, Tao J, Lee DD, Shen J, Hara M, Lopez J, Kuznetsov A, Philipson LH, Chong AS. Recovery of islet β-cell function in streptozotocin-induced diabetic mice: An indirect role for the spleen. Diabetes. 2006;55(12):3256–63.
156. Guz Y, Nasir I, Teitelman G. Regeneration of pancreatic beta cells from intra-islet precursor cells in an experimental model of diabetes. Endocrinology. 2001;142(11):4956–68.
157. Zorina TD, Subbotin VM, Bertera S, Alexander AM, Haluszczak C, Gambrell B, Bottino R, Styche AJ, Trucco M. Recovery of the endogenous beta cell function in the NOD

model of autoimmune diabetes. Stem Cells. 2003;21(4):377–88.
158. Kodama S, Kühtreiber W, Fujimura S, Dale EA, Faustman DL. Islet regeneration during the reversal of autoimmune diabetes in NOD mice. Science (80-). 2003;1223–7.
159. Chera S, Baronnier D, Ghila L, Cigliola V, Jensen JN, Gu G, Furuyama K, Thorel F, Gribble FM, Reimann F, Herrera PL. Diabetes recovery by age-dependent conversion of pancreatic δ-cells into insulin producers. Nature. 2014;514(7253):503–7.
160. Thorel F, Népote V, Avril I, Kohno K, Desgraz R, Chera S, Herrera PL. Conversion of adult pancreatic alpha-cells to beta-cells after extreme beta-cell loss. Nature. 2010;464(7292):1149–54.
161. Tschen SI, Dhawan S, Gurlo T, Bhushan A. Age-dependent decline in β-cell proliferation restricts the capacity of β-cell regeneration in mice. Diabetes. 2009;58(6):1312–20.
162. Wong ES, Le Guezennec X, Demidov ON, Marshall NT, Wang ST, Krishnamurthy J, Sharpless NE, Dunn NR, Bulavin DV. p38MAPK controls expression of multiple cell cycle inhibitors and islet proliferation with advancing age. Dev Cell. 2009;17(1):142–9.
163. Krishnamurthy J, Ramsey MR, Ligon KL, Torrice C, Koh A, Bonner-Weir S, Sharpless NE. p16INK4a induces an age-dependent decline in islet regenerative potential. Nature. 2006;443(7110):453–7.
164. Meier JJ, Butler AE, Saisho Y, Monchamp T, Galasso R, Bhushan A, Rizza RA, Butler PC. β-cell replication is the primary mechanism subserving the postnatal expansion of β-cell mass in humans. Diabetes. 2008;57(6):1584–94.
165. Edvell A, Lindström P. Development of insulin secretory function in young obese hyperglycemic mice (Umeå ob ob). Metabolism. 1995;44(7):906–13.
166. Hull RL, Kodama K, Utzschneider KM, Carr DB, Prigeon RL, Kahn SE. Dietary-fat-induced obesity in mice results in beta cell hyperplasia but not increased insulin release: Evidence for specificity of impaired beta cell adaptation. Diabetologia. 2005;48(7):1350–8.
167. Stamateris RE, Sharma RB, Hollern DA, Alonso LC. Adaptive β-cell proliferation increases early in high-fat feeding in mice, concurrent with metabolic changes, with induction of islet cyclin D2 expression. Am J Physiol Metab. 2013;305(1):149–59.
168. El Ouaamari A, Kawamori D, Dirice E, Liew CW, Shadrach JL, Hu J, Katsuta H, Hollister-Lock J, Qian WJ, Wagers AJ, Kulkarni RN. Liver-derived systemic factors drive β cell hyperplasia in insulin-resistant states. Cell Rep. 2013;3(2):401–10.
169. Parsons JA, Brelje TC, Sorenson RL. Adaptation of islets of Langerhans to pregnancy: increased islet cell proliferation and insulin secretion correlates with the onset of placental lactogen secretion. Endocrinology. 1992;130(3):1459–66.
170. Huang C, Snider F, Cross JC. Prolactin receptor is required for normal glucose homeostasis and modulation of β-cell mass during pregnancy. Endocrinology. 2009;150(4):1618–26.
171. Brelje TC, Parsons JA, Sorenson RL. Regulation of islet beta-cell proliferation by prolactin in rat islets. Diabetes. 1994;43(2):263–73.
172. Meier J, Butler A, Saisho Y, Monchamp T, Galasso R, Bhushan A, Rizza RA, Butler PC. Postnatal expansion of β-cell mass in humans. Diabetes. 2008;57(6):1584–94.
173. Carballar R, Canyelles MDL, Fernández C, Martí Y, Bonnin S, Castaño E, Montanya E, Téllez N. Purification of replicating pancreatic β-cells for gene expression studies. Sci Rep. 2017;7(1):17515.

174. Tyrberg B, Ustinov J, Otonkoski T, Andersson A. Stimulated endocrine cell proliferation and differentiation in transplanted human. Diabetes. 2001;1(2):301–7.
175. Alonso LC, Yokoe T, Zhang P, Scott DK, Kim SK, O'Donnell CP, Garcia-Ocaña A. Glucose infusion in mice: a new model to induce beta-cell replication. Diabetes. 2007;56(7):1792–801.
176. Levitt HE, Cyphert TJ, Pascoe JL, Hollern DA, Abraham N, Lundell RJ, Rosa T, Romano LC, Zou B, O'Donnell CP, Stewart AF, Garcia-Ocaña A, Alonso LC. Glucose stimulates human beta cell replication in vivo in islets transplanted into NOD-severe combined immunodeficiency (SCID) mice. Diabetologia. 2011;54(3):572–82.
177. Diiorio P, Jurczyk A, Yang C, Racki WJ, Brehm MA, Atkinson MA, Powers AC, Shultz LD, Greiner DL, Bortell R. Hyperglycemia-induced proliferation of adult human beta cells engrafted into spontaneously diabetic immunodeficient NOD-Rag1null IL2rγnull Ins2Akita mice. Pancreas. 2011;40(7):1147–9.
178. Boerner BP, George NM, Targy NM, Sarvetnick NE. TGF-β superfamily member Nodal stimulates human β-cell proliferation while maintaining cellular viability. Endocrinology. 2013;154(11):4099–112.
179. Aly H, Rohatgi N, Marshall CA, Grossenheider TC, Miyoshi H, Stappenbeck TS, Matkovich SJ, McDaniel ML. A novel strategy to increase the proliferative potential of adult human β-cells while maintaining their differentiated phenotype. PLoS One. 2013;8(6):e66131.
180. Dirice E, Walpita D, Vetere A, Meier BC, Kahraman S, Hu J, Dančík V, Burns SM, Gilbert TJ, Olson DE, Clemons PA, Kulkarni RN, Wagner BK. Inhibition of DYRK1A stimulates human β-cell proliferation. Diabetes. 2016;65(6):1660–71.
181. Ackeifi C, Wang P, Karakose E, Manning Fox JE, González BJ, Liu H, Wilson J, Swartz E, Berrouet C, Li Y, Kumar K, MacDonald PE, Sanchez R, Thorens B, DeVita R, Homann D, Egli D, Scott DK, Garcia-Ocaña A, et al. GLP-1 receptor agonists synergize with DYRK1A inhibitors to potentiate functional human β cell regeneration. Sci Transl Med. 2020;12(530).
182. Mezza T, Muscogiuri G, Sorice GP, Clemente G, Hu J, Pontecorvi A, Holst JJ, Giaccari A, Kulkarni RN. Insulin resistance alters islet morphology in nondiabetic humans. Diabetes. 2014;63(3):994–1007.
183. Brereton MF, Iberl M, Shimomura K, Zhang Q, Adriaenssens AE, Proks P, Spiliotis II, Dace W, Mattis KK, Ramracheya R, Gribble FM, Reimann F, Clark A, Rorsman P, Ashcroft FM. Reversible changes in pancreatic islet structure and function produced by elevated blood glucose. Nat Commun. 2014;5:4639.
184. Collombat P, Xu X, Ravassard P, Sosa-Pineda B, Dussaud S, Billestrup N, Madsen OD, Serup P, Heimberg H, Mansouri A. The ectopic expression of Pax4 in the mouse pancreas converts progenitor cells into α and subsequently β cells. Cell. 2009;138(3):449–62.
185. Druelle N, Vieira A, Shabro A, Courtney M, Mondin M, Rekima S, Napolitano T, Silvano S, Navarro-Sanz S, Hadzic B, Avolio F, Rassoulzadegan M, Schmid HA, Mansouri A, Collombat P. Ectopic expression of Pax4 in pancreatic δ cells results in β-like cell neogenesis. J Cell Biol. 2017;216(12):4299–311.
186. Courtney M, Gjernes E, Druelle N, Ravaud C, Vieira A, Ben-Othman N, Pfeifer A, Avolio F, Leuckx G, Lacas-Gervais S, Burel-Vandenbos F, Ambrosetti D, Hecksher-Sorensen J, Ravassard P, Heimberg H, Mansouri A, Collombat P. The inactivation of Arx

in pancreatic α-cells triggers their neogenesis and conversion into functional β-like cells. PLoS Genet. 2013;9(10):e1003934.
187. Chakravarthy H, Gu X, Enge M, Dai X, Wang Y, Damond N, Downie C, Liu K, Wang J, Xing Y, Chera S, Thorel F, Quake S, Oberholzer J, MacDonald PE, Herrera PL, Kim SK. Converting adult pancreatic islet α cells into β cells by targeting both Dnmt1 and Arx. Cell Metab. 2017;25(3):622–34.
188. Furuyama K, Chera S, van Gurp L, Oropeza D, Ghila L, Damond N, Vethe H, Paulo JA, Joosten AM, Berney T, Bosco D, Dorrell C, Grompe M, Ræder H, Roep BO, Thorel F, Herrera PL. Diabetes relief in mice by glucose-sensing insulin-secreting human α-cells. Nature. 2019;567(7746):43–8.
189. Pan FC, Bankaitis ED, Boyer D, Xu X, Van de Casteele M, Magnuson MA, Heimberg H, Wright CVE. Spatiotemporal patterns of multipotentiality in Ptf1a-expressing cells during pancreas organogenesis and injury-induced facultative restoration. Development. 2013;140(4):751–64.
190. Baeyens L, Lemper M, Leuckx G, De Groef S, Bonfanti P, Stangé G, Shemer R, Nord C, Scheel DW, Pan FC, Ahlgren U, Gu G, Stoffers DA, Dor Y, Ferrer J, Gradwohl G, Wright CVE, Van De Casteele M, German MS, et al. Transient cytokine treatment induces acinar cell reprogramming and regenerates functional beta cell mass in diabetic mice. Nat Biotechnol. 2014;32(1):76–83.
191. Akinci E, Banga A, Greder LV, Dutton JR, Slack JMW. Reprogramming of pancreatic exocrine cells towards a beta cell character using Pdx1, Ngn3 and MafA. Biochem J. 2011;442(3):539–50.
192. Zhou Q, Brown J, Kanarek A, Rajagopal J, Melton DA. In vivo reprogramming of adult pancreatic exocrine cells to beta-cells. Nature. 2008;455(7213):627–32.
193. Li W, Cavelti-Weder C, Zhang Y, Zhang Y, Clement K, Donovan S, Gonzalez G, Zhu J, Stemann M, Xu K, Hashimoto T, Yamada T, Nakanishi M, Zhang Y, Zeng S, Gifford D, Meissner A, Weir G, Zhou Q. Long-term persistence and development of induced pancreatic beta cells generated by lineage conversion of acinar cells. Nat Biotechnol. 2014;32(12):1223–30.
194. Cavelti-Weder C, Li W, Zumsteg A, Stemann-Andersen M, Zhang Y, Yamada T, Wang M, Lu J, Jermendy A, Bee YM, Bonner-Weir S, Weir GC, Zhou Q. Hyperglycaemia attenuates in vivo reprogramming of pancreatic exocrine cells to beta cells in mice. Diabetologia. 2016;59(3):522–32.
195. Clayton HW, Osipovich AB, Stancill JS, Schneider JD, Vianna PG, Shanks CM, Yuan W, Gu G, Manduchi E, Stoeckert CJ, Magnuson MA. Pancreatic inflammation redirects acinar to β cell reprogramming. Cell Rep. 2016;17(8):2028–41.
196. Lima MJ, Muir KR, Docherty HM, McGowan NWA, Forbes S, Heremans Y, Heimberg H, Casey J, Docherty K. Generation of functional beta-like cells from human exocrine pancreas. PLoS One. 2016;11(5):e0156204.
197. Sharma A, Zangen DH, Reitz P, Taneja M, Lissauer ME, Miller CP, Weir GC, Habener JF, Bonner-Weir S. The homeodomain protein IDX-1 increases after an early burst of proliferation during pancreatic regeneration. Diabetes. 1999;48(3):507–13.
198. Valdez IA, Dirice E, Gupta MK, Shirakawa J, Teo AKK, Kulkarni RN. Proinflammatory cytokines induce endocrine differentiation in pancreatic ductal cells via STAT3-dependent NGN3 activation. Cell Rep. 2016;15(3):460–70.

199. Zhang M, Lin Q, Qi T, Wang T, Chen CC, Riggs AD, Zeng D. Growth factors and medium hyperglycemia induce Sox9+ ductal cell differentiation into β cells in mice with reversal of diabetes. Proc Natl Acad Sci U S A. 2016;113(3):650–5.
200. Kopinke D, Murtaugh LC. Exocrine-to-endocrine differentiation is detectable only prior to birth in the uninjured mouse pancreas. BMC Dev Biol. 2010;10:38.
201. Yatoh S, Dodge R, Akashi T, Omer A, Sharma A, Weir GC, Bonner-Weir S. Differentiation of affinity-purified human pancreatic duct cells to beta-cells. Diabetes. 2007;56(7):1802–9.
202. Yoneda S, Uno S, Iwahashi H, Fujita Y, Yoshikawa A, Kozawa J, Okita K, Takiuchi D, Eguchi H, Nagano H, Imagawa A, Shimomura I. Predominance of β-cell neogenesis rather than replication in humans with an impaired glucose tolerance and newly diagnosed diabetes. J Clin Endocrinol Metab. 2013;98(5):2053–61.
203. Bonner-Weir S, Taneja M, Weir GC, Tatarkiewicz K, Song KH, Sharma A, O'Neil JJ. In vitro cultivation of human islets from expanded ductal tissue. Proc Natl Acad Sci U S A. 2000;97(14):7999–8004.
204. Gao R, Ustinov J, Korsgren O, Otonkoski T. In vitro neogenesis of human islets reflects the plasticity of differentiated human pancreatic cells. Diabetologia. 2005;48(11):2296–304.
205. Lee J, Sugiyama T, Liu Y, Wang J, Gu X, Lei J, Markmann JF, Miyazaki S, Miyazaki J, Szot GL, Bottino R, Kim SK. Expansion and conversion of human pancreatic ductal cells into insulin-secreting endocrine cells. Elife. 2013;2:e00940.
206. Yamada T, Cavelti-Weder C, Caballero F, Lysy PA, Guo L, Sharma A, Li W, Zhou Q, Bonner-Weir S, Weir GC. Reprogramming mouse cells with a pancreatic duct phenotype to insulin-producing β-like cells. Endocrinology. 2015;156(6):2029–38.
207. Slack JM. Developmental biology of the pancreas. Development. 1995;121(6):1569–80.
208. Talchai C, Xuan S, Kitamura T, DePinho RA, Accili D. Generation of functional insulin-producing cells in the gut by Foxo1 ablation. Nat Genet. 2012;44(4):406–12.
209. Banga A, Akinci E, Greder LV, Dutton JR, Slack JMW. In vivo reprogramming of Sox9+ cells in the liver to insulin-secreting ducts. Proc Natl Acad Sci. 2012;109(38):15336–41.
210. Chen YJ, Finkbeiner SR, Weinblatt D, Emmett MJ, Tameire F, Yousefi M, Yang C, Maehr R, Zhou Q, Shemer R, Dor Y, Li C, Spence JR, Stanger BZ. De novo formation of insulin-producing "neo-β cell islets" from intestinal crypts. Cell Rep. 2014;6(6):1046–58.
211. Ariyachet C, Tovaglieri A, Xiang G, Lu J, Shah MS, Richmond CA, Verbeke C, Melton DA, Stanger BZ, Mooney D, Shivdasani RA, Mahony S, Xia Q, Breault DT, Zhou Q. Reprogrammed stomach tissue as a renewable source of functional β cells for blood glucose regulation. Cell Stem Cell. 2016;18(3):410–21.
212. Seaberg RM, Smukler SR, Kieffer TJ, Enikolopov G, Asghar Z, Wheeler MB, Korbutt G, van der Kooy D. Clonal identification of multipotent precursors from adult mouse pancreas that generate neural and pancreatic lineages. Nat Biotechnol. 2004;22(9):1115–24.
213. Beamish CA, Strutt BJ, Arany EJ, Hill DJ. Insulin-positive, Glut2-low cells present within mouse pancreas exhibit lineage plasticity and are enriched within extra-islet endocrine cell clusters. Islets. 2016;8(3):65–82.
214. Razavi R, Najafabadi HS, Abdullah S, Smukler S, Arntfield M, van der Kooy D. Diabetes enhances the proliferation of adult pancreatic multipotent progenitor cells and biases their

differentiation to more β-cell production. Diabetes. 2015;64(4):1311–23.
215. Treutelaar MK, Skidmore JM, Dias-leme CL, Hara M, Zhang L, Simeone D, Martin DM, Burant CF. Nestin-Lineage Cells Contribute to the Microvasculature but Not Endocrine Cells of the Islet. Diabetes. 2003;52(10):2503–12.
216. van der Meulen T, Mawla AM, DiGruccio MR, Adams MW, Nies V, Dólleman S, Liu S, Ackermann AM, Cáceres E, Hunter AE, Kaestner KH, Donaldson CJ, Huising MO. Virgin beta cells persist throughout life at a neogenic niche within pancreatic islets. Cell Metab. 2017;25(4):911-926.e6.
217. Howe K, Clark MD, Torroja CF, Torrance J, Berthelot C, Muffato M, Collins JE, Humphray S, McLaren K, Matthews L, McLaren S, Sealy I, Caccamo M, Churcher C, Scott C, Barrett JC, Koch R, Rauch GJ, White S, et al. The zebrafish reference genome sequence and its relationship to the human genome. Nature. 2013;496(7446):498–503.
218. Delaspre F, Beer RL, Rovira M, Huang W, Wang G, Gee S, Vitery MC, Wheelan SJ, Parsons MJ. Centroacinar cells are progenitors that contribute to endocrine pancreas regeneration. Diabetes. 2015;64(10):3499–509.
219. Moss LG, Parsons MJ, Moss JB, Walter I, Koustubhan P, Greenman M. Regeneration of the Pancreas in Adult Zebrafish. Diabetes. 2009;58(8):1844–51.
220. Menke AL, Spitsbergen JM, Wolterbeek APM, Woutersen RA. Normal anatomy and histology of the adult zebrafish. Toxicol Pathol. 2011;39(5):759–75.
221. Biemar F, Argenton F, Schmidtke R, Epperlein S, Peers B, Driever W. Pancreas development in zebrafish: Early dispersed appearance of endocrine hormone expressing cells and their convergence to form the definitive islet. Dev Biol. 2001;230(2):189–203.
222. Argenton F, Zecchin E, Bortolussi M. Early appearance of pancreatic hormone-expressing cells in the zebrafish embryo. Mech Dev. 1999;87(1–2):217–21.
223. Yang YHC, Kawakami K, Stainier DY. A new mode of pancreatic islet innervation revealed by live imaging in zebrafish. Elife. 2018;7:e34519.
224. Moss LG, Caplan TV, Moss JB. Imaging beta cell regeneration and interactions with islet vasculature in transparent adult zebrafish. Zebrafish. 2013;10(2):249–57.
225. Field HA, Dong PDS, Beis D, Stainier DYR. Formation of the digestive system in zebrafish. ii. pancreas morphogenesis☆. Dev Biol. 2003;261(1):197–208.
226. Hesselson D, Anderson RM, Beinat M, Stainier DYR. Distinct populations of quiescent and proliferative pancreatic -cells identified by HOTcre mediated labeling. Proc Natl Acad Sci. 2009;106(35):14896–901.
227. Parsons MJ, Pisharath H, Yusuff S, Moore JC, Siekmann AF, Lawson N, Leach SD. Notch-responsive cells initiate the secondary transition in larval zebrafish pancreas. Mech Dev. 2009;126(10):898–912.
228. Wang Y, Rovira M, Yusuff S, Parsons MJ. Genetic inducible fate mapping in larval zebrafish reveals origins of adult insulin-producing β-cells. Development. 2011;138(4):609–17.
229. Alexander J, Rothenberg M, Henry GL, Stainier DYR. Casanova plays an early and essential role in endoderm formation in zebrafish. Dev Biol. 1999;215(2):343–57.
230. Alexander J, Stainier DYR. A molecular pathway leading to endoderm formation in zebrafish. Curr Biol. 1999;9(20):1147–57.
231. Yan C, Zheng W, Gong Z. Zebrafish fgf10b has a complementary function to fgf10a in liver and pancreas development. Mar Biotechnol. 2015;17(2):162–7.

232. Stafford D, White RJ, Kinkel MD, Linville A, Schilling TF, Prince VE. Retinoids signal directly to zebrafish endoderm to specify insulin-expressing β-cells. Development. 2006;133(5):949–56.
233. Chung WS, Andersson O, Row R, Kimelman D, Stainier DYR. Suppression of Alk8-mediated Bmp signaling cell-autonomously induces pancreatic β-cells in zebrafish. Proc Natl Acad Sci U S A. 2010;107(3):1142–7.
234. Chung WS, Stainier DYR. Intra-endodermal interactions are required for pancreatic beta cell induction. Dev Cell. 2008;14(4):582–93.
235. Bhushan A, Itoh N, Kato S, Thiery JP, Czernichow P, Bellusci S, Scharfmann R. Fgf10 is essential for maintaining the proliferative capacity of epithelial progenitor cells during early pancreatic organogenesis. Development. 2001;128(24):5109–17.
236. Kinkel MD, Prince VE. On the diabetic menu: Zebrafish as a model for pancreas development and function. BioEssays. 2009;31(2):139–52.
237. Tehrani Z, Lin S. Endocrine pancreas development in zebrafish. Cell cycle. 2011;10(20):3466–72.
238. Matsuda H. Zebrafish as a model for studying functional pancreatic β cells development and regeneration. Dev Growth Differ. 2018;60(6):393–9.
239. Prince VE, Anderson RM, Dalgin G. Zebrafish pancreas development and regeneration. In: Current Topics in Developmental Biology. 1st ed. Elsevier Inc.; 2017. p. 235–76.
240. Haumaitre C, Barbacci E, Jenny M, Ott MO, Gradwohl G, Cereghini S. Lack of TCF2/vHNF1 in mice leads to pancreas agenesis. Proc Natl Acad Sci U S A. 2005;102(5):1490–5.
241. Lancman JJ, Zvenigorodsky N, Gates KP, Zhang D, Solomon K, Humphrey RK, Kuo T, Setiawan L, Verkade H, Chi YI, Jhala US, Wright CVE, Stainier DYR, Dong PD. Specification of hepatopancreas progenitors in zebrafish by hnf1ba and wnt2bb. Dev. 2013;140(13):2669–79.
242. Song J, Kim HJ, Gong Z, Liu NA, Lin S. Vhnf1 acts downstream of Bmp, Fgf, and RA signals to regulate endocrine beta cell development in zebrafish. Dev Biol. 2007;303(2):561–75.
243. Sun Z, Hopkins N. Vhnf1, the MODY5 and familial GCKD-associated gene, regulates regional specification of the zebrafish gut, pronephros, and hindbrain. Genes Dev. 2001;15(23):3217–29.
244. Yee NS, Yusuff S, Pack M. Zebrafish pdx1 morphant displays defects in pancreas development and digestive organ chirality, and potentially identifies a multipotent pancreas progenitor cell. Genesis. 2001;30(3):137–40.
245. Huang H, Liu N, Lin S. Pdx-1 knockdown reduces insulin promoter activity in zebrafish. Genesis. 2001;30(3):134–6.
246. Zecchin E, Mavropoulos A, Devos N, Filippi A, Tiso N, Meyer D, Peers B, Bortolussi M, Argenton F. Evolutionary conserved role of ptf1a in the specification of exocrine pancreatic fates. Dev Biol. 2004;268(1):174–84.
247. Dong PDS, Provost E, Leach SD, Stainier DYR. Graded levels of Ptf1a differentially regulate endocrine and exocrine fates in the developing pancreas. Genes Dev. 2008;22(11):1445–50.
248. Manfroid I, Ghaye A, Naye F, Detry N, Palm S, Pan L, Ma TP, Huang W, Rovira M, Martial JA, Parsons MJ, Moens CB, Voz ML, Peers B. Zebrafish sox9b is crucial for

hepatopancreatic duct development and pancreatic endocrine cell regeneration. Dev Biol. 2012;366(2):268–78.
249. Seymour PA, Freude KK, Tran MN, Mayes EE, Jensen J, Kist R, Scherer G, Sander M. SOX9 is required for maintenance of the pancreatic progenitor cell pool. Proc Natl Acad Sci U S A. 2007;104(6):1865–70.
250. Flasse LC, Pirson JL, Stern DG, Von Berg V, Manfroid I, Peers B, Voz ML. Ascl1b and Neurod1, instead of Neurog3, control pancreatic endocrine cell fate in zebrafish. BMC Biol. 2013;11(1):1.
251. Moro E, Gnügge L, Braghetta P, Bortolussi M, Argenton F. Analysis of beta cell proliferation dynamics in zebrafish. Dev Biol. 2009;332(2):299–308.
252. Dalgin G, Prince VE. Differential levels of neurod establish zebrafish endocrine pancreas cell fates. Dev Biol. 2015;402(1):81–97.
253. Wendik B, Maier E, Meyer D. Zebrafish mnx genes in endocrine and exocrine pancreas formation. Dev Biol. 2004;268(2):372–83.
254. Dalgin G, Ward AB, Hao le T, Beattie CE, Nechiporuk A, Prince VE. Zebrafish mnx1 controls cell fate choice in the developing endocrine pancreas. Development. 2011;138(21):4597–608.
255. Li H, Arber S, Jessell TM, Edlund H. Selective agenesis of the dorsal pancreas in mice lacking homeobox gene Hlxb9. Nat Genet. 1999;23(1):67–70.
256. Harrison KA, Thaler J, Pfaff SL, Gu H, Kehrl JH. Pancreas dorsal lobe agenesis and abnormal islets of Langerhans in Hlxb9-deficient mice. Nat Genet. 1999;23(1):71–5.
257. Pauls S, Zecchin E, Tiso N, Bortolussi M, Argenton F. Function and regulation of zebrafish nkx2.2a during development of pancreatic islet and ducts. Dev Biol. 2007;304(2):875–90.
258. Binot AC, Manfroid I, Flasse L, Winandy M, Motte P, Martial JA, Peers B, Voz ML. Nkx6.1 and nkx6.2 regulate α- and β-cell formation in zebrafish by acting on pancreatic endocrine progenitor cells. Dev Biol. 2010;340(2):397–407.
259. Sussel L, Kalamaras J, Hartigan-O'Connor DJ, Meneses JJ, Pedersen RA, Rubenstein JL, German MS. Mice lacking the homeodomain transcription factor Nkx2.2 have diabetes due to arrested differentiation of pancreatic beta cells. Development. 1998;125(12):2213–21.
260. Naya FJ, Huang HP, Qiu Y, Mutoh H, DeMayo FJ, Leiter AB, Tsai MJ. Diabetes, defective pancreatic morphogenesis, and abnormal enteroendocrine differentiation in BETA2/neuroD-deficient mice. Genes Dev. 1997;11(18):2323–34.
261. Sander M, Sussel L, Conners J, Scheel D, Kalamaras J, Dela Cruz F, Schwitzgebel V, Hayes-Jordan A, German M. Homeobox gene Nkx6.1 lies downstream of Nkx2.2 in the major pathway of beta-cell formation in the pancreas. Development. 2000;127(24):5533–40.
262. Verbruggen V, Ek O, Georlette D, Delporte F, Von Berg V, Detry N, Biemar F, Coutinho P, Martial JA, Voz ML, Manfroid I, Peers B. The Pax6b homeodomain is dispensable for pancreatic endocrine cell differentiation in Zebrafish. J Biol Chem. 2010;285(18):13863–73.
263. Sander M, Neubüser A, Kalamaras J, Ee HC, Martin GR, German MS. Genetic analysis reveals that PAX6 is required for normal transcription of pancreatic hormone genes and islet development. Genes Dev. 1997;11(13):1662–73.

264. Collombat P, Mansouri A, Hecksher-Sørensen J, Serup P, Krull J, Gradwohl G, Gruss P. Opposing actions of Arx and Pax4 in endocrine pancreas development. Genes Dev. 2003;17(20):2591–603.
265. Djiotsa J, Verbruggen V, Giacomotto J, Ishibashi M, Manning E, Rinkwitz S, Manfroid I, Voz ML, Peers B. Pax4 is not essential for beta-cell differentiation in zebrafish embryos but modulates alpha-cell generation by repressing arx gene expression. BMC Dev Biol. 2012;12(1):1–16.
266. Sosa-Pineda B, Chowdhury K, Torres M, Oliver G, Gruss P. The Pax4 gene is essential for differentiation of insulin-producing beta cells in the mammalian pancreas. Nature. 1997;386(6623):399–402.
267. Wilfinger A, Arkhipova V, Meyer D. Cell type and tissue specific function of islet genes in zebrafish pancreas development. Dev Biol. 2013;378(1):25–37.
268. Ward AB, Warga RM, Prince VE. Origin of the zebrafish endocrine and exocrine pancreas. Dev Dyn. 2007;236(6):1558–69.
269. Singh SP, Janjuha S, Hartmann T, Kayisoglu Ö, Konantz J, Birke S, Murawala P, Alfar EA, Murata K, Eugster A, Tsuji N, Morrissey ER, Brand M, Ninov N. Different developmental histories of beta-cells generate functional and proliferative heterogeneity during islet growth. Nat Commun. 2017;8(1):664.
270. Zhang D, Golubkov VS, Han W, Correa RG, Zhou Y, Lee S, Strongin AY, Dong PDS. Identification of Annexin A4 as a hepatopancreas factor involved in liver cell survival. Dev Biol. 2014;395(1):96–110.
271. Janjuha S, Singh SP, Tsakmaki A, Mousavy Gharavy SN, Murawala P, Konantz J, Birke S, Hodson DJ, Rutter GA, Bewick GA, Ninov N. Age-related islet inflammation marks the proliferative decline of pancreatic beta-cells in zebrafish. Elife. 2018;7:e32965.
272. Salem V, Silva LD, Suba K, Georgiadou E, Neda Mousavy Gharavy S, Akhtar N, Martin-Alonso A, Gaboriau DCA, Rothery SM, Stylianides T, Carrat G, Pullen TJ, Singh SP, Hodson DJ, Leclerc I, Shapiro AMJ, Marchetti P, Briant LJB, Distaso W, et al. Leader β-cells coordinate Ca2+ dynamics across pancreatic islets in vivo. Nat Metab. 2019;1(6):615–29.
273. Nam YH, Hong BN, Rodriguez I, Ji MG, Kim K, Kim UJ, Kang TH. Synergistic potentials of coffee on injured pancreatic islets and insulin action via KATP channel blocking in zebrafish. J Agric Food Chem. 2015;63(23):5612–21.
274. Castañeda R, Rodriguez I, Nam YH, Hong BN, Kang TH. Trigonelline promotes auditory function through nerve growth factor signaling on diabetic animal models. Phytomedicine. 2017;36:128–36.
275. Olsen AS, Sarras MP, Intine RV. Limb regeneration is impaired in an adult zebrafish model of diabetes mellitus. Wound Repair Regen. 2010;18(5):532–42.
276. Intine RV, Olsen AS, Sarras MP. A zebrafish model of diabetes mellitus and metabolic memory. J Vis Exp. 2013;(72):1–7.
277. Tanvir Z, Nelson RF, DeCicco-Skinner K, Connaughton VP. One month of hyperglycemia alters spectral responses of the zebrafish photopic electroretinogram. DMM Dis Model Mech. 2018;11(10).
278. Benchoula K, Khatib A, Quzwain FMC, Che Mohamad CA, Wan Sulaiman WMA, Wahab RA, Ahmed QU, Ghaffar MA, Saiman MZ, Alajmi MF, El-Seedi H. Optimization of hyperglycemic induction in zebrafish and evaluation of its blood glucose level and

metabolite fingerprint treated with psychotria malayana Jack Leaf extract. Molecules. 2019;24(8):1506.
279. Shin E. An optimal establishment of an acute hyperglycemia zebrafish model. African J Pharm Pharmacol. 2012;6(42):2922–8.
280. Li M, Maddison LA, Page-McCaw P, Chen W. Overnutrition induces beta-cell differentiation through prolonged activation of beta-cells in zebrafish larvae. AJP Endocrinol Metab. 2014;306(7):799–807.
281. Li Z, Korzh V, Gong Z. DTA-mediated targeted ablation revealed differential interdependence of endocrine cell lineages in early development of zebrafish pancreas. Differentiation. 2009;78(4):241–52.
282. Pisharath H, Rhee JM, Swanson MA, Leach SD, Parsons MJ. Targeted ablation of beta cells in the embryonic zebrafish pancreas using E. coli nitroreductase. Mech Dev. 2007;124(3):218–29.
283. Ye L, Robertson MA, Hesselson D, Stainier DYR, Anderson RM. Glucagon is essential for alpha cell transdifferentiation and beta cell neogenesis. Development. 2015;142(8):1407–17.
284. Curado S, Anderson RM, Jungblut B, Mumm J, Schroeter E, Stainier DYR. Conditional targeted cell ablation in zebrafish: A new tool for regeneration studies. Dev Dyn. 2007;236(4):1025–35.
285. Oka T, Nishimura Y, Zang L, Hirano M, Shimada Y, Wang Z, Umemoto N, Kuroyanagi J, Nishimura N, Tanaka T. Diet-induced obesity in zebrafish shares common pathophysiological pathways with mammalian obesity. BMC Physiol. 2010;10(1).
286. Meguro S, Hasumura T, Hase T. Body fat accumulation in zebrafish is induced by a diet rich in fat and reduced by supplementation with green tea extract. PLoS One. 2015;10(3):e0120142.
287. Landgraf K, Schuster S, Meusel A, Garten A, Riemer T, Schleinitz D, Kiess W, Körner A. Short-term overfeeding of zebrafish with normal or high-fat diet as a model for the development of metabolically healthy versus unhealthy obesity. BMC Physiol. 2017;17(1):1–10.
288. Zang L, Shimada Y, Nishimura N. Development of a novel zebrafish model for type 2 diabetes mellitus. Sci Rep. 2017;7(1):1–11.
289. Capiotti KM, Antonioli R, Kist LW, Bogo MR, Bonan CD, Da Silva RS. Persistent impaired glucose metabolism in a zebrafish hyperglycemia model. Comp Biochem Physiol Part - B Biochem Mol Biol. 2014;171(1):58–65.
290. Alvarez Y, Chen K, Reynolds AL, Waghorne N, O'Connor JJ, Kennedy BN. Predominant cone photoreceptor dysfunction in a hyperglycaemic model of non-proliferative diabetic retinopathy. DMM Dis Model Mech. 2010;3(3–4):236–45.
291. Gleeson M, Connaughton V, Arneson LS. Induction of hyperglycaemia in zebrafish (Danio rerio) leads to morphological changes in the retina. Acta Diabetol. 2007;44(3):157–63.
292. Yin L, Maddison LA, Li M, Kara N, Lafave MC, Varshney GK, Burgess SM, Patton JG, Chen W. Multiplex conditional mutagenesis using transgenic expression of Cas9 and sgRNAs. Genetics. 2015;200(2):431–41.
293. Maddison LA, Joest KE, Kammeyer RM, Chen W. Skeletal muscle insulin resistance in zebrafish induces alterations in β-cell number and glucose tolerance in an age- and diet-

dependent manner. Am J Physiol - Endocrinol Metab. 2015;308(8):662–9.
294. Lu J, Liu K, Schulz N, Karampelias C, Charbord J, Hilding A, Rautio L, Bertolino P, Östenson C, Brismar K, Andersson O. IGFBP 1 increases β-cell regeneration by promoting α- to β-cell transdifferentiation. EMBO J. 2016;35(18):2026–44.
295. Ghaye AP, Bergemann D, Tarifeño-Saldivia E, Flasse LC, Von Berg V, Peers B, Voz ML, Manfroid I. Progenitor potential of nkx6.1-expressing cells throughout zebrafish life and during beta cell regeneration. BMC Biol. 2015;13(1):1–24.
296. Brissova M, Fowler MJ, Nicholson WE, Chu A, Hirshberg B, Harlan DM, Powers AC. Assessment of human pancreatic islet architecture and composition by laser scanning confocal microscopy. J Histochem Cytochem. 2005;53(9):1087–97.
297. Chung WS, Stainier DYR. Intra-endodermal interactions are required for pancreatic β cell induction. Dev Cell. 2008;14(4):582–93.
298. Bertrand JY, Chi NC, Santoso B, Teng S, Stainier DYR, Traver D. Haematopoietic stem cells derive directly from aortic endothelium during development. Nature. 2010;464(7285):108–11.
299. Hans S, Freudenreich D, Geffarth M, Kaslin J, Machate A, Brand M. Generation of a non-leaky heat shock-inducible Cre line for conditional Cre/lox strategies in zebrafish. Dev Dyn. 2011;240(1):108–15.
300. Boniface EJ, Lu J, Victoroff T, Zhu M, Chen W. FlEx-based transgenic reporter lines for visualization of Cre and Flp activity in live zebrafish. Genesis. 2009;47(7):484–91.
301. Mosimann C, Kaufman CK, Li P, Pugach EK, Tamplin OJ, Zon LI. Ubiquitous transgene expression and Cre-based recombination driven by the ubiquitin promoter in zebrafish. Development. 2011;138(1):169–77.
302. Engler C, Marillonnet S. Golden Gate Cloning. In: Valla S, Lale R, editors. DNA Cloning and Assembly Methods [Internet]. Totowa, NJ: Humana Press; 2014. p. 119–31. Available from: https://doi.org/10.1007/978-1-62703-764-8_9
303. Kawakami K, Takeda H, Kawakami N, Kobayashi M, Matsuda N, Mishina M. A transposon-mediated gene trap approach identifies developmentally regulated genes in zebrafish. 2004;7:133–44.
304. Kwan KM, Fujimoto E, Grabher C, Mangum BD, Hardy ME, Campbell DS, Parant JM, Yost HJ, Kanki JP, Chien CB. The Tol2kit: A multisite gateway-based construction kit for Tol2 transposon transgenesis constructs. Dev Dyn. 2007;236(11):3088–99.
305. Matsuda T, Cepko CL. Controlled expression of transgenes introduced by in vivo electroporation. Proc Natl Acad Sci U S A. 2007;104(3):1027–32.
306. Matsuda H, Parsons MJ, Leach SD. Aldh1-expressing endocrine progenitor cells regulate secondary islet formation in larval zebrafish pancreas. PLoS One. 2013;8(9):1–12.
307. McCarthy DJ, Campbell KR, Lun ATL, Wills QF. Scater: Pre-processing, quality control, normalization and visualization of single-cell RNA-seq data in R. Bioinformatics. 2017;33(8):1179–86.
308. Butler A, Hoffman P, Smibert P, Papalexi E, Satija R. Integrating single-cell transcriptomic data across different conditions, technologies, and species. Nat Biotechnol. 2018;36(5):411–20.
309. Stuart T, Butler A, Hoffman P, Hafemeister C, Papalexi E, Mauck WM, Hao Y, Stoeckius M, Smibert P, Satija R. Comprehensive integration of single-cell data. Cell. 2019;177(7):1888–902.

310. Toselli CM, Wilkinson BM, Paterson J, Kieffer TJ. Vegfa/vegfr2 signaling is necessary for zebrafish islet vessel development, but is dispensable for beta-cell and alpha-cell formation. Sci Rep. 2019;9(1):3594.
311. Sandlesh P, Juang T, Safina A, Higgins MJ, Gurova K. Uncovering the fine print of the CreERT2-LoxP system while generating a conditional knockout mouse model of Ssrp1 gene. PLoS One. 2018;13(6):e0199785.
312. Kristianto J, Johnson MG, Zastrow RK, Radcliff AB, Blank RD. Spontaneous recombinase activity of Cre–ERT2 in vivo. Transgenic Res. 2017;26(3):411–7.
313. Heffner CS, Herbert Pratt C, Babiuk RP, Sharma Y, Rockwood SF, Donahue LR, Eppig JT, Murray SA. Supporting conditional mouse mutagenesis with a comprehensive cre characterization resource. PLoS One. 2018;13(6):e0199785.
314. Muzumdar MD, Tasic B, Miyamichi K, Li L, Luo L. A global double-fluorescent Cre reporter mouse. Genesis. 2007;45(9):593–605.
315. Maddison LA, Chen W. Nutrient excess stimulates beta-cell neogenesis in zebrafish. Diabetes. 2012;61(10):2517–24.
316. Ninov N, Hesselson D, Gut P, Zhou A, Fidelin K, Stainier DYR. Metabolic regulation of cellular plasticity in the pancreas. Curr Biol. 2013;23(13):1242–50.
317. Roberts JA, Miguel-Escalada I, Slovik KJ, Walsh KT, Hadzhiev Y, Sanges R, Stupka E, Marsh EK, Balciuniene J, Balciunas D, Müller F. Targeted transgene integration overcomes variability of position effects in zebrafish. Dev. 2014;141(3):715–24.
318. Szabat M, Page MM, Panzhinskiy E, Skovsø S, Mojibian M, Fernandez-Tajes J, Bruin JE, Bround MJ, Lee JTC, Xu EE, Taghizadeh F, O'Dwyer S, van de Bunt M, Moon KM, Sinha S, Han J, Fan Y, Lynn FC, Trucco M, et al. Reduced insulin production relieves endoplasmic reticulum stress and induces β cell proliferation. Cell Metab. 2016;23(1):179–93.
319. Ye L, Robertson MA, Mastracci TL, Anderson RM. An insulin signaling feedback loop regulates pancreas progenitor cell differentiation during islet development and regeneration. Dev Biol. 2016;409(2):354–69.
320. Ramzy A, Mojibian M, Kieffer TJ. Insulin-deficient mouse β-Cells do not fully mature but can be remedied through insulin replacement by islet transplantation. Endocrinology. 2018;159(1):83–102.
321. Jabs N, Franklin L, Brenner MB, Gromada J, Ferrara N, Wollheim CB, Lammert E. Reduced insulin secretion and content in VEGF-A deficient mouse pancreatic islets. Exp Clin Endocrinol Diabetes. 2008;116:46–9.
322. Reinert RB, Brissova M, Shostak A, Pan FC, Poffenberger G, Cai Q, Hundemer GL, Kantz J, Thompson CS, Dai C, McGuinness OP, Powers AC. Vascular endothelial growth factor-a and islet vascularization are necessary in developing, but not adult, pancreatic islets. Diabetes. 2013;62(12):4154–64.
323. Lawson ND, Weinstein BM. In vivo imaging of embryonic vascular development using transgenic zebrafish. Dev Biol. 2002;248(2):307–18.
324. Nasevicius A, Larson J, Ekker SC. Distinct requirements for zebrafish angiogenesis revealed by a VEGF-A morphant. Yeast. 2000;1(4):294–301.
325. Bahary N, Goishi K, Stuckenholz C, Weber G, LeBlanc J, Schafer C, Berman SS, Klagsbrun M, Zon LI. Duplicate VegfA genes and orthologues of the KDR receptor tyrosine kinase family mediate vascular development in the zebrafish. Blood.

2007;110(10):3627–36.
326. Habeck H, Odenthal J, Walderich B, Maischein HM, Schulte-Merker S, Tübingen 2000 screen consortium. Analysis of a zebrafish VEGF receptor mutant reveals specific disruption of angiogenesis. Curr Biol. 2002;12(16):1405–12.
327. Hen G, Nicenboim J, Mayseless O, Asaf L, Shin M, Busolin G, Hofi R, Almog G, Tiso N, Lawson ND, Yaniv K. Venous-derived angioblasts generate organ-specific vessels during zebrafish embryonic development. Development. 2015;142(24):4266–78.
328. Dash SN, Hakonen E, Ustinov J, Otonkoski T, Andersson O, Lehtonen S. Sept7b is required for the differentiation of pancreatic endocrine progenitors. Sci Rep. 2016;6:24992.
329. Koenig AL, Baltrunaite K, Bower NI, Rossi A, Stainier DYR, Hogan BM, Sumanas S. Vegfa signaling promotes zebrafish intestinal vasculature development through endothelial cell migration from the posterior cardinal vein. Dev Biol. 2016;411(1):115–27.
330. Nikolova G, Jabs N, Konstantinova I, Domogatskaya A, Tryggvason K, Sorokin L, Fässler R, Gu G, Gerber HP, Ferrara N, Melton DA, Lammert E. The vascular basement membrane: A niche for insulin gene expression and β cell proliferation. Dev Cell. 2006;10(3):397–405.
331. Rombough P, Drader H. Hemoglobin enhances oxygen uptake in larval zebrafish (Danio rerio) but only under conditions of extreme hypoxia. J Exp Biol. 2009;212(6):778–84.
332. Marín-Juez R, Marass M, Gauvrit S, Rossi A, Lai SL, Materna SC, Black BL, Stainier DYR. Fast revascularization of the injured area is essential to support zebrafish heart regeneration. Proc Natl Acad Sci. 2016;113(40):11237–42.
333. Huang C, Lawson ND, Weinstein BM, Johnson SL. reg6 is required for branching morphogenesis during blood vessel regeneration in zebrafish caudal fins. Dev Biol. 2003;264(1):263–74.
334. Gerhard GS, Kauffman EJ, Wang X, Stewart R, Moore JL, Kasales CJ, Demidenko E, Cheng KC. Life spans and senescent phenotypes in two strains of Zebrafish (Danio rerio). Exp Gerontol. 2002;37(8–9):1055–68.
335. Gilbert MJH, Zerulla TC, Tierney KB. Zebrafish (Danio rerio) as a model for the study of aging and exercise: physical ability and trainability decrease with age. Exp Gerontol. 2013;50(1):106–13.
336. Hayes AJ, Reynolds S, Nowell MA, Meakin LB, Habicher J, Ledin J, Bashford A, Caterson B, Hammond CL. Spinal deformity in aged zebrafish Is accompanied by degenerative changes to their vertebrae that resemble osteoarthritis. PLoS One. 2013;8(9):e75787.
337. Shao J, Chen D, Ye Q, Cui J, Li Y, Li L. Tissue regeneration after injury in adult zebrafish: The regenerative potential of the caudal fin. Dev Dyn. 2011;240(5):1271–7.
338. Eames SC, Philipson LH, Prince VE, Kinkel MD. Blood sugar measurement in zebrafish reveals dynamics of glucose homeostasis. Zebrafish. 2010;7(2):205–13.
339. Steiner DJ, Kim A, Miller K, Hara M. Pancreatic islet plasticity: interspecies comparison of islet architecture and composition. Islets. 2010;2(3):135–45.
340. Zhang J, McKenna LB, Bogue CW, Kaestner KH. The diabetes gene Hhex maintains δ-cell differentiation and islet function. Genes Dev. 2014;28(8):829–34.
341. Quesada I, Todorova MG, Alonso-Magdalena P, Beltrá M, Carneiro EM, Martin F, Nadal A, Soria B. Glucose induces opposite intracellular Ca2+ concentration oscillatory patterns

in identified alpha- and beta-cells within intact human islets of Langerhans. Diabetes. 2006;55(9):2463–9.
342. Bosco D, Armanet M, Morel P, Niclauss N, Sgroi A, Muller YD, Giovannoni L, Parnaud G, Berney T. Unique arrangement of α- and β-cells in human islets of Langerhans. Diabetes. 2010;59(5):1202–10.
343. Kilimnik G, Jo J, Periwal V, Zielinski MC, Hara M. Quantification of islet size and architecture. Islets. 2012;4(2):167–72.
344. Bonner-Weir S, Sullivan BA, Weir GC. Human islet morphology revisited: human and rodent islets are not so different after all. J Histochem Cytochem. 2015;63(8):604–12.
345. Freudenblum J, Iglesias JA, Hermann M, Walsen T, Wilfinger A, Meyer D, Kimmel RA. In vivo imaging of emerging endocrine cells reveals a requirement for PI3K-regulated motility in pancreatic islet morphogenesis. Development. 2018;145(3):dev158477.
346. De Krijger RR, Aanstoot HJ, Kranenburg G, Reinhard M, Visser WJ, Bruining GJ. The midgestational human fetal pancreas contains cells coexpressing islet hormones. Dev Biol. 1992;153(2):368–75.
347. Portela-Gomes GM, Johansson H, Olding L, Grimelius L. Co-localization of neuroendocrine hormones in the human fetal pancreas. Eur J Endocrinol. 1999;141(5):526–33.
348. Pour PM. Pancreatic centroacinar cells. Int J Pancreatol. 1994;15(1):51–64.
349. Rovira M, Scott SG, Liss AS, Jensen J, Thayer SP, Leach SD. Isolation and characterization of centroacinar/terminal ductal progenitor cells in adult mouse pancreas. Proc Natl Acad Sci U S A. 2010;107(1):75–80.
350. Stanger BZ, Stiles B, Lauwers GY, Bardeesy N, Mendoza M, Wang Y, Greenwood A, Cheng KH, McLaughlin M, Brown D, DePinho RA, Wu H, Melton DA, Dor Y. Pten constrains centroacinar cell expansion and malignant transformation in the pancreas. Cancer Cell. 2005;8(3):185–95.
351. Kopinke D, Brailsford M, Pan FC, Magnuson MA, Wright CVE, Murtaugh LC. Ongoing Notch signaling maintains phenotypic fidelity in the adult exocrine pancreas. Dev Biol. 2012;362(1):57–64.
352. Peshavaria M, Larmie BL, Lausier J, Satish B, Habibovic A, Roskens V, LaRock K, Everill B, Leahy JL, Jetton TL. Regulation of pancreatic β-cell regeneration in the normoglycemic 60% partial-pancreatectomy mouse. Diabetes. 2006;55(12):3289–98.
353. Zhou J, Lin J, Zhou C, Deng X, Xia B. Cytotoxicity of red fluorescent protein DsRed is associated with the suppression of Bcl-xL translation. FEBS Lett. 2011;585(5):821–7.
354. Ganini D, Leinisch F, Kumar A, Jiang JJ, Tokar EJ, Malone CC, Petrovich RM, Mason RP. Fluorescent proteins such as eGFP lead to catalytic oxidative stress in cells. Redox Biol. 2017;12:462–8.
355. Laboulaye MA, Duan X, Qiao M, Whitney IE, Sanes JR. Mapping transgene insertion sites reveals complex interactions between mouse transgenes and neighboring endogenous genes. Front Mol Neurosci. 2018;11:385.
356. West AG, Gaszner M, Felsenfeld G. Insulators : many functions, many mechanisms. Genes Dev. 2002;16(3):271–88.
357. Hisano Y, Sakuma T, Nakade S, Ohga R, Ota S, Okamoto H, Yamamoto T, Kawahara A. Precise in-frame integration of exogenous DNA mediated by CRISPR/Cas9 system in zebrafish. Sci Rep. 2015;5:8841.

358. Ota S, Taimatsu K, Yanagi K, Namiki T, Ohga R, Higashijima SI, Kawahara A. Functional visualization and disruption of targeted genes using CRISPR/Cas9-mediated eGFP reporter integration in zebrafish. Sci Rep. 2016;6:34991.
359. Kawahara A. CRISPR/Cas9-Mediated Targeted Knockin of Exogenous Reporter Genes in Zebrafish. In: Methods in Molecular Biology. Genome Edi. Humana Press, New York, NY; 2017. p. 165–73.
360. Auer TO, Duroure K, De Cian A, Concordet JP, Del Bene F. Highly efficient CRISPR/Cas9-mediated knock-in in zebrafish by homology-independent DNA repair. Genome Res. 2014;24(1):142–53.
361. Jurczyk A, Roy N, Bajwa R, Gut P, Lipson K, Yang C, Covassin L, Racki WJ, Rossini AA, Phillips N, Stainier DYR, Greiner DL, Brehm MA, Bortell R, DiIorio P. Dynamic glucoregulation and mammalian-like responses to metabolic and developmental disruption in zebrafish. Gen Comp Endocrinol. 2011;170(2):334–45.
362. Zang L, Shimada Y, Nishimura Y, Tanaka T, Nishimura N. Repeated blood collection for blood tests in adult zebrafish. J Vis Exp. 2015;(102):53272.
363. Ye L, Robertson MA, Hesselson D, Stainier DYR, Anderson RM. Glucagon is essential for alpha cell transdifferentiation and beta cell neogenesis. Development. 2015;142(8):1407–17.
364. Li M, Maddison LA, Page-McCaw P, Chen W. Overnutrition induces β-cell differentiation through prolonged activation of β-cells in zebrafish larvae. Am J Physiol - Endocrinol Metab. 2014;306(7):799–807.
365. Grossman EJ, Lee DD, Tao J, Wilson RA, Park SY, Bell GI, Chong AS. Glycemic control promotes pancreatic beta-cell regeneration in streptozotocin-induced diabetic mice. PLoS One. 2010;5(1):e8749.
366. Dorsemans AC, Soulé S, Weger M, Bourdon E, Lefebvre d'Hellencourt C, Meilhac O, Diotel N. Impaired constitutive and regenerative neurogenesis in adult hyperglycemic zebrafish. J Comp Neurol. 2017;525(3):442–58.